2011

Development of modified p-y curves for Winkler Analysis to characterize the lateral load behavior of a single pile embedded in improved soft clay

Jin-wei Huang
Iowa State University

Development of modified p-y curves for Winkler Analysis to characterize the lateral load behavior of a single pile embedded in improved soft clay

by

Jin-Wei Huang

A thesis submitted to the graduate faculty

in partial fulfillment of the requirements for the degree of

MASTER OF SCIENCE

Major: Civil Engineering (Structural Engineering)

Program of Study Committee:
Sri Sritharan, Major Professor
Jeramy Ashlock
Jon Rouse
Shihwu Sung

Iowa State University

Ames, Iowa

2011

TABLE OF CONTENTS

LIST OF FIGURES

LIST OF TABLES

ABSTRACT

In the past decades, the behavior of pile foundations in liquefiable sands has been studied extensively; however, similar investigations of soft clays or static/seismic response of piles in improved soft clay soils are scarce. Despite the widespread presence of this soil type in high seismic regions and the frequent need to locate bridges and buildings in soft clay, only a few investigations have been carried out to guide engineers in evaluating the effectiveness of ground improvement techniques on increasing the lateral resistance of pile foundation embedded in soft clay, and no numerical models have been validated to evaluate this approach. Thus, the objective of this research was to develop modified *p-y* curves for Winkler analysis to characterize the lateral load behavior of a single pile embedded in a volume of improved clay surrounded by unimproved soft clays.

A detailed literature review was completed in the study, aiming to gain knowledge on the development and fields of applications together with limitations of different ground improvement techniques. The ability of each available analysis method for lateral loaded piles was assessed for determining lateral responses of pile foundation in a volume of improved soil surrounded by unimproved soil.

A method of developing *p-y* curve modification factors to account for the effect of the improved soil on enhancing the lateral load behavior of a single pile embedded in soft clay was developed by integrating the effectiveness of the improved soil into the procedures of constructing *p-y* curves for stiff clay recommended by Welch and Reese (1972). It was achieved by estimating the effective length for a infinitely long soil layer with soil improvement so that the fraction of the load resisted by the soil improved over a

limited horizontal extent could be accounted for by taking the ratio between the soil resistance attenuation at actual length of the soil improvement and the effective length. The accuracy of the method was verified against the centrifuge test data from Liu et al. (2010) and the full scale field test from Fleming et al. (2010). The verifications using experimental data demonstrated that the Winkler analysis with proposed *p-y* modification factors is able to capture the full range of elastic and inelastic pile responses with slopes that correspond well with the results obtained from both centrifuge and field testing, the effectiveness of the soil improvement can be adequately evaluated.

In addition, an analytical study on the effectiveness of the cement-deep-soil-mixing (CDSM) ground improvement technique on controlling the lateral displacement of pile foundations embedded in different clay soil conditions with and without ground improvement was carried out. A set of lateral load analyses was performed to establish permissible displacements for precast, prestressed concrete piles as well as open-ended steel pipe pile prior to reaching the curvature capacity of piles. The analysis results showed an average of 66% reduction on the permissible displacement limit by providing a volume of CDSM soil improvement around the prestressed precast concrete piles embedded in medium clay and soft clay. And an average of 79% reduction was observed on steel pipe pile embedded in CDSM improved medium clay and soft clay.

CHAPTER 1. INTRODUCTION

1.1 Historical Background

Pile foundations have been used to carry and transfer the structural loads to the bearing ground located at some depth below the ground surface for many years. In ancient times, villages and towns were located in river valleys on a stratum of weak soils, peats and on flood-prone sections due to the availability of the water and to ensure proper protection of the area from invaders. Therefore, the first types of piles in the form of stilts were used to strengthen the weak bearing ground as early as the late Neolithic Period (Ulitskii, 1995). Similarly, buildings have been preserved in Eastern Europe where some villages and settlements were built directly on peat covered with a layer of brush wood and strong fortifications around them on wooden piles (Ulitskii, 1995). In the modern "stone" age, buildings on piles, which were raised on rivers and lakes, were massive (Ulitskii, 1995). The presence of pile foundations makes it possible to construct structures in areas where the soil conditions are less than favorable for the design of shallow foundations (Prakash and Sharma, 1990).

1.2 Laterally Loaded Piles

In today's practice, piles usually made of steel or concrete. Sometimes, timber piles are also used. The common steel piles are the H-piles, in which case the standard H sections are used as the cross section of the pile, and the closed- or open-ended pipe-piles. For pipe piles, hollowed circular sections are used as cross section of the piles with the

bottom end is either sealed with a steel plate or left open. Concrete piles can be reinforced or prestressed piles, which are used in prefabricated form. Concrete piles can have square, rectangular or circular shape. The steel, timber and precast concrete piles are inserted into the ground by pile jacking or hammering. In the case of jacking, the pile is made to stand vertically on the ground and a sustained static load is placed on top which pushes the pile into the ground. In the case of hammering, instead of a static load, the pile is subjected to hammer blows at the top, which progressively forces the pile into the ground. Sometimes concrete piles are cast in situ (e.g., drilled shafts, continuous flight auger piles, drilled displacement piles). For cast-in-situ piles, a cavity (typically a cylindrical shape) of desired dimension is made in the ground (e.g., by the use of an auger) and the void is replaced by reinforcement and concrete.

Often, piles are grouped together under a column to ensure its stability (e.g., to restrain the rotation of a column base). Grouping of piles becomes essential when the loads from the superstructures are so large that a single pile cannot safely transfer the load. Such an arrangement, where piles are grouped under a thick reinforced concrete element known as the pile cap, is called a pile group.

Piles are commonly used to transfer vertical (axial) forces, arising primarily from gravity (e.g., the weight of a superstructure). Examples of structures where piles are commonly used as foundations are tall buildings, bridges, offshore platforms, defense structures, dams and lock structures, transmission towers, earth retaining structures, wharfs and jetties. However, in all these structures, it is not only the axial force that the piles carry; often the piles are subjected to lateral (horizontal) forces and moments. In

fact, there are some structures (e.g., oil production platforms, earth retaining structures, wharfs and jetties) where the primary function of piles is to transfer lateral loads to the ground.

Wind gusts are the most common cause of lateral force (and/or moment) that a pile has to resist. The other major cause of lateral force is seismic activity. The horizontal shaking of the ground during earthquakes generates lateral forces that the piles have to withstand. That apart, depending on the type of structure a pile supports, there can be different causes of lateral forces. For tall buildings and transmission towers, wind action is the primary cause. For offshore oil production platforms, quays, harbors, wharfs and jetties, wave action gives rise to lateral forces. In the case of bridge abutments and piers, horizontal forces are caused due to traffic, wind and thermal movement. Dams and lock structures have to withstand water pressures that transfer as horizontal forces on the supporting piles. Defense structures often have to withstand blasts that cause lateral forces. In the case of earth retaining structures, the primary role of piles is to resist lateral forces caused due to the lateral pressures exerted by the soil mass behind the retaining wall. Sometimes, piles are installed into slopes, where slow ground movements are taking place, in order to arrest the movement. In such cases, the piles are subjected only to lateral forces. Piles are used to support open excavations; here also, there is no axial force and the primary role of the piles is to resist lateral forces.

In the above examples, there are some cases where the external horizontal loads act at the pile head (i.e., at the top section of the pile). Such loading is called active loading (Fleming et al. 1992, Reese and Van Impe 2001). Common examples are lateral

loads (and moments) transmitted to the pile from superstructures like buildings, bridges and offshore platforms. Sometimes the applied horizontal load acts in a distributed manner over a part of the pile shaft; such a loading is called passive loading. Examples of passive loading are loads acting on piles due to movement of slopes or on piles supporting open excavations. There are cases where external horizontal loads are minimal or absent; even then external moments often exist because of accidental eccentricities caused by construction defects (e.g., out-of-plumb constructions), enabling axial loads to induce moments. Thus, piles in most cases are subjected to lateral loads. Consequently, proper analysis of laterally loaded piles is very important to the geotechnical and civil engineering profession.

1.2.1 Static Load Transfer Mechanism

A proper understanding of the load transfer mechanisms for piles is necessary for analysis and design. Piles transfer axial and lateral loads through different mechanisms. In the case of lateral loads, piles behave as transversely loaded beams. They transfer lateral load to the surrounding soil mass by using the lateral resistance of soil (Figure 1.1). When a pile is loaded laterally, a part or whole of the pile tries to shift horizontally in the direction of the applied load, causing bending, rotation and/or translation of the pile (Fleming et al. 1992, Salgado 2008). The pile presses against the soil in front of it (i.e., the soil mass presence in the direction of the applied load), developing compressive stresses and strains in the soil that offers resistance to the pile movement. This is the primary mechanism of load transfer for lateral loaded piles. The total soil resistance acting over the entire pile shaft balances the external horizontal forces, and the soil

resistance also allows satisfaction of moment equilibrium of the pile. Some frictional resistance between the pile shaft and the surrounding soil develops; however, the magnitude of the frictional resistance is much less compared with the compressive resistance and is usually neglected in the calculations.

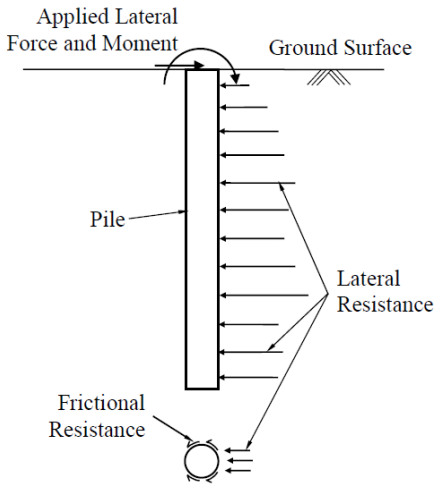

Figure 1.1 Load transfer mechanism of laterally loaded piles (Basu, 2006)

1.2.2 Kinematic Load Transfer Mechanism

The kinematics of axially loaded piles is simple: the pile moves vertically downward under the acting load and, if the resistive forces (i.e., shaft and base resistances) exceed the limiting values, then the pile suffers excessive vertical deflection (or plunging), leading to failure. The kinematics of laterally loaded piles is more complex and varies depending on the pile type. Since laterally loaded piles are transversely loaded, the pile may rotate, bend and/or translate. As the pile moves in the direction of the applied force, a gap may also open up between the back of the pile and the surrounding soil over the top few meters. If the pile is short and stubby, it will not bend much but will rotate or even translate (Figure 1.2). Such piles are called rigid piles. If the pile is long

and slender, then it bends because of the applied load (Figure 1.3). These piles are called flexible piles. In most practical situations, piles are long enough to behave as flexible piles. For flexible piles, the laterally loaded pile problem is a common soil-structure interaction (SSI) problem; i.e., the lateral deflection of the pile depends on the soil resistance, and the resistance of the soil, in turn, depends on the pile deflection.

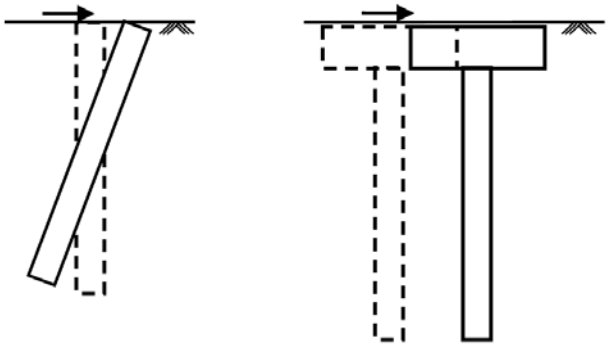

(a) Rotation (b) Translation

Figure 1.2 Kinematics of laterally loaded rigid piles

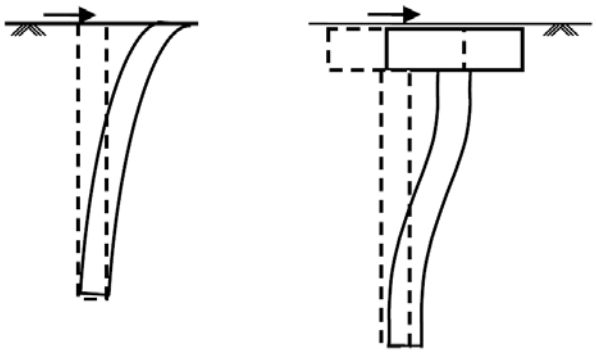

(a) Bending with free pile head (b) Bending with fixed pile head

Figure 1.3 Kinematics of laterally loaded flexible piles

1.3 Analysis Methods for Soil-Structure Interaction (SSI)

Many numerical methods have been developed over the years for the analysis of laterally loaded soil-pile systems (e.g., Broms, 1965; Thompson, 1977; Poulos, 1980; Georgiadis and Butterfield, 1982; and Reese, 1986). In most of these methods, the pile is modeled as a flexible beam. The main difference in the various methods is the approach used to capture the soil behavior in the analysis model. Therefore, the available analysis methods for pile subjected to lateral loading can be divided into three general approaches based on the soil modeling techniques:

1. The Winkler approach in which the pile is considered to be supported by a series of uncoupled springs. These springs may be taken to be linear elastic, but more correctly they should be modeled as nonlinear springs. The shape of the load-deformation relationships are described by *p-y* curves, where *p* is the soil resistance and *y* is the pile deflection. Finite difference techniques can then be used to determine the response of the pile and spring system to the applied lateral loads.
2. In the second approach, the soil surrounding the pile is modeled as homogeneous elastic continuum. The represented method of this approach is developed by Poulos (1971a, 1971b, 1972), who has presented an approximate numerical solution for laterally loaded pile and the pile is represented as an infinitely thin linearly elastic strip embedded in an elastic media. Some further development of elastic continuum analysis has been completed by Poulos and his colleagues (Poulos and Davis, 1980; Swane and Poulos, 1984).

3. Approaches in which the pile and the soil continuum surrounding it are modeled numerically using finite element methods make up the third modeling technique. The method can take into account the three-dimensional interaction, and both elastic and nonlinear soils can be simulated by giving inputs of elastic constants (e.g., Young's modulus and Poisson's ratio) or by plugging in appropriate nonlinear constitutive relationships.

All three of the analysis methods presented above will be further discussed in the next chapter to examine its ability of capturing the lateral response of a pile embedded in a type of soil profile which a volume of improved soil surrounded by unimproved soils.

1.4 Pile Performance in Soft Soils

1.4.1 Observed Pile Damages during Earthquakes

As discussed previously, the behavior of pile foundations under lateral loading is an important factor affecting the performance of many essential structures. Cases of damages to piles and pile-supported structures sited on soft soils have been frequently observed in the past earthquakes (San Francisco, 1906; Alaska, 1964; Niigata, 1964; Loma Prieta, 1989; and Kobe earthquakes, 1995; etc.), which gives excellent indication of pile performance under lateral load and insight into their modes of behavior and failure. Figure 1.4 shows a pile supported pier of the Salinas bridge during the 1906 San Francisco earthquake. The piles were observed to be unbroken at ground level, but the entire pier was inclined as shown in the figure (Wood, 1908). An example of liquefaction related pile failure is shown in Figure 1.5. During the 1964 Niigata earthquake, the large-diameter concrete piles supporting the NHK building were found to

be broken at two positions, near the top of the pile and near the base, and consistently inclined in the direction of the permanent ground displacement observed from aerial photographs after the event (Hamada, 1991). During the 1989 Loma Prieta earthquake, a pile-supported highway bridge across the Struve Slough collapsed. The piles did not show signs of settlement, but there were 30 to 45 cm wide gaps opened around the piles, indicating inadequate lateral support (Figure 1.6(a)). This inadequate lateral soil support resulted in excessive lateral pile deflections and flexural/shear failures at the pile to bent connections (Figure 1.6(b)). It appears that the failure was not due to the liquefaction as the upper foundation soils consisted of soft clay and organics, with some alluvial sands present (Reed et al., 1990).

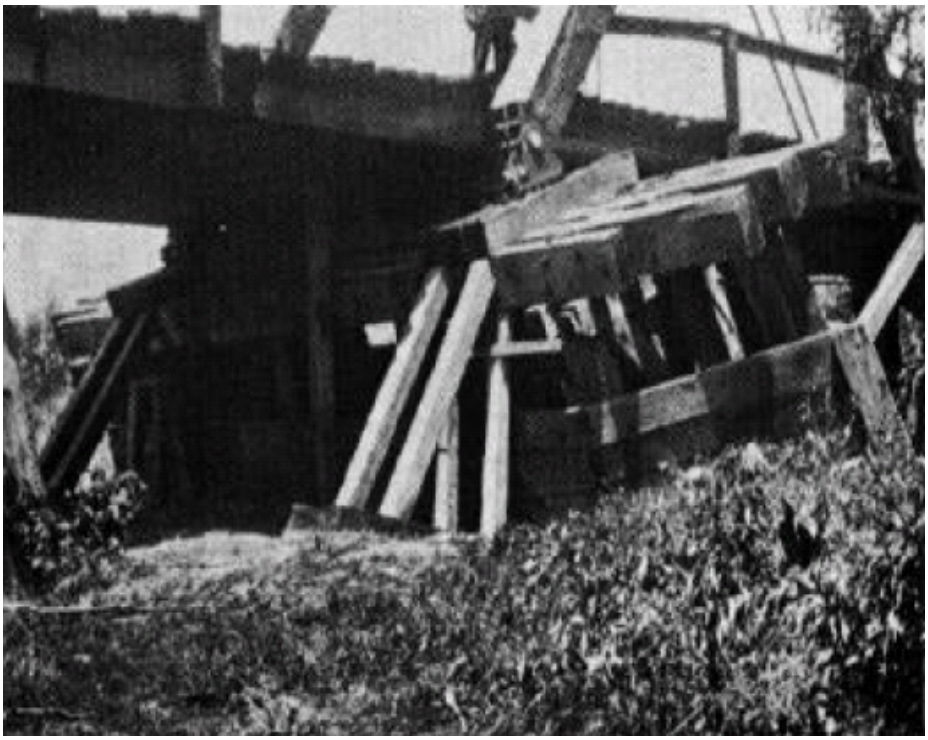

Figure 1.4 Failure of pile supported pier of the Salinas bridge during the 1906 San Francisco earthquake (Wood, 1908)

Figure 1.5. Piles supporting the NHK building sheared by lateral spreading during the 1964 Niigata earthquake (Hamada, 1991)

1.4.2 Analytical Work

The pile damages and its associated structural failures observed in the case histories indicates that many pile foundation failures during earthquake event are due to the loss of lateral soil support. In other words, strain softening of cohesive soils and/or liquefaction of cohesionless soils happens near the pile head and causes severe damages to the pile foundation and its supporting superstructures during earthquakes. An analytical work recently completed by Fanous et al. (2010) evaluated the lateral behavior of a precast, prestressed pile and established permissible limits of lateral displacement for the pile in different soil conditions. In this study, nine different soil types covering the full range of soil conditions defined in ASCE 7-05, including very dense soil and soft rocks, stiff soil and soft clay soil, were used. The "permissible limit" eventually defines the displacement that a specific pile, in a given soil, can undergo prior to experiencing

(a) Gap formation adjacent to one of the piles

(b) Flexural shear failure of pile to bent connection

Figure 1.6 Pile damages of the Struve Slough crossing during 1989 Loma Prieta earthquake (Reed et al., 1990)

failure. Through these analyses, Fanous et al. drew the following conclusion regarding the influence of the soil type on permissible limits of lateral displacement for the precase, prestressed pile:

- for piles embedded in clay, the permissible lateral displacement limits increases as the undrained shear strength and the effective unit weight decrease;

- for piles embedded in sand, the permissible lateral displacement limits increase as the friction angle, the initial modulus of subgrade reaction and the effective unit weight decrease;
- the displacements calculated for piles embedded in soft soils far exceed the displacements that may be permitted for these piles to experience under seismic lateral load without causing instability to the entire structure, and therefore structures should be designed with the consideration of serviceability limits and survival of the structures when piles have large lateral displacement capacities.

1.4.3 Solutions to Improving Pile Performance in Soft Soil

Both the qualitative observations and the quantitative analysis results made it clear that pile performance under seismic lateral loading is generally poor in soft ground. The behavior of pile foundations is very complex with the interaction between soils, piles and superstructures. It becomes further exacerbated with the presence of weak soil such as soft clay or liquefiable loose sand. The current seismic design practice calls for avoiding inelastic behavior of pile foundations by restricting their lateral displacements because it is difficult to detect damage to foundations below the ground following an earthquake. Limiting the lateral displacement of a pile foundation in competent soils is relatively easy to achieve. In cases of weak soils, the current practice is to use an increased number of more ductile, larger diameter piles that are more difficult to design and more expensive to construct (e.g., Zelinski et al. 1995). A more cost-efficient solution to this problem is to improve the soil surrounding the pile foundations. For structures undergoing seismic retrofit with existing pile foundations in weak soils,

improving the soils may also be the most cost efficient option to improve the seismic behavior of the foundation.

In ground improvement, different techniques may be used to improve different soil characteristics that match the desired results of a project, such as an increase in density and shear strength to aid problems of stability, the reduction of soil compressibility, influencing permeability to reduce and control ground water flow or to increase the rate of consolidation, or to improve soil homogeneity. Among the variety of the ground improvement techniques, distinction is made between methods of compaction or densification and methods of soil reinforcement through the introduction of additional material into the ground. This distinction offers the opportunity to divide the topics into several groups, which are:

- surface compaction and deep compaction, in which surface compaction is used to increases the soil unit weight by forcing the soil particles into a tighter state and reducing air voids by adding either static or dynamic forces; while deep compaction is used to reduce the soils compressibility and increase the soil strength by packing soil particles together with high energy vibrations as the probe is progressively inserted to and withdrawn from thick soil deposit;
- grouting, in which the voids in the ground is filled with liquids grout mixes under pressure with the aim to increase soil resistance against deformation, to supply cohesion, shear strength and uniaxial compressive strength of week soils; and

- in-situ deep soil mixing, which has been extensively used to improve soil strength and deformation behavior. In this method, soils are mixed in situ with different stabilizing binders, which chemically react with the soil and/or the groundwater.

The development and fields of applications together with limitations of each technique will be discussed further in Chapter 2.

1.5 Scope of Research

In the past decades, the behavior of pile foundations in liquefiable sands has been studied extensively (e.g., Boulanger and Tokimatsu 2006; Ohtomo 1996); however, similar investigations of soft clays or static/seismic response of piles in improved soft clay soils are scarce despite the widespread presence of this soil type in high seismic regions and the frequent need to locate bridges and buildings in soft clay. In the current study, a methodology is developed to account for the effect of the cement-deep-soil-mixing (CDSM) improved soil on the lateral behavior of a single pile foundation in soft clay using the Winkler analysis approach.

The CDSM ground improvement technique is not widely used in seismic regions due to lack of fundamental understanding of the behavior of improved and unimproved soils and the interactions between them as well as with the piles during earthquakes. However, this ground improvement method is a more cost-efficient solution to improve the seismic performance of pile foundation in soft clay comparing to the current practice of using an increased number of more ductile, larger diameter piles. With the newly developed methodology, the lateral behavior of the CDSM-improved pile foundations

will be investigated analytically in this study with the emphasis on developing a method that can be easily used during design of piles in improved soft clay.

Among all the available analysis methods for SSI problems, the Winkler analysis approach, in which the soil is discredited as a set of nonlinear springs, appears to represent a versatile and practical approach for routine analyses. However, the traditional Winkler analysis approach does not allow analysis of a pile foundation embedded in a volume of improved soil surrounded by unimproved soil because the the one-dimensional simplification of the soil-pile model (*p-y* curves) ignores the radial and three-dimensional components of interaction at each depth along the pile length. Based on this deficiency, the current project is undertaken with the overall scope is to develop modified *p-y* curves for Winkler analysis to characterize the lateral load behavior of a single pile embedded in a volume of CDSM-improved clay surrounded by unimproved soft clays. In order to develop the modified *p-y* curves, the project will focus on the following:

1. Detailed examinations on ground improvement techniques and available analysis methods for laterally loaded piles through literature review;
2. The development of the modifications to *p-y* curves for capturing the lateral load responses of a single pile embedded in CDSM improved clay surrounded by unimproved soft clay using Winkler analysis method;
3. Verification of the methodology developed for modifying *p-y* curves using centrifuge test and full-scaled field test; and
4. Determination of the permissible lateral displacements that the prestressed concrete pile and the open-ended steel pile will be able to withstand in

unimproved and improved clay soils using the Winkler analysis method with modified *p-y* curves.

1.6 Report Layout

The remainder of this report includes a detailed description of the procedures of this project. Chapter 1 gives the introduction to the project by providing background information and scope of the research undertaken in this project. The second chapter includes a detailed literature review on the ground improvement techniques and current available analysis methods for lateral loaded piles, as well as the recent investigations on pile performance in soft clay with ground improvement. A complete description of the development of the modified *p-y* curves, which can be used for the Winkler analysis to capture lateral load response of a single pile embedded in CDSM improved clay soil surrounding by unimproved soft clay, is presented in Chapter 3. Next, Chapter 4 provides verification of the Winkler analysis method with previously developed *p-y* curves using a set of cyclic load test result from centrifuge testing of small-scale piles and field testing of large scale piles. Chapter 5 presents an evaluation of the effectiveness of CDSM ground improvement by establishing the permissible lateral displacements for single pile foundations in different clay soils with and without CDSM improvement using the Winkler analysis. Finally, the conclusions and recommendations drawn from the completion of the study are included in the Chapter 6.

CHAPTER 2 LITERATURE REVIEW

2.1 Introduction

Pile foundations have been widely used in the design of structures built on poor soil conditions and heavy marine environment. However, a loss of lateral soil support has been frequently observed during the past earthquakes to have caused pile damages and associated structural failure in cases where soft ground presents. Given the focus of this thesis on developing an method that can be easily used during design of pile foundations in improved soft clay, this chapter is dedicated to the current practice in ground improvement techniques, the available analysis methods for SSI problem and the ability of each method for determining lateral response of a pile embedded in a volume of improved soil surrounded by unimproved soil, and a few recent investigations in evaluating the effectiveness of the ground improvement on increasing lateral resistance of pile foundation in soft clay.

2.2 Ground Improvement Methods

In general, the term soft ground includes soft clay soil, soils with large fractions of fine particles such as silts, clay soils which have high moisture content, peat foundations, and loose sand deposits near or under water table (Kamom and Bergado, 1991). A soil/ground improvement technique is used to increase the soil shear strength, the reduction of soil compressibility, and the reduction of soil permeability (Bergado et al., 1996). As previously noted, the ground improvement techniques can be generally classified in to two categories, namely: a) techniques involving only the soil itself such as compaction or densification, and b) methods that introduces additional materials into the

ground such as the use of chemical admixtures and the utilization of various soil reinforcements. It is important to select appropriate method suitable for specific soil conditions, type of structures, expected loadings and period of constructions.

2.2.1 Compaction

The mechanical behavior of granular soils is markedly influenced by their density. Loose soils are softer and can provide much less shear resistance than dense soils. Loose cohesionless soils are usually less uniform and tend to liquefaction. Consequently, there is a demand for the densification of loose granular soils for construction purposes. The method of compaction is being used with success for many years to achieve the densification of soil.

In general, ground improvement by compaction can be characterized into two subcategories, which are surface compaction and deep compaction. Surface compaction is the most traditional and the cheapest method of ground improvement. It increases the soil unit weight by forcing the soil particles into a tighter state and reducing air voids by adding either static or dynamic forces (Bergado et al., 1996). Figure 2.1 shows the schematic diagram of the reduction of voids of the soil due to compaction. In the case of cohesive soil, the compaction leads to higher density and higher internal friction angle. For cohesive soils, the compaction gives closer particle arrangement and more cohesion. This reduction of voids provides soil with less potential for deformation and less changes in moisture contents. Furthermore, the voids reduction will directly reduce soil permeability, especially for cohesive-frictional soils, because of restricted channels of flow (Bergado et al., 1996). In the field, surface compaction can be achieved by applying

energy in three ways, which are applying pressure by rolling and kneading, by ramming, and by vibrations.

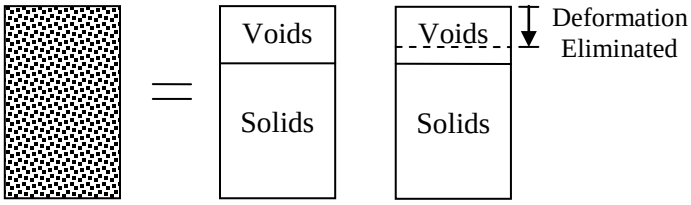

Figure 2.1 Compaction Process

Deep compaction is to reduce the soils compressibility and increase the soil strength by packing soil particles together with high energy vibrations as the probe is progressively inserted into and withdrawn from thick soil deposit (Sondermann and Wehr, 2004). The objectives for deep compaction are to reduce total and differential settlements, increase shear strength, increase resistance to soil liquefaction during earthquakes, and reduce the cost of foundation systems. The increase in density of the foundation subsoil may also allow the utilization of a shallow foundation rather than the more expensive deep foundation. The application of deep compaction techniques varies from simple vibrating poker for clean sands such as the Terraprobe, Resonance Compaction, and Vibroflotation, to dropping of heavy weight such as Dynamic Compaction for more complicated sites with silty and clayey sands, old mine quarries, mine quarries, mine spoils and landfills (Bergado et al., 1996).

2.2.2 Grouting

Grouting generally is used to fill voids in the ground with the aim to increase resistance against deformation, to supply cohesion, shear-strength and uniaxial compressive strength or to reduce conductivity and interconnected porosity in an aquifer

(Stadler, 2004). It uses liquids which are injected under pressure into the pores and fissures of ground (sediments and rock). Liquid grout mixes mainly consist of mortar and chemical products like polyurethane, acrylate or epoxy. Piston or crew-feed pumps deliver grout through lances, perforated pipes and puckered or sleeved pipes into the soil. By displacing gas or groundwater, these grouts fill pores and fissures in the ground and thus improving the properties to the subsoil. The performance of the improved soil is dictated by the degree of saturation and the properties of the grout after the setting and hardening.

Grouting originated from mining and applications in hydro-engineering, and although its history dates back approximately 200 years now, these two sectors remain where today's applications prevail. City excavations for high-rise structures and subways haven prominently added to these examples. A typical example of applications of grouting may be given with the grouting of horizontal barriers (blankets) in the sands below city excavations in Berlin. Internationally renowned agencies and institutions established headquarters in the revived city around Potsdamer Platz, requiring more than 250,000 m^2 of deep, water-sealing blankets in pervious sands during the 1990's. Figure 2.2 shows respective foundation works for the new Offices of the German President of State. To reduce seepage during excavation of construction pits at gradients of approximately 10, it was necessary to reduce permeabilities to around 1×10^{-7} m/s, which corresponded to seepage values of 1.5 l/s per 1000 m^2. Microfine binders barely met the requirement, and it was mainly silicates and aluminate-hardeners which were used to supply a soft gel in a single-shot treatment campaign, i.e. grouting one phase only

through one single port outlet, sufficient to achieve the required impermeabilization and to withstand washout for more than 12 months.

Figure 2.2 Single port grout pipes used in the foundation work for the new Offices of the German President of State (Semprich and Stadler, 2002)

In today's practice, the injection of chemicals into the ground as presented above is increasingly prohibited for environmental reasons (Kirsch and Moseley, 2004). It has been largely replaced by jet grouting, which one of the most versatile ground improvement technique commonly used today. With this technique, it is possible to strengthen the soil, cut-off ground water and provide structural rigidity with a single application. Figure 2.3 shows the principle method of application whereby either high-pressure water or grout is used to physically disrupt the ground, in the process modifying it and thereby improving it. In normal operation, the drill string is advanced to the required depth and then high-pressure water or grout is introduced while withdrawing the rods. There are many applications that suit jet grouting, such as groundwater control,

improving the ground to prevent failure through inadequate bearing, transferring foundation load through weak material to a competent strata and providing support to piles or walls to prevent or reduce lateral movement. A practical case history briefy

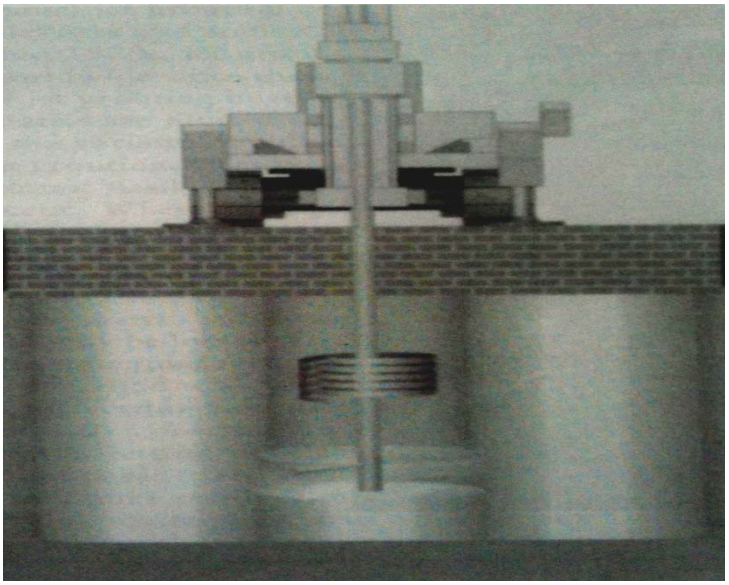

Figure 2.3 Jet grout column construction (Essler and Yoshida, 2004)

explains the application of controlling lateral displacement of walls. As shown in Figure 2.4, the work required an excavation of 10 m depth in a soft clayey layer for basement construction but adjacent houses were so close to the site that they were afraid of being largely undermined due to displacement of walls for shoring. Consequently, jet grouting-produced props of just 1 m thickness at the bottom of excavation have proved successful together with a row of conventional strutting at ground level. By adding a row of grouted props enabled the reduction of lateral displacement by approximately 80% as clear shown in Figure 2.4.

2.2.3 Soil Mixing

Soil mixing has been extensively used to improve inherent properties of the soil such as strength and deformation behavior. An increment in strength, a reduction in

compressibility, an improvement of the swelling or squeezing characteristics and increasing the durability of soil are the main aims of the soil mixing. In this method of ground improvement, soils are mixed in situ with different stabilizing binders, which

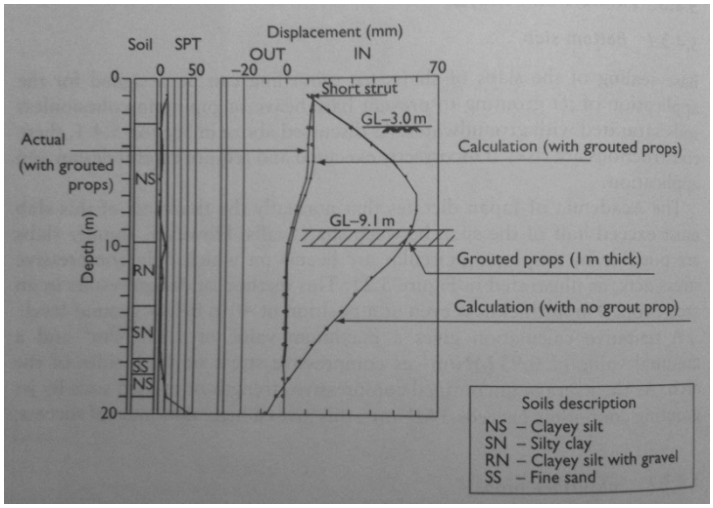

Figure 2.4 Comparison of calculated and actual wall displacements (Yahiro, 1996)

chemically react with the soil and/or the groundwater. By cation exchange at the surface of clay minerals, bonding of soil particles and/or filling of voids by chemical reaction products, ground improvement can be effectively achieved (Topolnicki, 2004). The most common and important binders are cements and limes. However, blast furnace slag, gypsum, ashes as well as other secondary products and compound materials are also used.

Soil mixing technology can be subdivided into two general methods: the Deep Soil Mixing (DSM) method and the Shallow Soil Mixing (SSM) method. The DSM is more frequently used and better developed for stabilization of the soil to a minimum depth of 3 m (a limit depth proposed by CEN TC 288, 2002) and is currently limited to treatment depth of about 50 m (Topolniki, 2004). The binders are injected into the soil in dry and slurry form through hollow rotating mixing shafts tipped with various cutting tools. The mixing shafts are also equipped with discontinuous auger flights, mixing

blades or paddles to increase the efficiency of the mixing process. In some methods, the mechanical mixing is enhanced by simultaneously injecting fluid grout at high velocity through nozzles in the mixing or cutting tools (Topolniki, 2004), as shown in Figure 2.5.

(a) (b)

Figure 2.5 DSM mixing tools: (a) COLMIX mixing tools (Hiway GeoTechnical, 2010); (b) Bauer mixing tool (Bauer Technologies, 2010)

The SSM method is developed to reduce the cost of improving loose or soft superficial soils overlying substantial area a few meters thick. It can be achieved by installing vertical overlapping columns with up and down movements of rotating mixing tools, as in the case of DSM method, and is most cost-effective when using large diameter mixing augers or multiple shaft arrangements. It is important to notice that the difference between DSM and SSM methods is not solely attributed to the available depth of treatment criteria because soil mixing at shallow depth can also be performed with DSM method.

Soil mixing is a versatile ground improvement method. It can be used to stabilize a wide range of soils, including soft clays, silts and fine grained sands. The main areas of soil mixing applications are: foundation support, retention systems, ground treatment, liquefaction mitigation, hydraulic cut-off walls and environmental remediation. An example of controlling vertical settlement of foundation using DSM is presented in Figures 2.6 (a) and (b). A multistory building in Poland was designed with a shallow foundation slab of 1497 m^2 with a thickness of 45 cm. The soil on site consists of soft soils extending 3 to 3.5 m below the slab level, including: silt, organic clay, fine sand, peat inclusions 0.5 to 0.8 m thick. Analysis performed before construction showed an expected settlement of 70 to 500 mm without ground improvement. In order to control the excessive vertical settlement, 461 of cement DSM columns with a diameter of 0.8 m and length varying between 5 to 9.2 m were constructed below the foundation slab. By

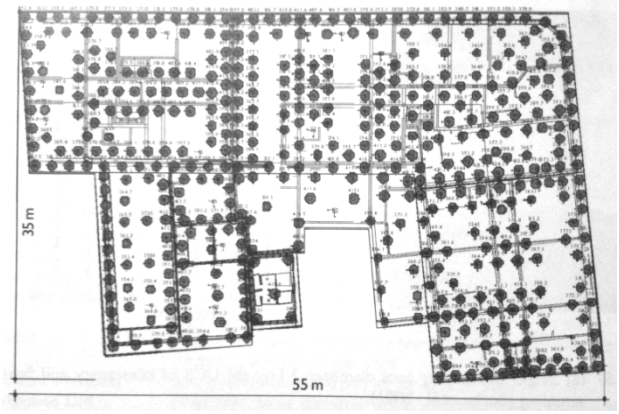

(a)

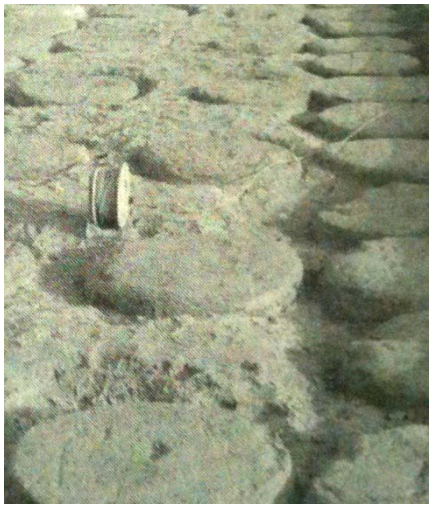

(b)

Figure 2.6 DSM improved foundation for a multistory building in Poland: (a) arrangement of DSM columns; (b) constructed DSM columns (Topolnicki, 2004)

improving the soil using DSM, the vertical settlement of the building was able to be controlled within 10 mm.

2.3 Available Analysis Methods for Laterally Loaded Piles

Having assessed the different ground improvement techniques in current engineering practice, the next step is to examine the available analysis methods for lateral loaded piles so that the ability of each method for determining lateral response of a pile embedded in a volume of improved soil surrounded by unimproved soil can be assessed.

Research on analysis of laterally loaded piles started more than five decades ago. As a consequence of such sustained research, there are a number of analysis methods available that can be used for design of pile foundations. Broadly, the methods of analysis can be classified into three approaches: 1) beam-on-Winkler foundation approach, 2) elastic continuum approach, and 3) finite element approach.

2.3.1 Beam-on-Winkler Foundation Method

Long before the research on laterally loaded pile started, foundation engineers had looked into the possibility of representing shallow foundations that are long and flexible enough (e.g., strip footings) as beams resting on foundations. In the context of beam-on-Winkler foundation approach, the beam represents the foundation (e.g., footings, piles etc.) and the foundation represents the soil mass. As early as 1867, Winkler (1867) proposed that the vertical resistance of a ground against external forces can be assumed to be proportional to the ground deflection. By extending this idea, researchers represented the ground with a series of elastic springs so that the compression (or extension) of the spring, which is the same as the deflection of the ground, is proportional to the applied

load. The spring constant represents the stiffness of the supporting ground against the applied loads.

This concept was extended by placing an Euler-Bernoulli beam on top of the elastic foundation and applying loads on top of the beam (Figure 2.7). Hetenyi (1946) presented solutions for beams on foundation with linear response with a fourth-order differential equation governing the beam deflection. The input parameters required are the elastic modulus and geometry of the beam, the spring constant of the foundation (soil) and the magnitude and distribution of the applied load. As a result of the analysis, the beam deflection, bending moment and shear force along the span of the beam can be determined.

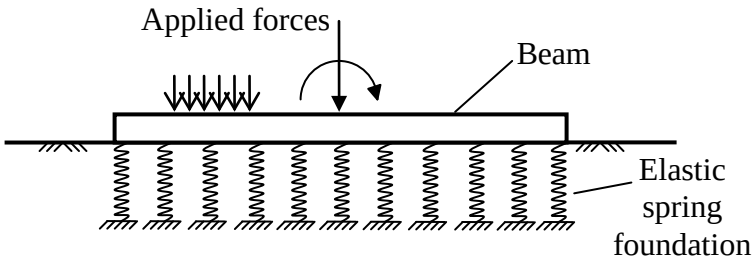

Figure 2.7 Beam on an elastic foundation

The beam-on-Winkler foundation approach can also be called subgrade-reaction approach because the foundation spring constant can be related to the modulus of subgrade reaction of a soil mass (Terzaghi, 1955). Terzaghi suggested values of the subgrade modulus that can be used in the standard beam equation, which was developed earlier by Hetenyi, to solve for deflection and bending moment, but he failed to give any experimental data or analytical procedure to validate his recommendations.

The beam-on-foundation concept was later adapted by the researchers on laterally loaded piles because, in most cases, the piles behave as flexible beams against lateral

(transverse) loads and the problem can be looked upon as a beam-on-Winkler foundation rotated by 90° (Figure 2.8). Matlock and Reese (1960) presented a generalized iterative solution method for rigid and flexible laterally loaded piles embedded in soils with two forms of varying modulus with depth. Davisson and Gill (1963) investigated the case of a laterally loaded pile embedded in a layered soil system with a constant (but different) modulus of subgrade reaction for each layer, but it was varied between layers. They concluded that the near surface modulus was the controlling factor for the pile response, and that soil investigations and characterization should be focused in this zone. In classic companion papers, Broms (1964a, b) described a method for analyzing lateral pile response in cohesive and cohesionless soils. His method for computing ground surface deflections of rigid and flexible fixed and free head piles was based on a modulus of subgrade reaction using values suggested by Terzaghi (1955). For undrained loading, Broms designated that a constant subgrade modulus be used with a value of $9S_u$ for the ultimate lateral soil resistance, where S_u is the undrained shear strength of the soil. For drained loading cases, a subgrade modulus linearly increasing with depth was specified and a Rankine earth pressure-based method was used for computing an ultimate resistance assumed equal to $3K_pD_p\sigma'_v$, where K_p is the passive lateral earth pressure coefficient, D_p is the pile diameter, and σ'_v is the effective vertical stress of the soil layer.

However, the problem of laterally loaded pile is more complex because soils in real field situations behave nonlinearly, particularly that surrounding the top part of the pile. The linear springs, as hypothesized by Winkler (1867), could no longer be used for laterally loaded piles, and were replaced by nonlinear springs (for which the value of the spring constant changes with pile deflection). As a result, the governing fourth order

differential equation became nonlinear and the finite difference method was used to iteratively solve the equation (McClelland and Focht, 1958).

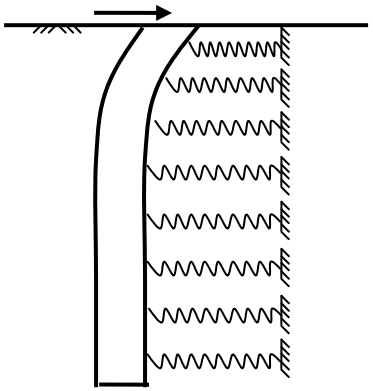

Figure 2.8 A laterally loaded pile modeled with a bed of springs

Further modification of the beam-on-Winkler foundation approach led to the p-y method, in which the soil around the pile is replaced by a set of mechanisms that merely indicate the soil resistance *p* is a nonlinear function of pile deflection *y* (Figure 2.9). McClelland and Focht (1958) can be said to be the originators of the *p-y* method of laterally loaded pile analysis. They proposed a procedure for correlating triaxial stress-strain data to *p-y* curve at discrete depths and estimating the modulus of subgrade reaction at each layer.

In a series of reports to Shell Development Company, Matlock and his co-workers conducted static and cyclic field and laboratory tests of laterally loaded piles in soft clay. He described the *p-y* concept as the relationship that relates the soil resistance "*p*" arising from the non-uniform stress field surrounding the pile mobilized in response to a lateral soil displacement "*y*" (see Figure 2.10). For a single pile, a family of *p-y* curves can be described; their stiffness will typically increase with depth. In 1970, Matlock proposed

procedures for constructing *p-y* curves of soft clay under static and cyclic loading (described in Chapter 3) and is codified in the API Recommended Practice (API, 1993).

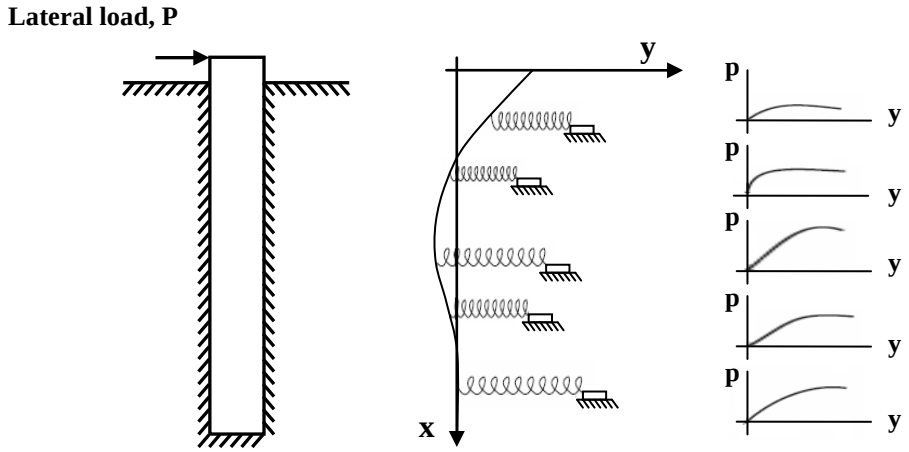

Figure 2.9 Model of a pile subjected to lateral loading with *p-y* curves (Ensoft, Inc. 2004)

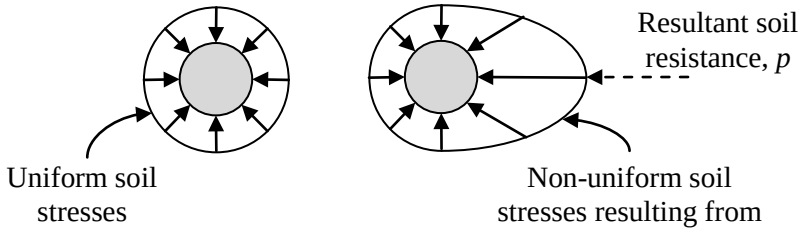

Figure 2.10 Distribution of soil stresses surrounding a pile: (a) before, and (b) after lateral deflection (after Thompson, 1977)

The API recommended method for constructing p-y curves in sand was the result of work by Reese et al. (1974) from the results of static and cyclic lateral load tests. In their method, the ultimate soil resistance was determined from the lesser of two expressions reflecting shallow wedge failure and deep flow failure geometries, and modified for pile diameter, depth, and loading regime. Perhaps Reese's most influential contribution has been the introduction of the computer programs COM624P (Reese, 1984) and LPILE (Reese and Wang, 1989), first presented as COM622 in Reese (1977). These

analytical tools provide highly efficient platforms for *p-y* analysis of static and cyclic laterally loaded piles in layered soils.

Over the years, many other different *p-y* curves have been developed for different soil and/or ground conditions. Georgiadis (1983) proposed a method of constructing *p-y* curves for layered soil by introducing an equivalent depth of all the layers existing below the upper layer. Ismael (1990) presented an approach for computing *p-y* curves for soil with both cohesion and a friction angle by using an approximate ultimate resistance of *c-φ* soils recommended by Evans and Duncan (1982). Modifications to *p-y* curves for sloping ground, weak rock and effect of inclinations of the pile are also available now for lateral loaded pile analysis using beam-on-Winkler foundation approach.

Using the p-y method of Winkler analysis, pile deflection can be estimated as a function of applied load under working load conditions. In other words, designs against the serviceability limit state of tolerable lateral deflection can be done using this method. Since the serviceability limit state is the primary concern in the design of laterally loaded piles, the beam-on-Winkler foundation approach has become the most widely used analysis method for calculating the response of lateral loaded piles. However, there is a singular disadvantage exists. The one-dimensional simplification of the soil-pile model ignores the radial and three-dimensional components of interaction. This deficiency limits the p-y curves to only representing homogeneous soil at each depth along the pile length, and therefore the analysis of pile foundations embedded in a volume of improved soil surrounded by unimproved soil cannot be directly achieved by using the *p-y* method.

2.3.2 Elastic Continuum

Analysis of laterally loaded piles is done by treating the soil surrounding the pile as a three-dimensional continuum. Such an approach is conceptually more appealing than the beam-on-Winkler foundation approach because the interaction of the pile and the soil is indeed three-dimensional in nature. The elastic continuum analytical method is based on Mindlin's (1936) closed form solution for the application of point loads to a semi-infinite mass. The accuracy of these solutions is directly related to the evaluation of the Young's modulus and the other elastic parameters of the soil.

Research in this direction was pioneered by Poulos (1971a, b), who treated the soil mass as an elastic continuum and the pile as a strip, which applied pressure on the continuum. Referring to Figure 2.11, the pile in Poulos's elastic continuum approach is divided into $n + 1$ elements with equal length. Each element is acted upon by a uniform horizontal pressure p, which is assumed constant across the width of the pile. By equating the horizontal displacements of the soil and pile at the center of each elements, Poulos derived the expression for soil displacements at all points along the pile as:

$$\{\rho_s\} = \frac{d}{E_s}[I_s]\{p\} \tag{2.1}$$

where, d = diameter of the pile;

E_s = Young's modulus of the soil;

$\{\rho_s\}$ = $n + 1$ column vector of horizontal soil displacement;

$\{p\}$ = $n + 1$ column vector of horizontal loading between soil and pile; and

$[I_s]$ = $n + 1$ by $n + 1$ matrix of soil-displacement-influence factors, which the elements I_{ij} of $[I_s]$ are evaluated by integration over a rectangular area of

the Mindlin equation for the horizontal displacement of a point within a semi-infinite mass caused by horizontal point-load with the mass.

In determing the pile displacements, Poulos obtained the following equation using the differential equation for bending of a thin beam:

$$-\{p\} = \frac{E_p I_p n^4}{dL^4}[D]\{\rho_p\} + \frac{E_p I_p}{dL^4}\{A\} \tag{2.2}$$

where, $E_p I_p$ = flexural rigidity of the pile;

L = the total length of the pile;

$\{\rho_p\}$ = the n - 1 column vector of pile displacements;

$[D]$ = $n + 1$ by $n + 1$ matrix of finite deference coefficients;

$$[A] = \begin{Bmatrix} \frac{ML^2}{n^2 E_p I_p} \\ 0 \\ 0 \\ \vdots \\ 0 \end{Bmatrix}_{n-1} .$$

The soil and pile displacements from Eqs. (2.1) and (2.2) can be equated, and the resulting equations, together with the appropriate equilibrium equation, the displacements can be solved for different boundary conditions at the top of the pile. Poulos and Davis (1980) presented a comprehensive set of analysis and design methods for pile foundations based on analysis method presented above. Poulos (1982) described a procedure for degradation of soil-pile resistance under cyclic lateral loading and compared it to several case studies. However, the method is less popular than the *p-y* method, most likely because the analysis steps are relatively involved.

Other elastic continuum-based analysis methods are also available (Baguelin et al., 1977; Pyke and Beikae, 1984; Lee et al., 1987; Lee and Small, 1991; Sun, 1994a; Guo

and Lee, 2001; Einav, 2005; Basu, 2006). Due to the three-dimensional nature of this analysis method, the ability of analyzing pile foundations embedded in a volume of improved soil surround by unimproved soil is enabled. However, the analysis steps in this type of approach are always relatively involved and more complex comparing to the *p-y* method. As a result, complicated mathematical solution techniques are required within the analysis, which do not provide simple, practical steps for obtaining pile deflection as a function of applied load under working condition. Furthermore, the methods are limited in the sense that nonlinear soil-pile behavior is difficult to incorporate, which does not represent the real field situations, and therefore the elastic continuum method is rarely used by practitioners.

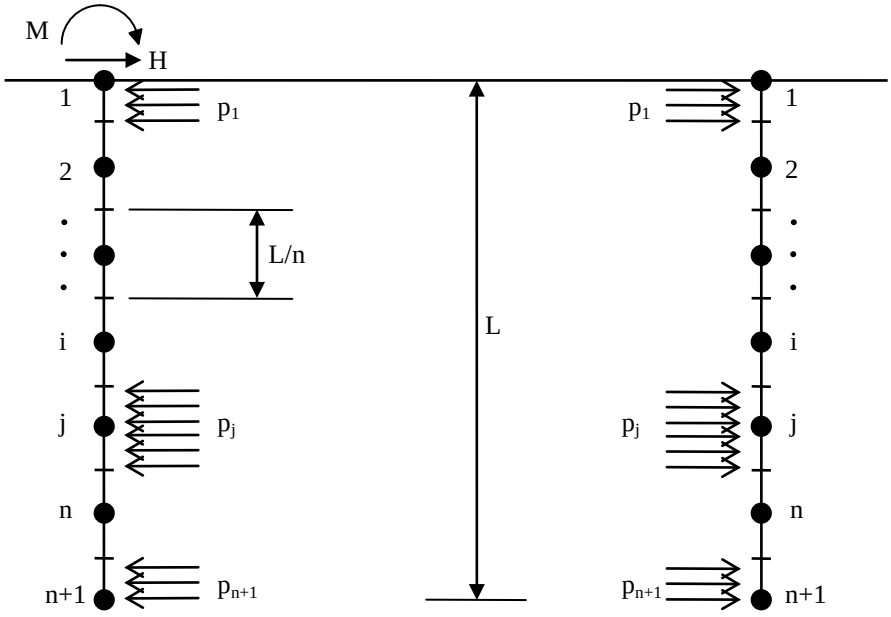

(a) Pile (b) Soil adjacent to pile

Figure 2.11 Poulos elastic analysis model for laterally loaded floating pile (Poulos and Davis, 1980)

2.3.3 Finite Element

The finite element method potentially provides the most powerful means for conducting soil-foundation-structure-interaction (SFSI) analyses. The advantages of a finite element approach include the capability of performing the SFSI analysis of pile or pile groups in a fully-coupled manner, without resorting to independent calculations of site or superstructure response for even the complex dynamic loadings, or application of pile group interaction factors. At the same time, it is possible to model any arbitrary soil profile and to study the 3-D effects.

Yegian and Wright (1973) implemented a two-dimensional finite element analysis with a radial soil-pile interface element that described the nonlinear lateral pile response of single piles and pairs of piles subjected to static loading. Desai and Appel (1976) presented a three-dimensional finite element solution with interface elements for the laterally loaded pile problem. Thompson (1977) used a plane-stress finite element model and obtained soil-response curves that agreed well with results near the ground surface from full-scale experiments. Trochianis et al. (1988) investigated nonlinear monotonic and cyclic soil-pile response in both lateral and axial modes with a three-dimensional finite element model of single and pairs of piles, incorporating slippage and gapping at the soil-pile interface. They deduced a simplified model accommodating pile head loading only. Koojiman (1989) described a quasi-three-dimensional finite element model that substructured the soil-pile mesh into independent layers with a Winkler type assumption. Brown et al. (1989) obtained *p-y* curves from three-dimensional finite element simulations that showed only fair comparison to field observations. Wong et al. (1989) modeled soil-drilled shaft interaction with a specially developed three-

dimensional thin layer interface element. Bhowmik and Long (1991) devised both two-dimensional and three-dimensional finite element models that used a bounding surface plasticity soil model and provided for soil-pile gapping. Brown and Shie (1991) used a three-dimensional finite element model to study group effects on modification of *p-y* curves. Portugal and Seco e Pinto (1993) used the finite element method based on *p-y* curves to obtain a good prediction of the observed lateral behavior of the foundation piles of a bridge in Portugal. Cai et al. (1995) analyzed a three-dimensional nonlinear finite element subsystem model consisting of substructured solutions of the superstructure and soil-pile systems.

Research is continuing with three-dimensional, nonlinear finite elements; however no proposals have been made for a practical method of design due to the different challenges associated with the successful implementation of this analysis technique. Providing appropriate soil constitutive models that can model small to very large strain behavior, rate dependency, degradation of resistance, and still prove practical for use is essential in developing results that can be used in practice, while special features to account for pile installation effects and soil-pile gapping should also be implemented.

2.4 Lateral Loaded Piles in Soft Clay with Ground Improvement

Over the years, a significant amount of studies have been completed on the topics of laterally loaded pile foundations and ground improvement techniques in separate topics, however, the investigations of laterally loaded piles in soft clay and improved soils are still scarce despite the widespread presence of the soft clay soil in high seismic regions and the frequent need to locate bridges and buildings in this soil type. Limited

work (Basack and Purkayastha 2007; Levy et al. 2007) has been recently carried out by the offshore community to examine the pile foundations in soft clays under cyclic loading. Their work reveals that the lateral load capacity of pile foundations in soft clay degrades with cyclic loading. Lok (1999) and Mayoral et al. (2005) measured *p-y* curves for a pile in an artificial soft clay. Wilson et al. (1997a&b) and Boulanger et al. (1999) studied seismic behavior of a soft clay overlying dense sand using centrifuge tests and analysis. Again, no ground improvement effects were considered in the above-listed researches. Only recently, a few investigations have been carried out to guide engineers in evaluating the effectiveness of the ground improvement on increasing the lateral resistance of pile foundation embedded in soft clay.

2.4.1 Tomisawa and Miura (2007)

Tomisawa and Nishikawa (2005a, 2005b) developed a practical foundation design method, in which the ground was improved around the heads of the pile foundations in soft ground and ground subjected to liquefaction. In this method, the increased shear strength of the improved soil is reflected in the horizontal resistance. The construction method studied uses a combination of pile foundation construction together with common ground improvement methods including deep mixing, preloading and sand compaction piling; and is referred to as the composite ground pile method. In this study, the authors presented a design procedure for the composite ground pile method for establishing the range of influence of the horizontal resistance of piles. The necessary range of ground improvement was proposed to be a three-dimensional domain formed with the gradient of the surface of passive failure $\theta = (45° + \frac{\varphi}{2})$, where φ is the angle of shear resistance of soil, from the depth of the characteristic length of pile, *1/β*, which is the depth of

influence of the horizontal resistance of piles on the basis of the limit equilibrium and the Mohr-Coulomb failure criterion. As a result, the necessary range of improvement can be set as a three-dimensional inverted cone shape centered on the pile. However, it should be recognized that it is difficult to conduct ground improvement in a cone shape. A cubic body covering the range of the invert cone shape shown in Figure 2.12 was proposed by the authors for the range for ground improvement.

A series of dynamic centrifuge model tests was conducted in this study to evaluate the earthquake resistance of the composite ground pile. Figure 2.13 shows the setup of the test model. A 50 g centrifugal acceleration field was adopted for the test to create a 1:50 model to prototype scale on the stress level. A model pile with outer

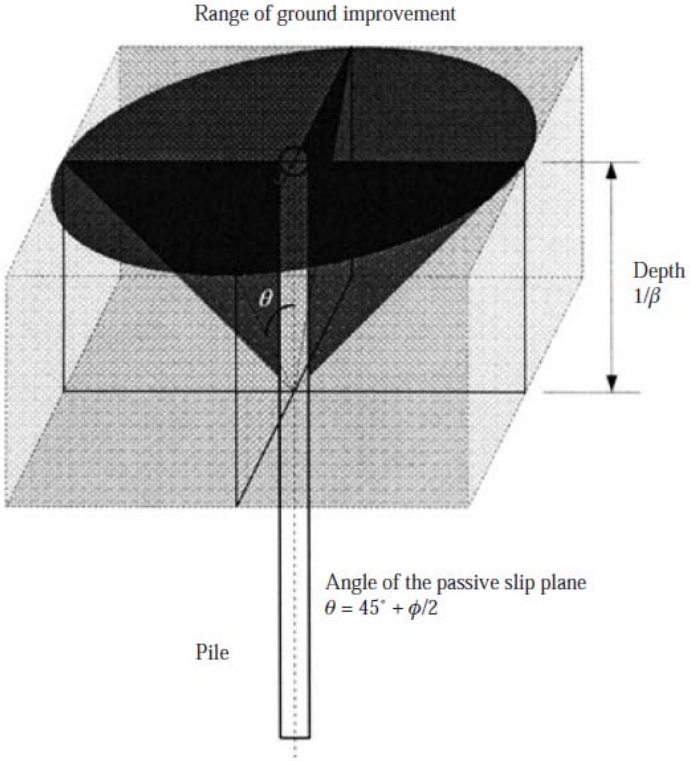

Figure 2.12 The proposed range of ground improvement region subjected by Tomisawa and Miura for laterally loaded pile (2007)

diameter of 0.01 m, and thickness of 0.002 m, and pile length of 0.4 m was made from steel pipe to simulate a prototype steel pile with outer diameter of 0.5 m and thickness of 0.01 m in the centrifugal acceleration field. A steel block with a weight of 3.92 N (equivalent to 490 kN at the prototype scale) was fixed to the pile head to simulate the substructure. To form the test soils, a single layer of dry kaolin clay was prepared to simulate the uniform soft ground, and the improved ground was prepared by replacing kaolin clay with Toyoura sand in the area around the pile head to simulate ground improvement using sand compaction pile with a relatively high improvement rate. Table 2.1 shows the properties of kaolin clay and Toyoura sand.

A sine-wave was used as input motion for the shaking tests. The acceleration level of the input motion was set as 10 m/s^2 (equivalent to 20 g at the prototype scale) to

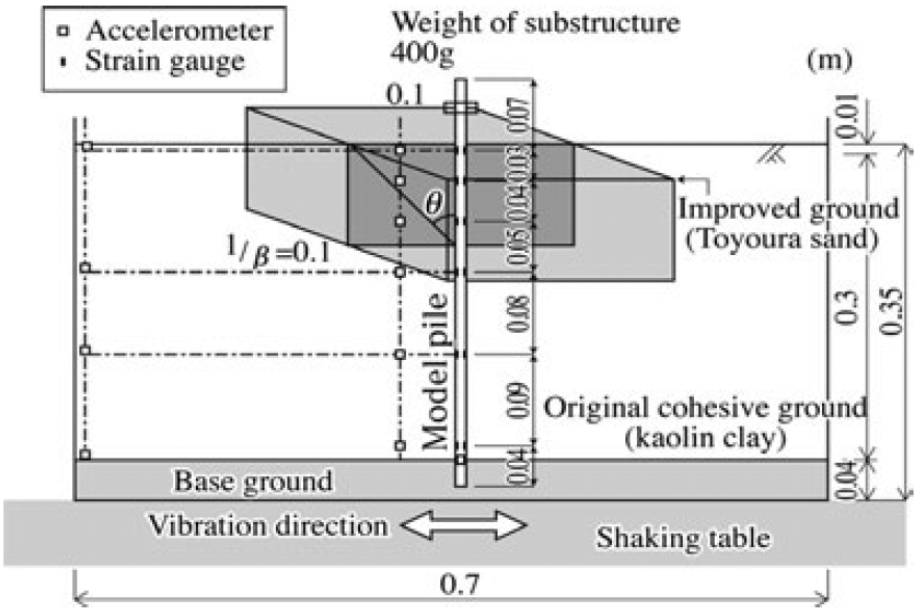

Figure 2.13 Composite-ground-pile model setup for the centrifuge shaking test conducted by Tomisawa and Miura, all units are in meters (2007)

Table 2.1 Physical properties of kailin clay and Toyoura sand

		Kaolin clay	Toyoura Sand
Unit weight	kN/m^3	10.101	15.574
Particle percentage			
Sand	%	-	97.3
Silt	%	50.3	0.8
Clay	%	49.7	1.9
Cone index q_c	MN/m^2	1.0	3.3

simulate the behavior of the pile and ground over a small range of deformation. From the data obtained during shaking, the following conclusions were made by the authors:

- the maximum displacement of the piles in the improved ground using Toyoura sand was 1/6 of that of piles in uniform ground of kaolin clay;
- the maximum bending moment occurred within the range of depth $1/\beta$ was 1/2.5 of that in uniform ground of kaolin clay and converged within the range f improved ground with Toyoura sand;
- by using ground improvement around the pile head, a certain amount of earthquake resistance that restricts pile displacement and bending moment against earthquake motion was achieved, though careful attention should be paid to the shortening of the natural frequency of pile foundations in improved ground.

2.4.2 Rollins et al. (2010)

Rollins et al. (2010) performed several lateral load tests on a full-scale pile cap in untreated virgin soft clay (Figure 2.14) along with pile groups involving (a) excavation and replacement with sand backfill (Figure 2.15), (b) a soilcrete wall along the side of the pile group (Figure 2.16), and (c) a jet grouted zone below the pile cap (Figure 2.17). The soil profile at the test site consists predominantly of cohesive soils; however, some thin

sand layers were located throughout the profile. The cohesive soils near the ground surface were classified as CL or CH materials with plasticity indices of about 20 to 25. In contrast, the soil layer from a depth of 4.5 to 7.5 m consists of interbedded silt (ML) and sand (SM) layers. The water table was at a depth of 0.6 m.

The pile group consisted of nine test piles which were driven in a 3 x 3 orientation with a nominal center to center spacing of 0.9 m. The test piles were 324 mm OD pipe piles with 9.5 mm thickness and they were driven closed-ended to a depth of approximately 13.4 m below the ground surface. The steel conformed to ASTM A252 Grade 2 specifications with a yield strength of 400 MPa and moment of inertia of 14,235 cm^4. The steel pipe piles were filled with concrete which had an average unconfined compressive strength of 34.5 MPa. A 2.84 m x 2.75 m rectangular concrete pile cap was constructed by excavating 0.76 m into the virgin clay with steel reinforcing mats placed in the top and bottom of each cap. A 0.55 m tall and 1.22 m wide concrete corbel was constructed on top of each cap to allow the lateral load to apply above the ground surface without affecting the soil around the pile cap.

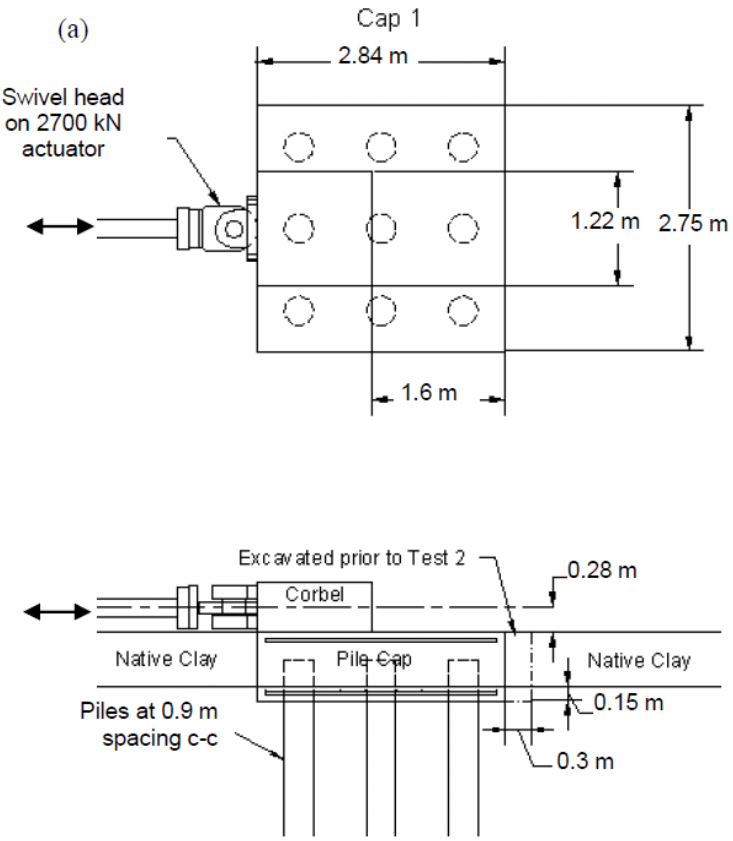

Figure 2.14 Plan and profile drawings of pile groups in untreated virgin clay (Rollins et al., 2010)

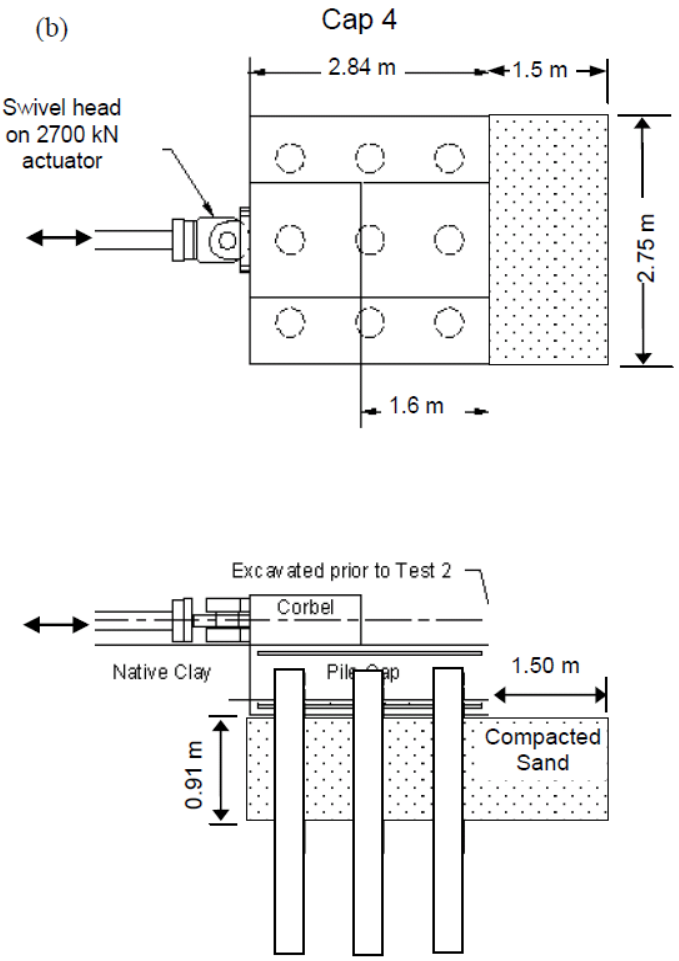

Figure 2.15 Plan and profile drawings of pile groups with compacted sand (Rollins et al., 2010)

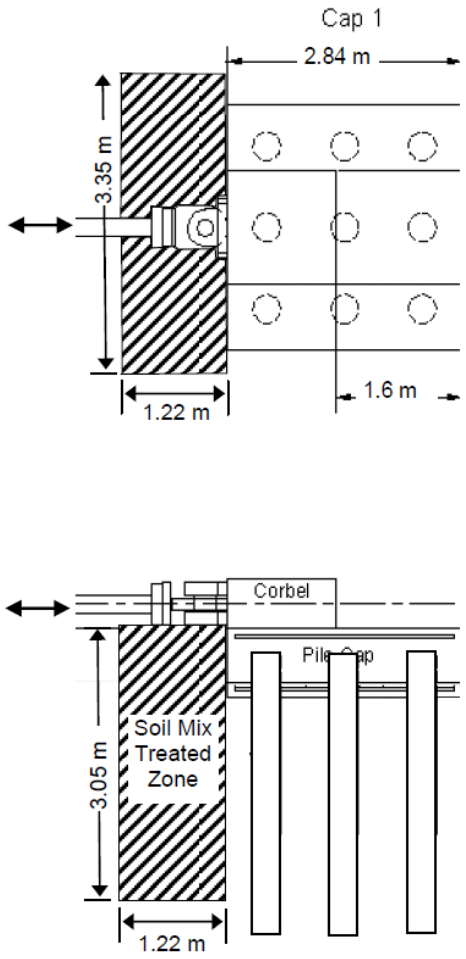

Figure 2.16 Plan and profile drawings of pile groups with soil mixed treated wall on one side (Rollins et al., 2010)

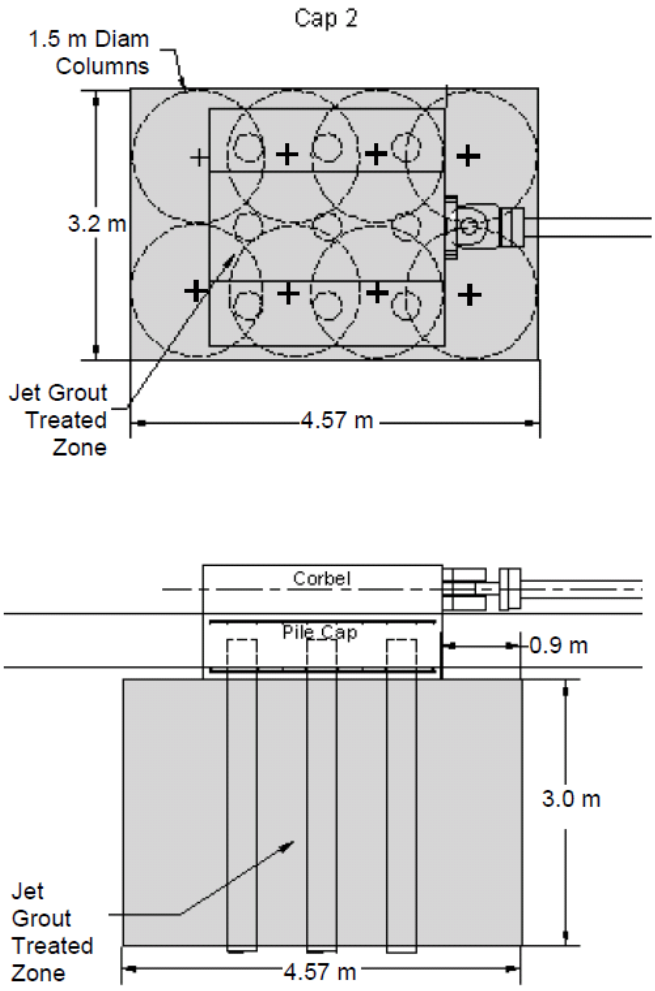

Figure 2.17 Plan and profile drawings of pile groups with jet grout tratmet under the pile cap (Rollins et al., 2010)

The lateral pile group load tests were conducted using one or two 2700 kN hydraulic actuators to apply load to the pile group. A displacement control approach was used for the tests with target pile cap displacement increments of 3, 6, 13, 19, 25 and 38 mm. During this process the actuator extended or contracted at a rate of about 40 mm/min. In addition, at each displacement increment 10 cycles with a peak pile cap amplitude of ±1.25 mm were applied with a frequency of approximately 1 Hz to evaluate dynamic response of the pile cap.

In completing the analysis of the test results, the following conclusions are drawn by the authors:

- excavation and replacement of about 1 m of clay with compacted sand (94% relative compaction) led to an 18% increase in lateral resistance of the pile group relative to the pile group in untreated soil;
- mass mixing with a cement content of approximately 200 kg/m^3 (i.e., 10% by weight) was able to increase the compressive strength of a soft, plastic clay from a value between 40 to 60 kPa to an average of 970 kPa while jet grouting with a cement content of about 400 kg/m^3 produced an average compressive strength of 3170 kPa;
- construction of a mass mixed “soilcrete” wall adjacent to an existing pile cap increased the lateral resistance and initial stiffness of the pile group by about 65%;
- construction of eight 1.5 m diameter jet grout columns around the pile group increased the lateral pile group resistance to 3475 kN relative to the 1253 kN resistance for the pile group in untreated virgin clay, which represented an increase in lateral resistance of about 180%;
- jet grouting treatment of the pile group also increased the lateral stiffness of the pile group from 140 kN/mm to 700 kN/mm, which is an increase of 400%;
- soil improvement technique, such as soil mixing and jet grouting, provide the opportunity to significantly increase the lateral resistance of existing pile group foundations with relatively little investment of time, effort and expense relative to approaches that rely on incorporating additional structural elements.

2.4.3 Kirupakaran et al. (2010)

An analytical investigation was conducted by Kirupakaran et al. as a part of current project using a fully coupled finite element computer code TeraDysac to study the seismic behavior of pile foundations with varying degrees of the cement-deep-soil-mixing (CDSM) soil improvement around. In this study, a planned centrifuge model test of single pile foundations with various extents of CDSM improvement in saturated soft clay was selected for the analysis in TeraDysac. Figure 2.18 shows the centrifuge model with the prototype dimensions. The soil profile consists of approximately 10 m of soft clay underlain by 8 m of dense sand. Table 2.2 and 2.3 list the soil parameters used in the analysis. Four single piles with an outside diameter of 0.36 m, pile length of 16.4 m and density of 2500 kg/m^3 were simulated with various extents of CDSM around the piles as shown in Figure 2.12. The above ground piers were 1.5 m long and have the same diameter and density of the piles. A mass of 7630 kg was used to simulate the superstructures on top of the piers. All the structural elements had a Young's modulus of 24.1 GPa.

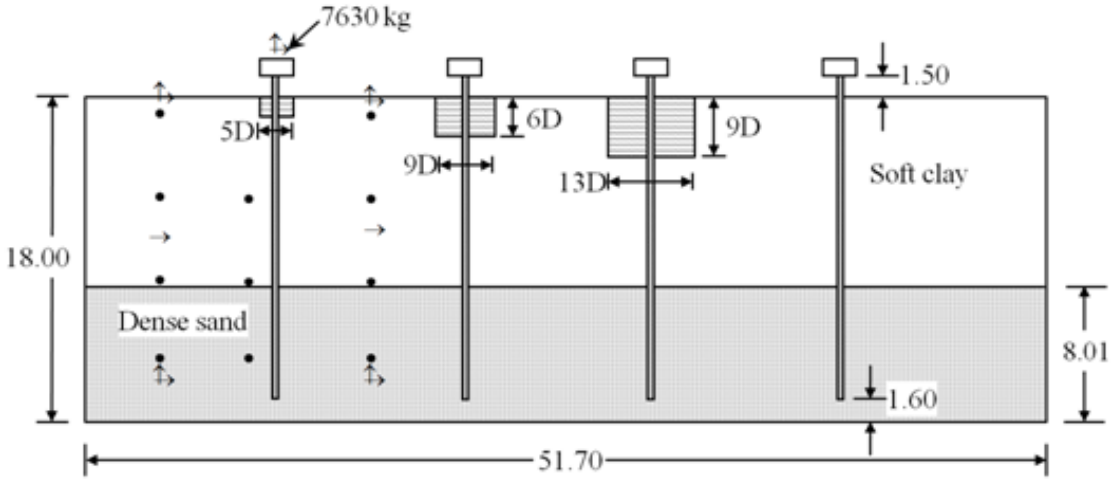

Figure 2.18 Centrifuge model, all units are in meters (Kirupakaran et al., 2010)

Table 2.2 Model parameters of soft and improved clays used by Kirupakaran et al. for TeraDysac analysis (2010)

Parameter	Soft Clay	Improved Clay
Slope of the isotropic consolidation line on $e - \ell n\ p'$ plot (λ)	0.182	0.015
Slope of an elastic rebound line on $e - \ell n\ p'$ plot (κ)	0.026	0.002
Slope of the critical state line in $q - p'$ space (compression) (M_c)	0.984	2.952
Permeability (m/s)	9.26×10^{-10}	1.85×10^{-10}

Table 2.3 Other model parameters and soil properties used by Kirupakaran et al. for TeraDysac analysis (2010)

Parameter	Value
Initial void ratio (e_0)	1.20
Specific gravity	2.70
Traditional Model Parameters	
Poisson's ratio (ν)	0.30
Ratio of extension to compression value of M (M_e / M_c)	1.00
Bounding Surface Configuration Parameters	
Value of parameter defining the ellipse1 in compression (R_C)	2.40
Value of parameter defining the hyperbola in compression (A_C)	0.01
Parameter defining the ellipse 2 (tension zone) (T)	0.01
Projection center parameter (C)	0.00
Elastic nucleus parameter (S)	1.00
Ratio of triaxial extension to compression value of R (R_e / R_c)	0.92
Ratio of triaxial extension to compression value of A (A_e / A_c)	1.20
Hardening Parameters	
Hardening parameter (m)	0.02
Shape hardening parameter in triaxial compression (h_c)	3.00
Ratio of triaxial extension to compression value of h (h_e/h_c)	1.00
Hardening parameter on I-Axis (h_o)	2.00

The finite element mesh and the base motion used for the analysis are shown in Figure 2.19 and 2.20, respectively. The soil was modeled using four-noded quadrilateral (2-D) and eight-noded brick (3-D) isoparametric elements and the piles were modeled with Timoshenko beam elements.

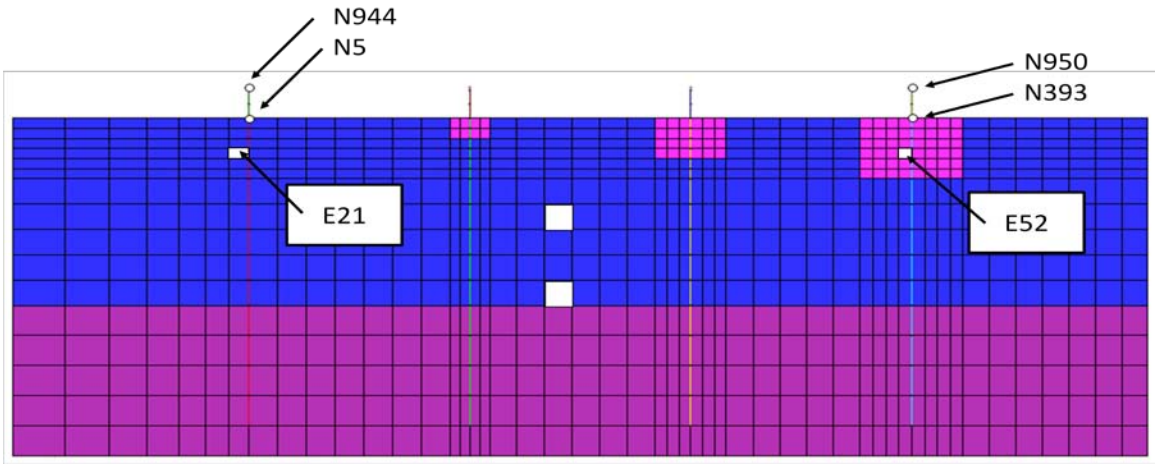

Figure 2.19 Finite element mesh generated by TeraDysac (Kirupakaran et al., 2010)

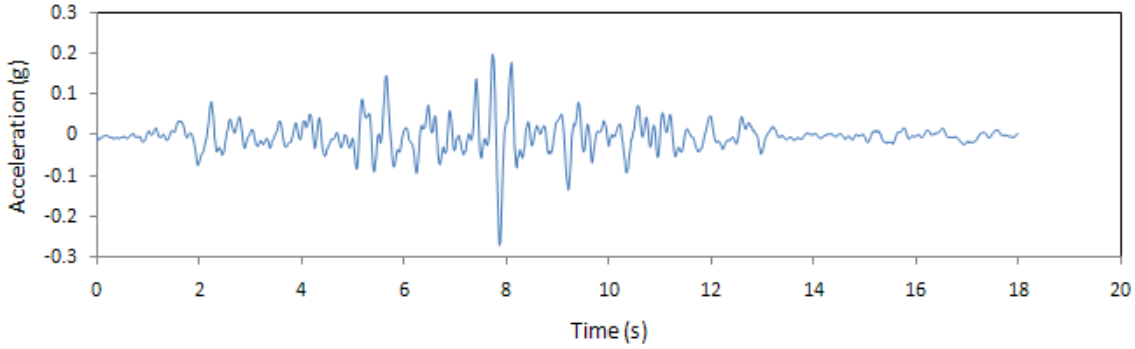

Figure 2.20 Horizontal base motion (Kirupakaran et al., 2010)

The following observations were made by the authors based on the finite element simulations:

- comparing to the unimproved clay, the CDSM improved clay around Pile 4, i.e. the pile with largest extent of CDSM improvement, reduced the maximum superstructure and ground surface displacements by about 2 cm and 1 cm, respectively;

- excess pore pressure increases are predicted by the fully coupled computer code TeraDysac within the improved and unimproved clay; the pore pressure increases are, however, substantially larger within the unimproved clay;
- CDSM ground improvement, however, increased the bending moments within the piles according to the analysis results.

2.4.4 Summary

Although soil improvement techniques have the potential for being more cost-effective and reducing construction time, only a few tests (Tomisawa and Miura, 2007; Rollins et al., 2010) have been performed to guide engineers in evaluating the actual effectiveness of this approach on improving the lateral resistance of pile foundations. In addition, numerical models to evaluate this approach have not been validated (Kirupakaran et al., 2010). As a result, the main objective of the current study is to develop a numerical method to evaluate the effectiveness of the soil improvement on laterally loaded piles, and validate the method through experimental testing.

CHAPTER 3. FORMULATION OF WINKLER ANALYSIS USING P-Y METHOD FOR LATERALLY LOADED PILES IN IMPROVE SOIL SURROUNDED BY SOFT CALY

3.1 Objective

The preceding chapter included an overview of the current practice of ground improvement techniques, available analysis methods for SFSI problems, and the recent investigations on improving pile performance in soft clay through ground improvement. The discussion concluded that both elastic continuum and finite element approaches has the ability to analyze laterally loaded piles embedded in a volume of improved soil surrounded by soft clay. However, computational cost of these fully coupled analysis methods is expensive and do not provide simple, practical steps for use in routine design practice. Furthermore, no numerical models have been verified in conducting analysis that can be used in evaluating the effectiveness of soil improvement on laterally loaded piles. Therefore, the objective of this project is to develop modified *p-y* curves for use in the Winkler analysis, which is a simplified approach to conduct lateral SFSI analyses, to characterize the lateral load behavior of a pile in improved soil surrounded by soft clay.

3.2 General Concept of the Winkler Analysis Method

In the Winkler analysis method, pile and its surrounding soils are divided into a number of discrete layers, as shown in Figure 3.1. The pile is represented by a series of beam-column elements, which are characterized by the moment resistance and corresponding bending stiffness, E_pI_p, where E_p is the modulus of elasticity of the pile

and I_p is the moment of inertia of the pile cross-section. The soil surrounding the pile is replaced by a set of mechanisms that merely indicate that the soil resistance p is a nonlinear function of pile deflection y. The mechanisms, and the corresponding p-y curves that represent their behavior, are considered to vary continuously with depth.

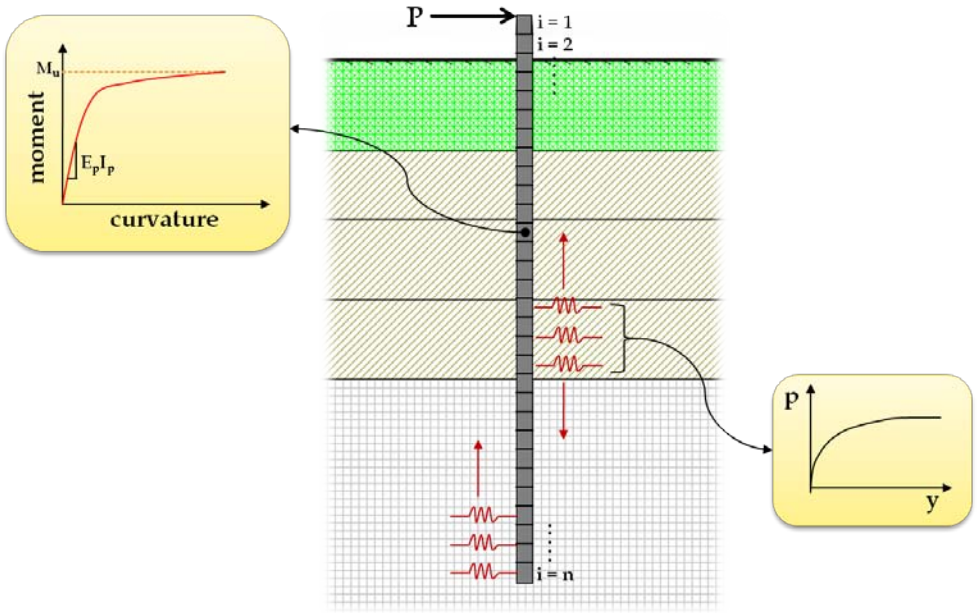

Figure 3.1. Model for pile under lateral loading with Winkler analysis method

By defining the moment-curvature response of the pile sections, the p-y curves of surrounding soils, and the appropriate boundary conditions at top and bottom of the pile, the nonlinear responses of a lateral loaded pile can be determined by solving the standard beam-column equation, Eq.(3.1). This fourth-order differential equation is developed by Hetenyi (1946) based on the structural equilibrium in a beam-column element shown in Figure 3.2.

$$E_p I_p \frac{d^4y}{dx^4} + P_x \frac{d^2y}{dx^2} - p = 0, \qquad p = -k_{py} y \tag{5.1}$$

where E_pI_p = bending stiffness of the pile foundation;

y = lateral deflection of the pile and soil at point x along the length of the pile;

P_x = axial load on the pile foundation;

p = soil resistance per unit length; and

k_{py} = the secant soil modulus of the soil-resistance curve.

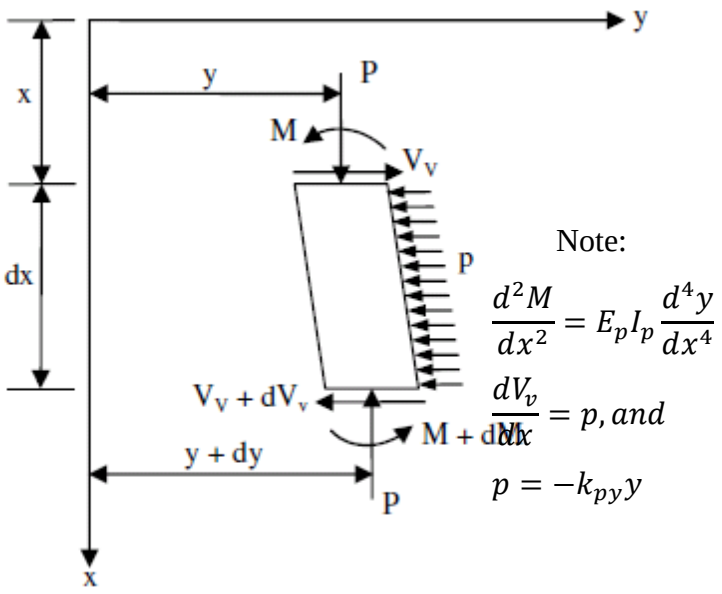

Figure 3.2. Element from beam-column (after Hetenyi 1946)

Furthermore, the finite difference method can be employed for general solution of the beam-beam column equation, which allows E_pI_p to be nonlinear and a function of the computed values of bending moment. An axial load can also be considered in the solution with respect to its effect on bending but not in regard to computing the required length to support a given axial load.

3.3 Current Recommendations on p-y Curves for Clay Soil

For the Winkler analysis concept presented in the preceding section, a key component is to accurately define the resistance of the soil surrounding the pile foundation through use to the *p-y* curves. To commence the development of modified *p-y* curves for a volume of CDSM-improved soil surrounded by soft clay, the current

recommendations for obtaining *p-y* curves for clay soils are studied in the subsequent sections as the starting point. These recommendations are developed based on the results of full-scale experiments with instrumented piles and have been used extensively in the design of pile-supported offshore platforms. In these experiments, bending moment was accurately measured by the use of strain gauges. The deflection of the pile can be obtained by two integrations of the moment curves, while the computation of the soil resistance was achieved by taking two differentiations of the moment curves. With families of curves showing the distribution of deflection and soil resistance, *p-y* curves was plotted by the investigators to develop the recommendations presented in the subsequent sections. Verifications of the suggested procedures of obtaining *p-y* curves were made by back calculating the bending-moment curves using the computed *p-y* curves. The computed bending moments was in close agreement with those from experimental testing.

3.3.1 Response of Piles in Soft Clay

Matlock (1970) performed lateral-load tests on full-scaled steel-pipe piles in soft clay near Lake Austin, Texas. After analyzing series of experimental data, this researcher proposed procedures for constructing *p-y* curves of soft clay under short-time static loading and cyclic loading as illustrated by Figure 3.3. The detailed procedures can be summarized as follows:

- For short-term static loading condition (as illustrated in Figure 3.3 (a)):
    1. Obtain the best possible estimate of the variation of undrained shear strength, c_u, effective unit weight, γ, and the strain corresponding to one-half the

maximum principal stress difference, ε_{50}. If stress-strain curves are unavailable, a typical value of 0.02 may be used.

2. Compute the ultimate soil resistance per unit length of pile, using the smaller of the values calculated by the following equations:

$$p_{ult} = \left[3 + \frac{\gamma}{c_u} z + \frac{J}{b} z\right] c_u b \tag{5.2}$$

$$p_{ult} = 9 c_u b \tag{5.3}$$

where z = depth from the ground surface to *p-y* curve;

J = coefficient of geometrically related restraint, which should be taken as 0.5;

b = width or diameter of pile.

3. Compute the deflection, y_{50}, at one-half the ultimate soil resistance from the following equation:

$$y_{50} = 2.5 \varepsilon_{50} b \tag{5.4}$$

4. Compute the points describing the *p-y* curve of soft clay using the following equation:

$$\frac{p}{p_{ult}} = 0.5 \left(\frac{y}{y_{50}}\right)^{\frac{1}{3}} \tag{5.5}$$

- For cyclic loading condition (as illustrated in Figure 3.3 (b)):

1. For p less than $0.72 p_{ult}$, construct the *p-y* curve in the same manner as for short-term static loading.

2. Compute the depth at the transition point, z_r, by solving Equations 3.2 and 3.3. If the effective unit weight and undrained shear strength are constants in the upper zone, then compute z_r from the following equation:

$$z_r = \frac{6c_u b}{\gamma b + Jc_u} \tag{5.6}$$

If the effective unit weight and undrained shear strength vary with depth, z_r should be computed with the soil properties at the depth where *p-y* curve is desired.

3. If the depth of the *p-y* curve is greater than or equal to z_r, p is equal to $0.72p_{ult}$ for all values of y greater than $3y_{50}$.

4. If depth of the *p-y* curve is less than z_r, compute p for values of y between $3y_{50}$ to $15y_{50}$ from following equation:

$$p = 0.72p_{ult}\left(\frac{z}{z_r}\right) \tag{5.7}$$

The value of p remains constant beyond $y = 15y_{50}$.

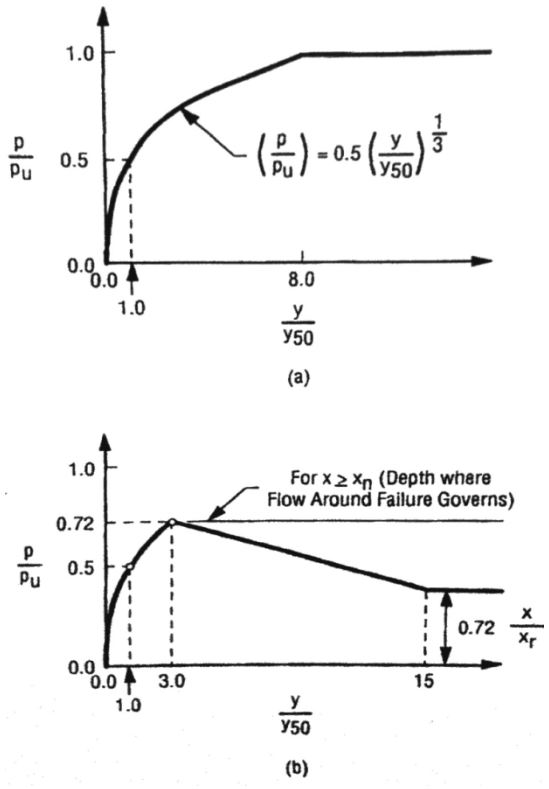

Figure 3.3 Characteristic shapes of p-y curves for soft clay: (a) static loading; (b) cyclic loading (after Matlock, 1970)

3.3.2 Response of Pile Stiff Clay

Welch and Reese (1972) performed experimental testing on full-scaled drilled shafts in a stiff to very stiff clay, known as the Beaumont clay. After completing the analysis of the test data, the following procedures were suggested to determine the *p-y* curves for stiff clay and are illustrated in Figure 3.4 and 3.5.

- For short-term static loading condition (as illustrated in Figure 3.4 (a)):
    1. Obtain the best possible estimate of the variation of undrained shear strength, c_u, effective unit weight, γ, and the strain corresponding to one-half the maximum principal stress difference, ε_{50}. If stress-strain curves are

unavailable, use a value of 0.010 or 0.005 with the larger value resulting in a smaller stiffness for the *p*-y curve, and consequently being more conservative.

2. Compute the ultimate resistance per unit length of pile, using the smaller of the values given by Eq. (3.2) and (3.3).
3. Compute the deflection at one-half the ultimate soil resistance from Eq. (3.4).
4. Points describing *p-y* curve may be computed from the relationship below:

$$\frac{p}{p_{ult}} = 0.5\left(\frac{y}{y_{50}}\right)^{0.25} \tag{5.8}$$

5. Beyond $y = 16y_{50}$, p is equal to p_{ult} for all values of y.

- For cyclic loading condition (as illustrated in Figure 3.4 (b)):
  1. Determine the *p-y* curve for short-term static loading by the procedure previously given.
  2. Determine the number of times the design lateral load will be applied to the pile.
  3. For several values of p/p_{ult}, obtain the parameter, C, describing the effect of repeated loading on deformation from laboratory tests. In the absence of tests, the value of C can be estimated using the following equation:

$$C = 9.6\left(\frac{p}{p_{ult}}\right)^{4} \tag{5.9}$$

  4. At the value of p corresponding to the values of p/p_{ult} selected in Step 3, compute new values of deflection for cyclic loading from the following equation:

$$y_c = y_s + y_{50}C\ logN \tag{5.10}$$

where y_c = deflection under *N*-cycle of load;

y_s = deflection under short-term static load; and

y_{50} = deflection under short-term static load at one-half the ultimate resistance.

5. The *p-y* curve defines the soil response after *N*-cycles of load.

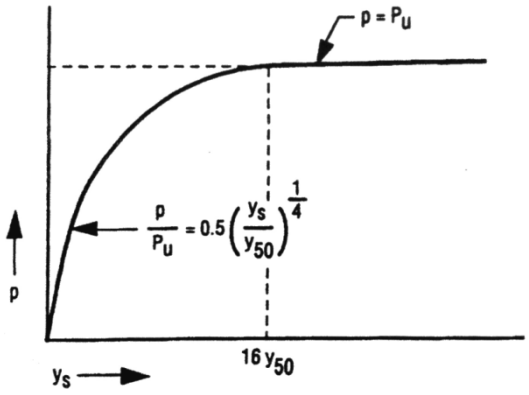

(a)

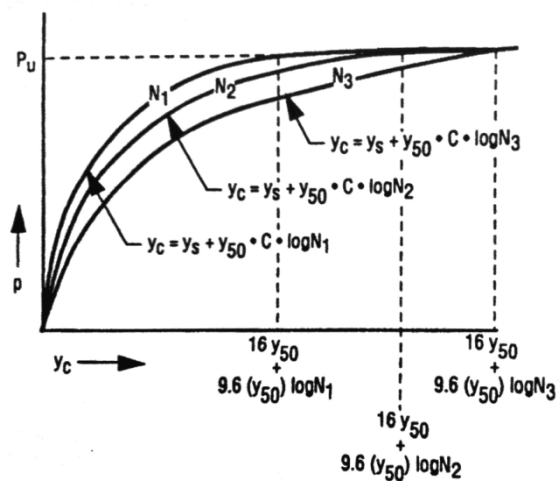

(b)

Figure 3.4 Characteristic shapes of p-y curves for stiff clay (a) static loading; (b) cyclic loading (after Welch and Reese, 1972)

3.4 Modifications to p-y Curve for CDSM-Improved Soft Clay Soil

The study summarized in Section 3.3 concludes that the current recommendations for p-y curves used for modeling the response of clay soils are limited to homogeneous soil layers at each depth along the pile length. In order to analyze the behavior of a lateral loaded pile in a volume of CDSM-improved soil surrounded by soft clay, modifications must be made to account for the lateral load resisted by the soil improved to a limited horizontal extent.

By extending the general concept of the Winkler analysis, as shown in Figure 3.5, the nonlinear behavior of the CDSM-improved soil and unimproved soft clay within each discrete layer could be represented by two nonlinear springs connected in series. The aim of this *p-y* curve modification is to model this unimproved and improved clay soil system as a homogenous equivalent material, requiring the two nonlinear springs connected in series to be represented by one single spring with combined properties. Consequently, the analysis can then follow the Winkler analysis concept to address the effect of the soil improvement surrounding the pile.

3.4.1 Effective Length of the Infinitely Long CDSM-Improved Soil

The modifications to *p-y* curves for soil with CDSM improvement can be developed by integrating the effectiveness of the improved soil into the procedures of constructing *p-y* curves for stiff clay. This was achieved by estimating the effective length for the infinitely long soil layer with CDSM so that the fraction of the load resisted by the soil improved over a limited horizontal extent could be accounted for by taking the ratio between the actual length of the soil with CDSM and the effective length. The effective length of the soil improved with CDSM over the infinite length can be determined by

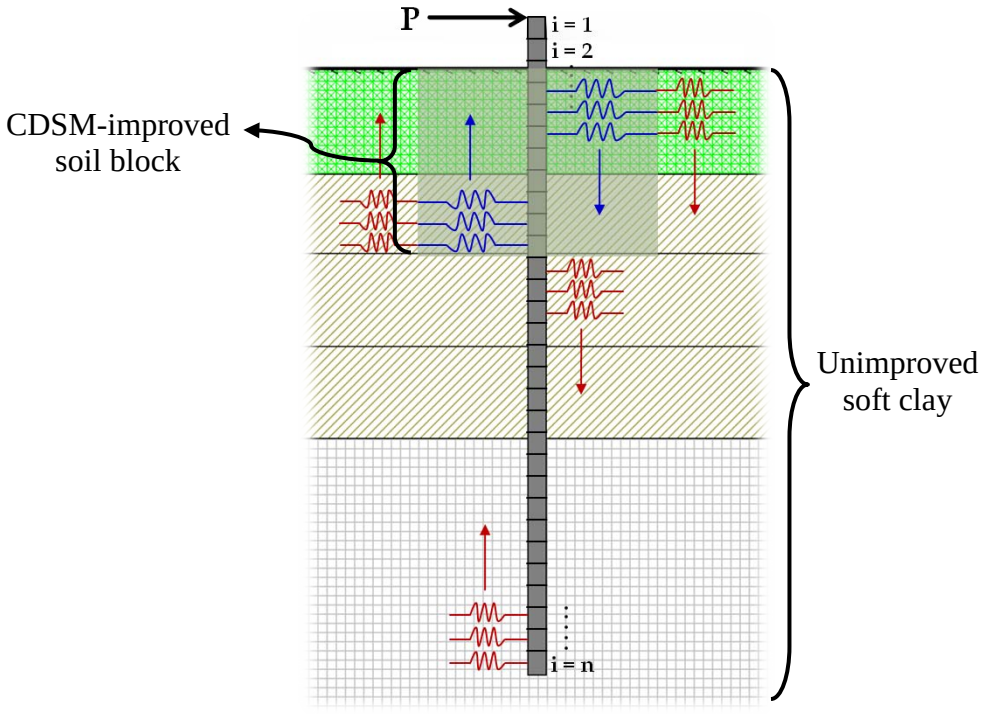

Figure 3.5 Winkler analysis model with improved soil profile

following Welch and Reese's recommendations for establish *p-y* curves for stiff clay. From the current recommendation for obtaining *p*-y curve presented in Section 3.3, the relevance of the stress-strain curve to *p*-y curves was dictated by the strain corresponding to one-half the maximum principal stress difference, ε_{50}. In other words, ε_{50} was selected as the single parameter to characterize the stiffness of the stress-strain curves. Therefore, the stiffness of soils can be found by taking the secant stiffness modulus of the corresponding *p-y* curves at one-half of the soil resistance as shown in Figure 3.6. By considering the CDSM soil block as a solid homogeneous region, its stiffness may be quantified by AE_s/L, where A is the cross-sectional area of the soil layer, E_s and L are the modulus of elasticity and horizontal length of the soil improved with CDSM, respectively.

Therefore, the effective length of a infinitely long CDSM-improved soil layer can be calculated using the following equation:

$$L_{eff} = \frac{AE_s}{k_{i,CDSM}} \tag{5.11}$$

where $k_{i,CDSM}$ is the initial stiffness of the CDSM-improved soil, which is obtained by taking the secant stiffness modulus of the corresponding *p-y* curves at one-half of the soil resistance, as previously disscussed. Because the stiffness of the improved soil increases with its depth due to the increased vertical effective stress, the effective length for the horizontal extent of the soil with CDSM should decrease with increasing depth.

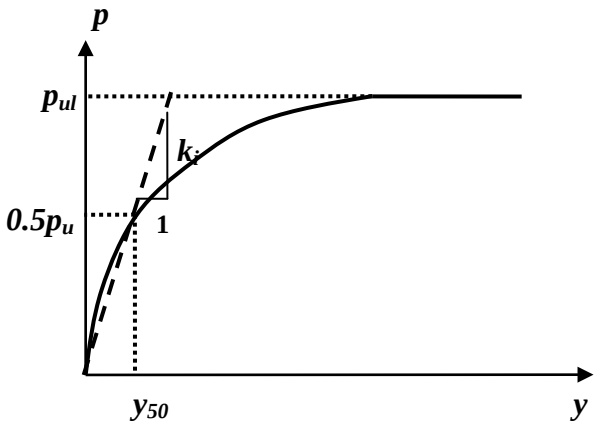

Figure 3.6 Initial soil stiffness estimation

3.4.2 Effective Stiffness of the Homogenized Equivalent Material

As described previously, modeling the soil with CDSM and unimproved soft clay as a homogenized composite material can be achieved by replacing a two-nonlinear-spring system with a single-nonlinear spring having the combined properties. The effective stiffness of a homogenized equivalent material for a CDSM soil region with a length of *l* surrounded by unimproved soft clay can be represented by:

$$k_{eff} = \frac{P_{total}}{\Delta_{CDSM} + \Delta_{soft\ clay}} \tag{5.12}$$

where, P_{total} = lateral load resisted by the soil layer at a specific depth;

Δ_{CDSM} = horizontal deflections of the CDSM-improved soil caused by the lateral load acting on the pile; and

$\Delta_{soft\ clay}$ = horizontal deflections of the soft clay caused by the lateral load acting on the pile.

The horizontal deflections of the CDSM-improved soil and soft clay in above equation can be calculated as follows:

$$if\ l < l_{eff}, \qquad \Delta_{CDSM} = \frac{P_{total} \times \left(\frac{l}{l_{eff}}\right)}{k_{i,CDSM}}\ \ and\ \ \Delta_{soft\ Clay} = \frac{P_{total} \times \left(1 - \frac{l}{l_{eff}}\right)}{k_{i,Soft\ Clay}} \tag{5.13}$$

$$if\ l > l_{eff}, \qquad \Delta_{CDSM} = \frac{P_{total}}{k_{i,CDSM}}\ \ and\ \ \Delta_{soft\ Clay} = 0 \tag{5.14}$$

In Eq. (3.13), the lateral load applied to the pile is divided into two components acting separately on the soft clay and soil with CDSM, where the length ratio l/l_{eff} determines the fraction of the load acting on each part. In ground improvement scenarios, in which the actual length of the CDSM soil region is greater than the effective length, the soft clay has no contribution to the effective stiffness since the CDSM soil block is wide enough to resist the entire lateral load. This is reflected in Eq. (3.14).

3.4.3 p and y-Modification Factors

To develop the *p-y* curve for the homogenized equivalent material describing the CDSM-improved soil surrounded by soft clay, *p*- and *y*-modification factors are introduced to modify the *p-y* curve for soil with CDSM improved to infinite length, i.e.

the *p-y* curve generated using the procedures developed by Welch and Reese (1972). As shown in Figure 3.7, the development of the *p*- and *y*-modification factors can be carried out using the linear interpretation approach. By setting the point, P_1, on the modified *p-y* curve in line with the other two points, P_2 and P_3, on *p-y* curves for unimproved soil and CDSM improved soil with infinite length, respectively, the modification factors can be found by solving the equations below:

$$\Omega_p\left(0.5p_{ult,CDSM}\right) = k_{eff}\left[\Omega_y\left(y_{50,CDSM}\right)\right] \tag{5.15}$$

$$\Omega_p\left(0.5p_{ult,CDSM}\right) = A\left[\Omega_y\left(y_{50,CDSM}\right)\right] + B \tag{5.16}$$

where, Ω_p = *p*-modification factor;

Ω_y = *y*-modification factor;

$A = \frac{0.5\left(p_{ult,CDSM} - p_{ult,soft\ clay}\right)}{y_{50,CDSM} - y_{50,soft\ clay}}$;

$B = 0.5p_{ult,CDSM} - Ay_{50,CDSM}$;

$p_{ult,CDSM}$ = ultimate soil resistance of CDSM-improved soil, the smaller of the values given by Eq. (3.2) and (3.3);

$p_{ult,soft\ clay}$ = ultimate soil resistance of CDSM-improved soil, the smaller of the values given by Eq. (3.2) and (3.3);

$y_{50,CDSM}$ = deflection of the CDSM-improved soil at one-half the ultimate soil resistance, calculated using Eq. (3.4); and

$y_{50,soft\ clay}$ = deflection of the CDSM-improved soil at one-half the ultimate soil resistance, calculated using Eq. (3.4).

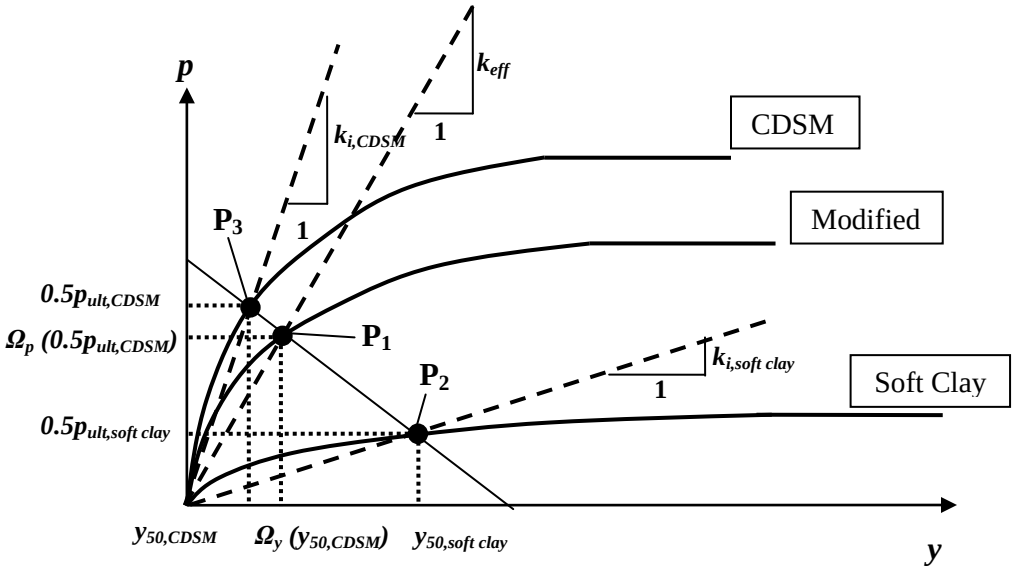

Figure 3.7 Estimation of the *p- and y-modification factors*

It is important to notice that the modification factors, Ω_p and Ω_y, has different values at different depths within the improved soil layer. This is because of the increase in soil stiffness along the pile length. As a result, the effective stiffness of the homogenized equivalent material, k_{eff}, increases as the depth of the improved soil layer increases.

The *p-y* curves for the soil with CDSM improved to infinite length can be modified by multiplying all the *p* and *y* values on the curve by the respective Ω value at each layer depth. The modified *p-y* curves can then be used in the Winkler analysis to represent the combined nonlinear behavior of the CDSM-improved soil and its surrounding soft clay.

3.5 Improvement to the Preliminary P-Y Curve Modifications

A key component in developing modifications to *p-y* curve for CDSM-improved soil surrounded by soft clay is to accurately estimate the amount of the lateral load resisted by the soil improved over a limited horizontal extent. In the preliminary

modification method presented in Section 3.4, this was accounted for by simply taking the length ratio of l/l_{eff}, considering the improved soil as a solid homogeneous block. This simplification did not provide the capability for the modified *p-y* curve to reflect the actual pattern of lateral resistance attenuation in the surrounding soil. Based on this deficiency, an improvement is made to the preliminary modification method with the emphasis on developing the lateral resistance attenuation within the CDSM-improved soil region.

3.5.1. Soil Displacement Attenuation

When pile is subjected to a lateral load, a part or whole length of the pile tries to shift horizontally. The pile presses against the soil in front of it and developing compressive stresses and strains in the soil that offers resistance to the pile movement. The soil resistance in the soil surrounding the pile is then attenuatted with a distance away from the pile. The displacement of the soil in the direction of the loading also diminishes with the resistance attenuation.

Based on a concept developed by Guo and Lee (2001), the decay of soil displacement in the direction of loading can be estimated by employing a radial attenuation function for soil displacement, $\varphi(r)$, where r is radial distance away from the center of the pile section. In Guo and Lee (2001)'s model, a load transfer approach was developed by introducing a simplified stress field in the elastic soil continuum surrounding a laterally loaded pile. As presented in Figure 3.8, the displacement field is nonaxisymmetric, and normally dominated by radial displacement u, and circumferential displacement v; while the vertical displacement, w, is negligible lateral loading. Thus, the fields may be expressed as following:

$$u = y(z)\varphi(r)cos\theta, \qquad v = -y(z)\varphi(r)sin\theta, \qquad w = 0 \tag{5.17}$$

$$\sigma_r = 2G_s y\frac{d\varphi}{dr}cos\theta, \qquad \sigma_\theta = \sigma_z = 0,$$
$$\tau_{r\theta} = -G_s y\frac{d\varphi}{dr}sin\theta, \qquad \tau_{\theta z} = -G_s\frac{dy}{dz}\varphi sin\theta, \qquad \tau_{zr} = G_s\frac{dy}{dz}\varphi cos\theta \tag{5.18}$$

where, $y(z)$ = pile body displacement at depth z;

$\varphi(r)$ = attenuation of soil displacement at r from the pile axis;

θ = angle between the interesting point and the loading direction;

G_s = soil shear modulus;

σ_r = radial stress within the surrounding soil;

σ_θ = circumferential stress within the surrounding soil;

σ_z = vertical stress within the surrounding soil;

$\tau_{r\theta}$ = shear stress within the r-θ plane;

$\tau_{\theta z}$ = shear stress within the θ-z plane; and

τ_{rz} = shear stress within the r-z plane.

In Eq. (3.17), the expressions show that the soil displacement in the direction of loading at a distance r from the pile axis is a resultant of the radial displacement, u, and the circumferential displacement v, and will always equal to the radial displacement at a point where the angle between this point and the loading direction is zero. Therefore, the decay of soil displacement in the direction of loading can also be estimated using the radial attenuation function for soil displacement, $\varphi(r)$,

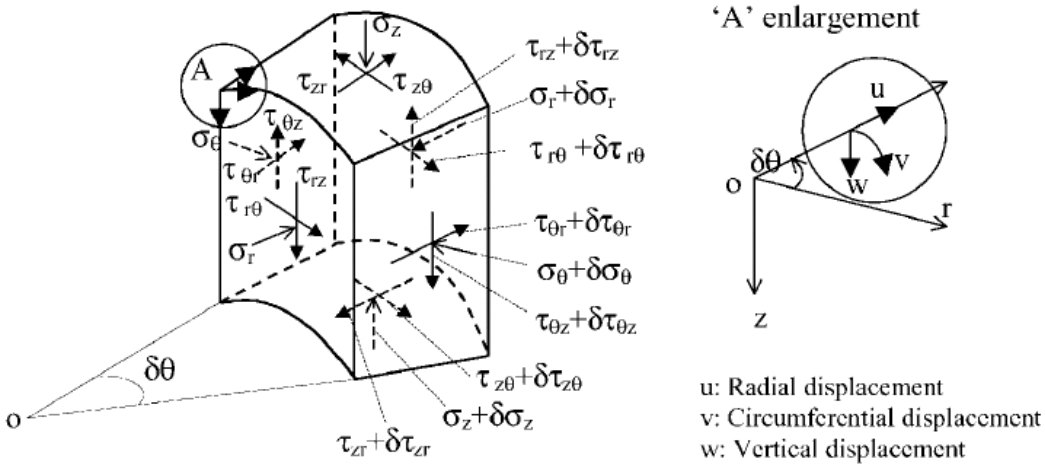

Figure 3.8 Stress and displacement field adopted in the load transfer analysis (Guo and Lee, 2001)

Using the displacement field from Eq. (3.11) and the stress field from Eq. (3.12), the variation of potential energy of the pile-soil system, δU, may be expressed as:

$$\delta U = E_p I_p \int_0^L \frac{d^2y}{dz^2}\delta\left(\frac{d^2y}{dz^2}\right)dz + \pi R^2 \int_L^\infty G_s \frac{dy}{dz}\delta\left(\frac{dy}{dz}\right)dz + \iiint \sigma_{ij}\delta\varepsilon_{ij}\, r\, dr\, d\theta\, dz \qquad (5.19)$$

where, R = the radius of an equivalent cylinder pile;

σ_{ij} = stress components (from Eq. (3.12)) in the surrounding soil of the pile; and

ε_{ij} = strain components in the surrounding soil of the pile.

The virtual work, δW, done by the lateral load, P, and the moment, M_0, due to small displacement, δy, and rotation, $\delta(dy/dz)$, may be expressed as:

$$\delta W = P\delta y|_{z=0} + M_0\delta(dy/dz)|_{z=0} \qquad (5.20)$$

Equilibrium of the pile-soil system leads to:

$$\delta U + \delta W = 0 \qquad (5.21)$$

By expanding Eq.(3.15) and collecting the coefficients of $\delta\varphi$ for $R \le r < \infty$, the governing equation for the radial attenuation function, $\varphi(r)$, can be obtained as:

$$r^2\frac{d^2\varphi}{dr^2}+r\frac{d\varphi}{dr}-\left(\frac{\beta}{R}\right)^2 r^2\varphi=0 \tag{5.22}$$

where β is a nondimensional parameter that determines how rapidly the radial displacements diminish with the radial distance r. By satisfying the finite condition at $r\to\infty, \varphi(\infty)=0$, and unit condition at $r=R, \varphi(R)=1$, Eq. (3.16) may be solved and expressed as modified Bessel functions of the second kind of order zero, $K_0(\beta)$:

$$\varphi(r)=\frac{K_0\left(\frac{\beta r}{R}\right)}{K_0(\beta)} \tag{5.23}$$

3.5.2. Determination of Parameter β

Based on the variation approach, iterative procedure is needed for determination of the nondimensional parameter, β. Guo and Lee (2001) generated the values of, β, using a purpose written program operating in Mathcad, with different pile-soil relative stiffness, loading characteristics (P or M_0), and pile-head and base conditions. These values are then summarized statistically and expressed in the following form:

$$\beta=k_1\left(\frac{E_p}{G^*}\right)^{k_2}\left(\frac{L_e}{R}\right)^{k_3} \tag{5.24}$$

where, k_1, k_2, k_3 = coefficients given in Table 3.1;

G^* = modified soil modulus = $(1+0.75\nu_s)G_s$;

L_e = pile length embedded in the soil; and

ν_s = Poisson's ratio of soil.

The values of k_1, k_2, and k_3 in Table 3.1 were determined for cases wherein the pile is subjected either to lateral load P or moment M_0 at the ground surface level. In cases where the pile is subjected to a load and moment simultaneously, the value of β should lie

in between the value of β for the load P and that for the moment M_0. The maximum difference in the radial attenuation function, $\varphi(r)$, for the P and M_0 is generally less than 10%. Thus, the value of β for the combined loading condition has been taken as the average of the β for the load P and that for the moment M_0 in this study, which gives rise to a much smaller difference in the prediction of $\varphi(r)$ from using the exact β generated with the variation approach.

Table 3.1 Parameters for estimating load transfer factor, γ

	Long Piles: $\frac{E_p}{G^*} \leq \left(\frac{E_p}{G^*}\right)_c^{\S}$			Short Piles: $\frac{E_p}{G^*} > \left(\frac{E_p}{G^*}\right)_c^{\S}$		
Items	k_1	k_2	k_3	k_1	k_2	k_3
FeHCP[§§] (P)	1.00	-0.25	0	1.90	0	-1.00
FeHFP (P)	1.00	-0.25	0	2.14	0	-1.00
FeHCP (M_0)	2.00	-0.25	0	2.38	-0.04	-0.84
FeHFP (M_0)	2.00	-0.25	0	3.80	0	-1.00
FxHCP (P)	0.65	-0.25	-0.04	1.50	-0.01	-0.96
FxHFP (P)	0.65	-0.25	-0.04	0.76	0.06	-1.24

§ $\left(\frac{E_p}{G^*}\right)_c$ is the critical pile-soil stiffness, to be obtained as: $\left(\frac{E_p}{G^*}\right)_c \approx \frac{0.05}{1+0.75\nu_s}\left(\frac{L}{R}\right)^4$.

§§ FeH = free-head; CP(P) or CP (M_0) = clamped piles due to a lateral load, P or moment, M_0, respectively; FP(P) or FP (M_0) = floating piles due to a lateral load, P or moment, M_0, respectively; FxH = fixed-head.

3.5.3 Soil Resistance Attenuation

As described previously, the soil displacement attenuates as the soil resistance diminishes with a increasing distance away from the pile. Therefor, by using the relationship (Eq. (3.8)) developed by Welch and Reese (1972) for determining *p-y* curve of stiff clay, the relationship between attenuation of soil resistance and displacement can be derived by normalizing the soil resistance corresponding to the soil displacement at a horizontal distance, r, away from the center of the pile, $p(r)$, with the respect to the soil resistance at the pile-soil interface, $p(R)$:

$$\psi(r) = \frac{p(r)}{p(R)} = \frac{0.5p_{ult}\left(\frac{y\phi(r)}{y_{50}}\right)^{0.25}}{0.5p_{ult}\left(\frac{y\phi(R)}{y_{50}}\right)^{0.25}} \tag{5.25}$$

where, $\psi(r)$ = attenuation of soil resistance at r from the pile axis; and

y = lateral deflection of the pile-soil interface.

Since the attenuation function for soil displacement, $\varphi(r)$, satisfies the unit condition at $r = R$, Eq. (3.19) can then be simplified to the following form:

$$\psi(r) = [\phi(r)]^{0.25} \tag{5.26}$$

3.5.4 Modified Effective Length of the Infinitely Long CDSM-Improved Soil

In Eq. (3.17) and (3.19), the solutions to attenuation functions $\varphi(r)$ and $\psi(r)$ satisfy the finite conditions at $r \to \infty, \varphi(\infty) = 0;\ \psi(\infty) = 0$. This idealized condition resulted in an infinitely large stiffness for soil at a small displacement, which is overly conservative compare to the initial stiffness of the soil continuum. Therefore, a modified effective length, l'_{eff}, is estimated by allowing the lateral stiffness of the soil to be increased to a limiting value. After calibration with two sets of centrifuge test results, which will be presented in Chapter 4, l_{eff}, was defined by following relationship:

$$\frac{\psi(l'_{eff})}{\phi(l'_{eff})} = 8\left(\frac{\psi(R)}{\phi(R)}\right) \tag{5.27}$$

Eq. (3.27) indicates that the lateral resistance of the imporved soil and its corresponding displacement can be considered to diminish to a value of zero when the normalized lateral stiffness of the soil at a horizontal distance l'_{eff} away from the center of the pile increased to eight times larger than that at the pile-soil interface. As a result, the original soil attenuation functions $\varphi(r)$ and $\psi(r)$ needs to be modified to include this change as

well. By satisfying the zero conditions at $r = l'_{eff}$, and the original function, $\varphi(r)$ and $\psi(r)$ can be modified as follows:

$$\phi'(r) = \phi(r) - \left(\frac{r-R}{l_{eff}-R}\right)\phi(l_{eff}) \tag{5.28}$$

$$\psi'(r) = \psi(r) - \left(\frac{r-R}{l_{eff}-R}\right)\psi(l_{eff}) \tag{5.29}$$

where, $\varphi'(r)$ = modified attenuation of soil displacement at r from the pile axis; and

$\psi'(r)$ = modified attenuation of soil lateral resistance at r from the pile axis.

An example of the modified attenuation of soil displacement and lateral resistance are plotted in Figure 3.9. As shown in this figure, at $r = R, \varphi'(R) = 1, \psi'(R) = 1$; and as $r = l_{eff}, \varphi'(l_{eff}) = 0, \psi'(l_{eff}) = 0$.

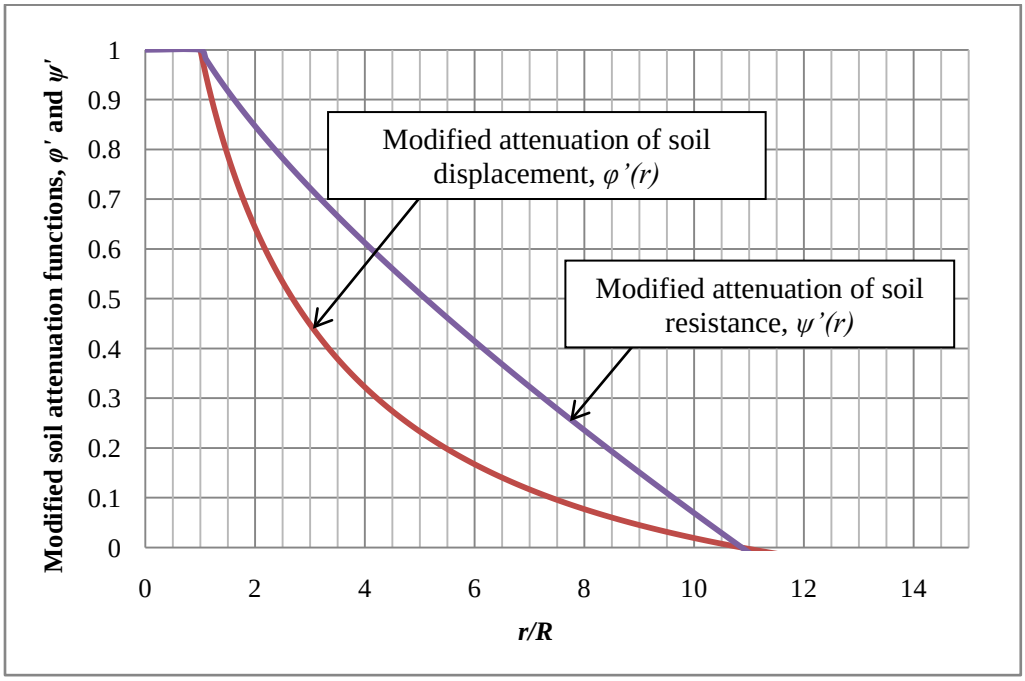

Figure 3.9 An example of the modified attenuation of soil displacement and lateral resistance

3.5.5 Modified Effective Stiffness of the Homogenized Equivalent Material

By estimating the attenuation of the soil resistance, the amount of lateral loads resisted by soil improved over a limited extent can be directly accounted for when establishing the effective stiffness of the homogenized equivalent material. As described in Section 3.4.2, the effective stiffness of a homogenized equivalent material for a CDSM soil region with a length of *l* surrounded by unimproved soft clay can be represented by:

$$k_{eff} = \frac{P_{total}}{\Delta_{CDSM} + \Delta_{soft\ clay}} \tag{5.30}$$

The horizontal deflections of the CDSM-improved soil and soft clay in above equation can be modified as the soil resistance attenuation at a distance *r* away from the center of the pile, $\psi(r)$, determines the amount of the load acting on each part:

$$if\ l < l'_{eff}, \qquad \Delta_{CDSM} = \frac{P_{total} \times \left(1 - \psi'(l)\right)}{k_{i,CDSM}}\ \ and\ \ \Delta_{soft\ Clay} = \frac{P_{total} \times \psi'(l)}{k_{i,Soft\ Clay}} \tag{5.31}$$

$$if\ l > l'_{eff}, \qquad \Delta_{CDSM} = \frac{P_{total}}{k_{i,CDSM}}\ \ and\ \ \Delta_{soft\ Clay} = 0 \tag{5.32}$$

After the stiffness is establish using Eqs (3.30) to (3.32), the modified *p-y* curve accounting for the resistance attenuation within the soil surrounding the pile can be obtained using the same procedures described in Section 3.4.3, and then be used in the Winkler analysis to represent the combined nonlinear behavior of the CDSM-improved soil and its surrounding soft clay.

3.6 LPILE

In the preceding sections, a modified *p-y* curve representing a volume of CDSM improvement surrounded by soft clay can be constructed using the modification factors. To continue the current study in lateral load behavior of the piles, LPILE Plus Version

5.0 (Ensoft, Inc. 2004) was utilized. LPILE is a commercial program that includes the capability to analyze a pile subjected to lateral loading using the Winkler analysis concept (see Section 3.2). The p-y curves of various soil types can be internally generated in LPILE by follow published recommendations available in the literature and are discussed in detail later in this section. The nonlinear behavior of a pile can be accommodated in LPILE by defining the moment-curvature response of the pile sections at appropriate places. For a given problem with appropriate boundary conditions, LPILE can analyze the response of a pile under monotonic loading and produce deflection, shear, bending moment, and soil response along the pile length.

3.6.1 Solution Process

As discussed in Section 3.2, the standard beam-column equation (Eq.(3.1)) can be used to determine the deformation of a pile subjected to axial and lateral loads. LPILE uses the finite difference method to develop a solution of this forth-order differential equation. In the finite difference method, the pile is divided into several segments with equal lengths that are referred to as beam elements. Figure 3.11 shows an undeformed and deformed pile that is subdivided into segments. Eq. 3.1 can be expressed in the following form:

$$\begin{aligned} y_{m-2}R_{m-1} + y_{m-1}(-2R_{m-1} - 2R_m + Qh^2) \\ + y_m(R_{m-1} + 4R_m + R_{m+1} - 2Qh^2 + k_m h^4) \\ + y_{m+1}(-2R_m - 2R_{m+1} + Qh^2) + y_{m+2}R_{m+1} = 0 \end{aligned} \tag{5.33}$$

where $R_m = E_m I_m$ (flexural rigidity of pile at depth m); and

$k_m = E_{sm}$ (secant modulus of the soil-response curve at depth m).

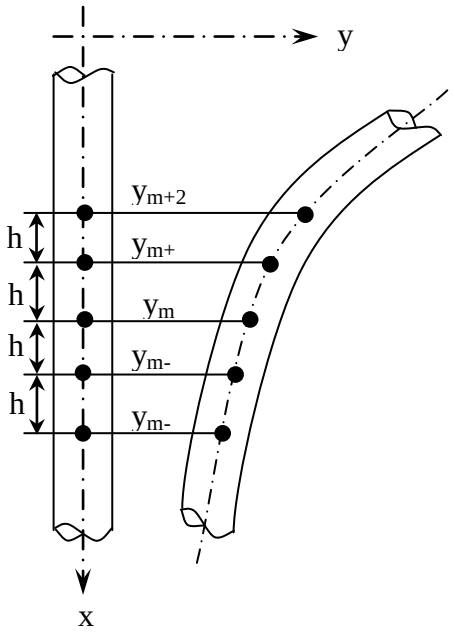

Figure 3.10. Subdivided pile model as used in LPILE for the finite difference solution (Ensoft Inc. 2005)

The relations needed to calculate the slope, curvature, shear, and load are shown below.

$$\frac{dy}{dx} = \frac{y_{m-1} + y_{m+1}}{2h} \tag{5.34}$$

$$\frac{d^2y}{dx^2} = \frac{y_{m-1} - 2y_m + y_{m+1}}{h^2} \tag{5.35}$$

$$\frac{d^3y}{dx^3} = \frac{-y_{m-2} + 2y_{m-1} - 2y_{m+1} + y_{m+2}}{2h^3} \tag{5.36}$$

$$\frac{d^4y}{dx^4} = \frac{y_{m-2} - 4y_{m-1} + 6y_m - 4y_{m+1} + y_{m+2}}{h^4} \tag{5.37}$$

To calculate the moment and shear within each element, the flexural rigidity, E_pI_p, is needed. However, the flexural rigidity changes according to the state of deformation within each element, thus inducing a nonlinear effect on the pile. LPILE has the capabilities to account for the nonlinear behavior of each element according to a user-specified moment-curvature relationship.

For the above equations, LPILE uses the following steps to find the solution for a prescribed lateral load or displacement. A set of p-y curves is internally generated along the length of the pile for the selected soil profile. A linear relation is established between the soil resistance, *p*, to the deflection, *y*, with the slope of the line representing the soil modulus at a given *y*. The soil modulus values are established from each of the p-y curves that were generated along the pile length. In order to complete the computation, LPILE uses the computed values of the soil modulus and continues iterations on the deflection until the difference in the calculated deflections is less than a specified tolerance. Once the deflections have been computed, the derivatives of deflections equation can be utilized to compute the rotation, bending moment, shear, and soil reaction as presented in Eqs. 3.36, 3.37, 3.38 and 3.39.

3.6.2 Features of LPILE

To accomplish the completion of a typical analysis required in the current study, the following input are needed: selection of the analysis type, identification of the pile properties, selection of the loading type, selection of the boundary conditions, and selection of the soil surrounding the pile. In addition, a brief list of LPILE features relevant to the lateral analysis of piles and how these features were used in the current study are presented below.

- As previously noted, a user defined moment-curvature response can be defined for the pile section, thereby enabling accurate representation of the confinement effects on the pile response in the analysis. This was achieved by running moment-curvature analyses of the pile sections using a software framework,

OpenSees (see Section 3.6), and defining EI as M/ϕ, where M is the moment output and ϕ is the corresponding section curvature.

- Five sets of boundary conditions are available to model the pile head. Depending on the boundary conditions, the pile-head loading may consist of a lateral load, a bending moment, a specific lateral displacement, or a specific pile-head rotation. The boundary conditions of interest for this study were a pinned connection, a fixed connection. By keeping the moment value zero and incrementally changing the displacement, a pinned connection at the pile head was established. By keeping the pile-head rotation zero and incrementally changing the lateral displacement, a fixed connection at the pile head was established. Upon selecting the boundary condition, ten different incremental displacement steps may be applied at the pile head for a single analytical run, enabling observation of the pile behavior for a displacement range for a given set of boundary conditions.
- If provided with basic soil properties, soil-resistance (i.e., p-y curves) curves can be internally generated by the program for 11 different types of soil: Soft Clay (Matlock, 1970), Stiff Clay with Free Water (Reese, 1975), Stiff Clay without Free Water (Reese, 1975), Sand (as recommended by Reese et al., 1974), Vuggy Limestone (Strong Rock), Silt (with cohesion and internal friction angle), API Sand (as recommended by API, 1997), Weak Rock (Reese, 1997), Liquefiable Sand (as recommended by Rollins, 2003), and Stiff Clay without free water with specified initial k. In addition, any user-specified p-y modification factors may be utilized in LPILE to represent soil conditions that were not included in the 11

predefined soil types. For the current study, soft clay soils based on Matlock (1970) and sand properties as per API (1997) were used to model the unimproved soil profile, as the stiff clay without free water based on Reese (1975) together with a set of p-y modification factors developed using the proposed methods were used to model the CDSM improved soil surrounded by soft clay soils.

3.7 Section Analysis Tool

In order to define the structural behavior of the individual pile elements within LPILE for a fully inelastic analysis, performing a moment-curvature analysis is necessary. OpenSees, an acronym for Open System for Earthquake Engineering Simulation, is a software framework that allows users to simulate the seismic response of both structural and geotechnical systems (Mazzoni et al., 2004). It aims to improve the modeling and computational simulation through community input, and is thus continually developing. The capabilities of this software include modeling and analyzing the nonlinear response of systems. In OpenSees, moment-curvature analyses are performed as an incremental analysis on a zero length section, defined by two nodes, both located at (0.0, 0.0). The zero-length section is defined using a fiber-based approach, which is outlined below.

- Identify a set of key points that will define the section of the pile.
- Create the nodes for the model.
- Create the models for materials represented in the section and assign each region of the section with the corresponding material model (i.e., structural steel, confined concrete, unconfined concrete, prestress strands, etc.).
- Define the element type to be utilized.

- Define the external axial load and set the analysis parameters.

OpenSees allows sections to be defined by either circles or polygons, or a combination of the two. Figure 3.12 shows an example of octagonal pile sections defined in the program. Any of the moment-curvature analyses reported within the remainder of this report were performed using OpenSees.

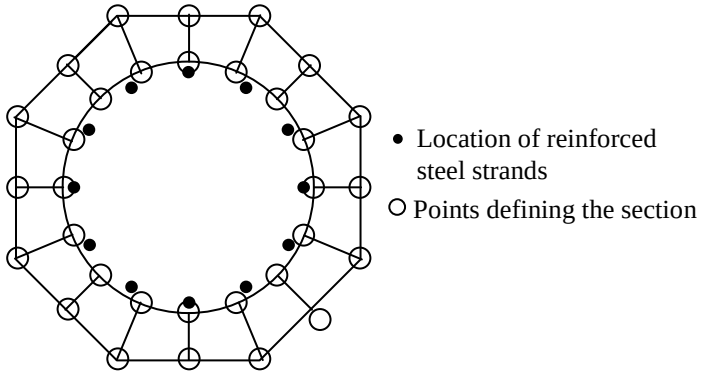

Figure 3.11 Definition of an octagonal pile section in OpenSees

CHAPTER 4. EXPERIMENTAL VALIDATIONS

4.1 Introduction

Chapter 3 presented the Winkler analysis using *p-y* method to characterize the lateral load behavior of a single pile embedded in a volume of improved soil surrounded by soft clay utilizing the newly developed *p-y* curve modification factors. Two different experimental investigations were conducted to determine the actual effectiveness of the CDSM soil improvement on increasing the lateral load resistance of pile foundations and validate the analytical methodology proposed in Chapter 3. The remainder of this chapter will first discuss in detail the two experimental investigations that were performed for verification of the proposed methodology. The ability of the *p-y* method to handle the lateral response of a single pile in a volume of improved soil surrounded by unimproved soft clay is then demonstrated by comparing the experimental data with the analysis results obtained using LPILE.

4.2 Small-Scale Centrifuge Testing

As a part of the current project, two centrifuge tests were performed by Liu et al. (2010) at the Center for Geotechnical Modeling at UC Davis to investigate the lateral load behavior of pile foundations in soft clay with and without CDSM ground improvement. Figures 4.1 to 4.4 show the configurations of the centrifuge testing. Each centrifuge model consisted of seven single piles with three different ground improvement configurations. Both centrifuge tests were carried out under a centrifugal acceleration of 30g. Table 4.1 lists the scaling factors that were used to convert the data from the centrifuge scale to the prototype scale. A complete description of the scaling laws can be

found in Kutter et al. (1992). The flexible shear beam container was used to provide continuity for the soil in both centrifuge tests. The piles were defined in the format of X-YDUV, for which X represents the test number, YD stands for the depth of the CDSM improved soil block surrounding the pile in meters, and UV are the two letters assigned to the strain gages attached to each pile. All dimensions reported in the following sections are at the prototype scale.

Table 4.1 Scaling factors for centrifuge tests

Quantity	Prototype Parameter : Model Parameter
Time / Displacement / Length	30 : 1
Acceleration / Gravity / Frequency	1 : 30
Pressure / Stress / Strain / Density	1 : 1
Force	900 : 1

4.2.1 Soil Properties

According to Peck et al. (1974), soft clays have undrained shear strength lower than 25 kPa (3.63 psi). To satisfy the requirements of the soft clay for the centrifuge testing, i.e., low strength and acceptable permeability to finish consolidation of the clay layers in the centrifuge model in a reasonable time period, commercially available Kaolin clay from Old Hickory Clay Company in Kentucky and white fine sand from George Townsend & Co. Inc. in Oklahoma were selected to make the soft clay mixture. The mixture consisted of 50/50 clay/sand by weight with an initial water content of 64% (or 2LL). The bottom two layers of test soil were composed of dense Nevada sand. These dense sand layers were used to satisfy the double drainage conditions during soft clay consolidation and were also used to anchor the piles.

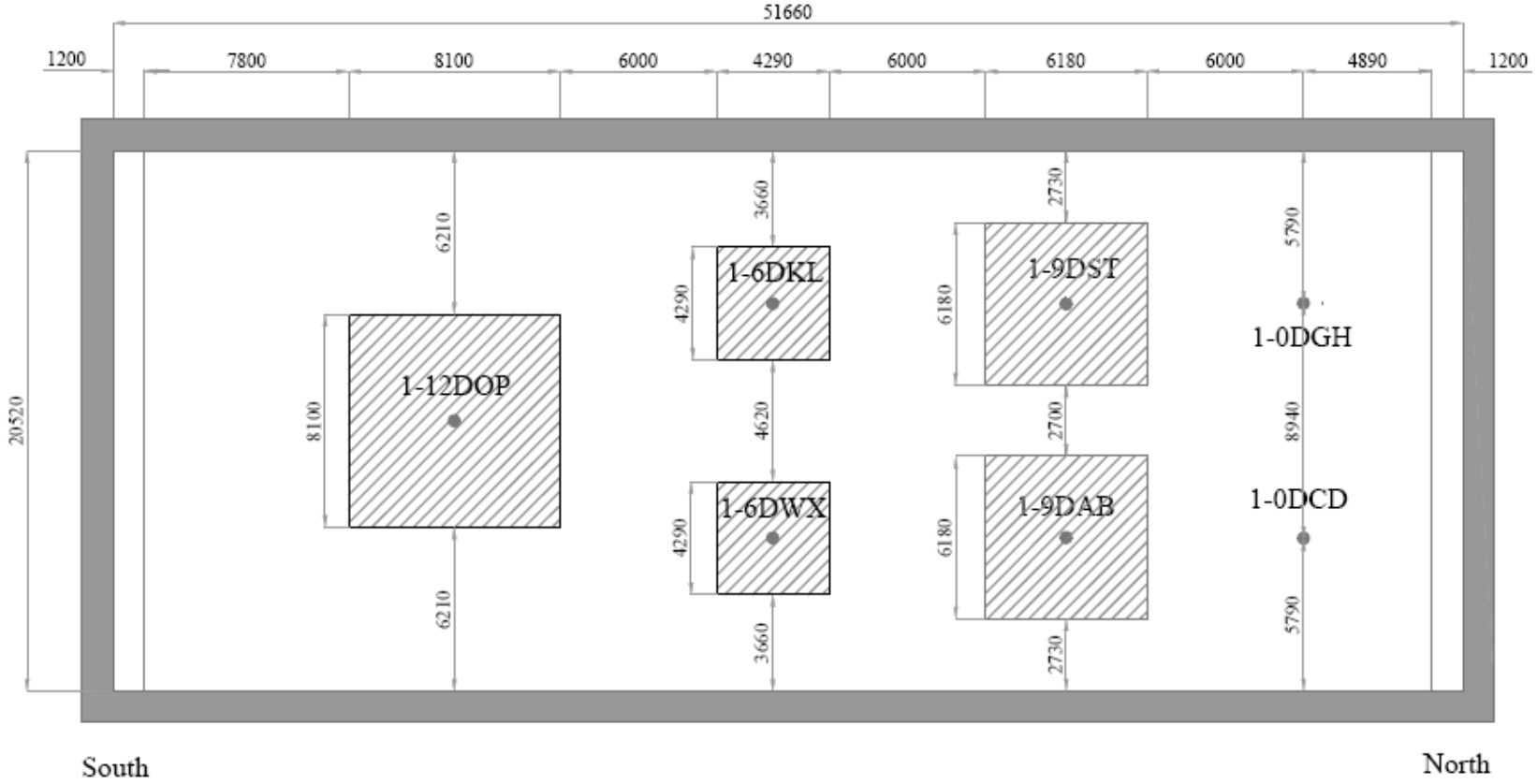

Figure 4.1 Plan view of the centrifuge model setup for test #1, all dimensions in mm; 1 mm = 0.0394 in. (Liu et al., 2010)

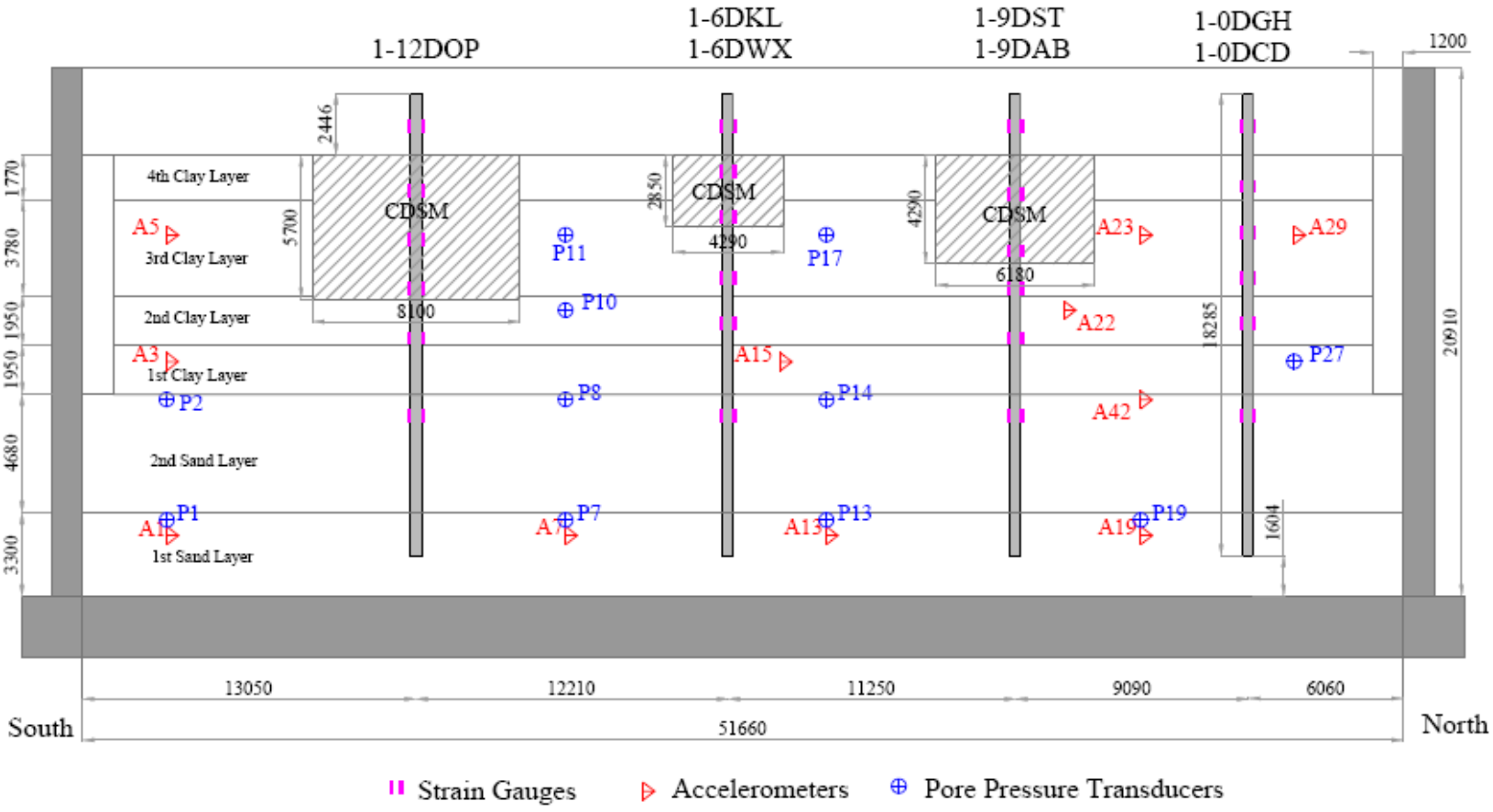

Figure 4.2 Elevation view of the centrifuge model setup for test #1, all dimensions in mm; 1 mm = 0.0394 in. (Liu et al., 2010)

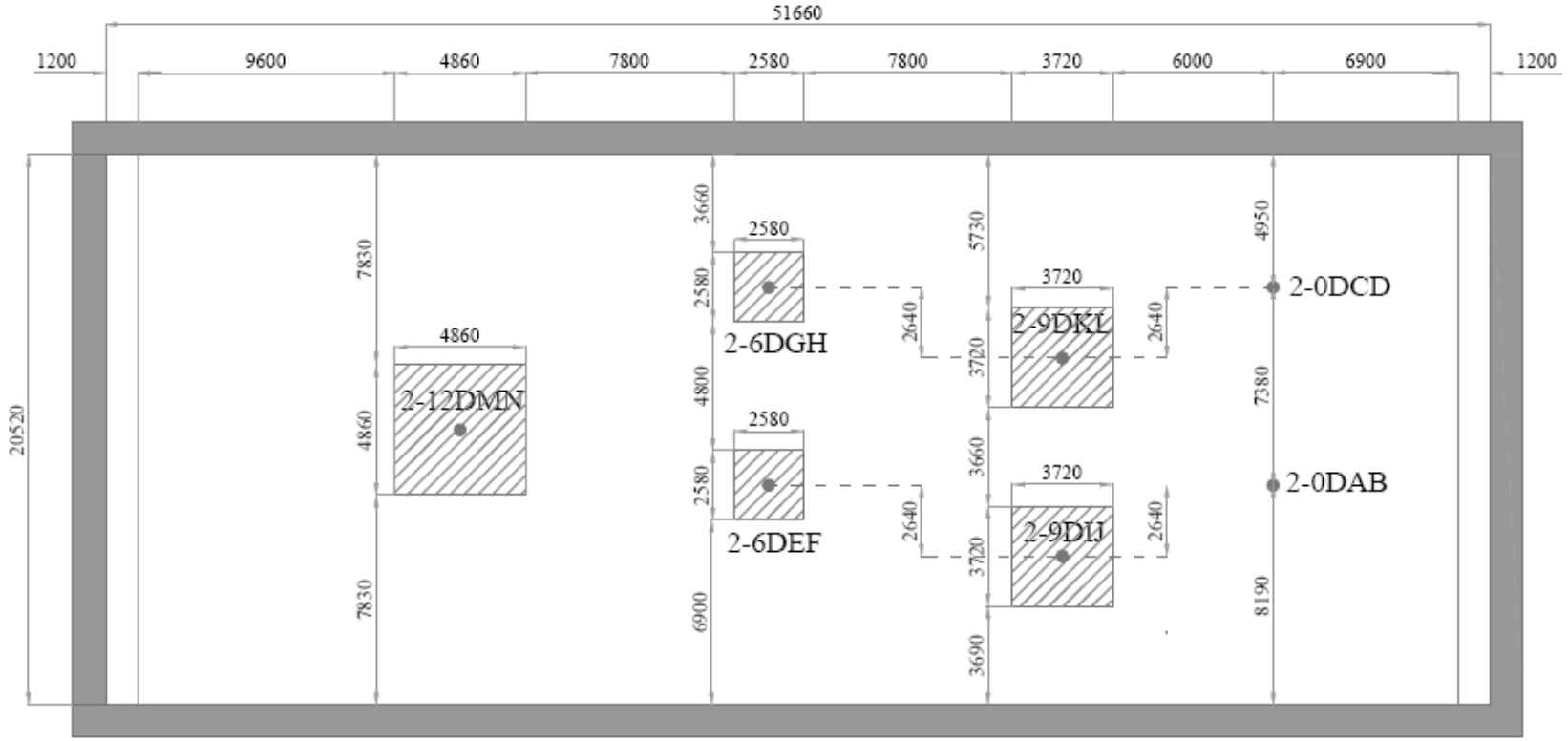

Figure 4.3 Plan view of the centrifuge model setup for test #2, all dimensions in mm; 1 mm = 0.0394 in. (Liu et al., 2010)

Figure 4.4 Elevation view of the centrifuge model setup for test #2, all dimensions in mm; 1 mm = 0.0394 in. (Liu et al., 2010)

also used to anchor the piles.

The recipe for the CDSM improved soil was selected such that the clay:sand ratio to be 1:1 and the mixing water content for the soil to be 34%. The cement-dry soil mix ratio was 1:10 by weight. The water-cement weight ratio was 1:1. Figure 4.5 shows the variation of unconfined strength of the cement/soil mix with curing time.

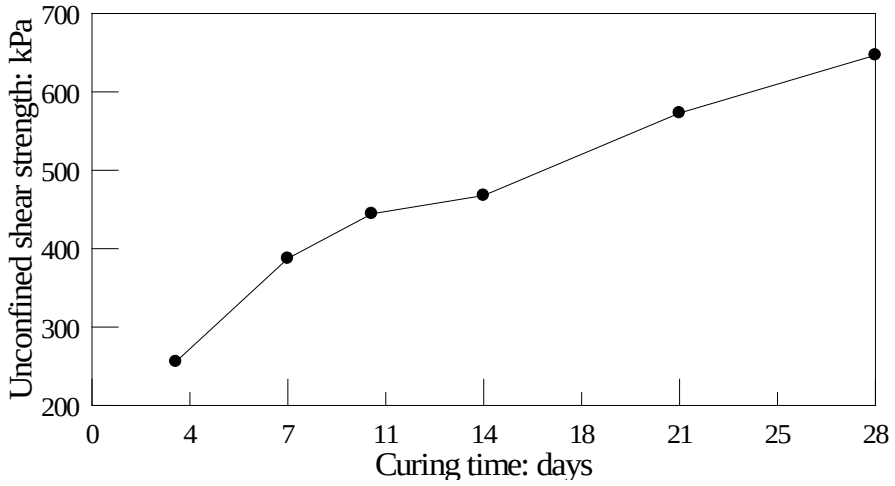

Figure 4.5 Unconfined shear strength of CDSM-improved soil (Liu et al., 2010)

As shown in Figures 4.2 and 4.4, the soil profile used in both tests consisted of 4 layers of soft clay and 2 layers of dense sand. In Test #1, the bottom first sand layer had a thickness of 3.300 m (130 in.) with a void ratio of 0.567, while the second sand layer was 4.680 m (184 in.) thick with a void ratio of 0.531. The soft clay layers No. 1, 2, 3, and 4 in Test #1 were each consolidated to target vertical effective stresses of 190 kPa (28 psi), 150 kPa (22 psi), 55 kPa (8 psi) and 25 kPa (4 psi), respectively, with the final thickness after consolidation to be 1.950 m (77 in.), 1.950 m (77 in.), 3.780 m (149 in.) and 1.770 m (70 in.). In Test #2, the first sand layer was 4.230 m (167 in.) thick with a void ratio of 0.570 and the second sand layer was 3.810 m (150 in.) thick with a void ratio of 0.506. The four soft clay layers were consolidated under vertical effective

stresses of 95 kPa (14 psi), 70 kPa (10 psi), 45 kPa (7 psi) and 25 kPa (4 psi), respectively. The thickness of each soft layer from the bottom to the top was 2.520 m (99 in.), 2.250 m (89 in.), 2.490 m (98 in.) and 2.742 m (108 in.), respectively. For both tests, the dimensions of the CDSM-improved soil blocks were: 9D×9D×6D, 13D×13D×9D and 17D×17D×12D (Note: D was the outside diameter of the pile). There were two small, two medium and one large CDSM blocks in each test. Based on the soil properties of the test soil and CDSM-improved soil blocks, equivalent soil profiles were established for the use of development *p-y* curve modification factors as well as the lateral load analysis using LPILE. The parameters of the equivalent soil profiles are summarized for centrifuge test #1 and #2 in tables 4.2 and 4.3, respectively.

Table 4.2 Soil properties of centrifuge Test #1

Soil Type	**Soil Parameters**			
	Depth	**Effective unit weight, γ'**	**Undrained shear strength, c_u**	**Strain at 50% of the maximum principal stress difference, ε_{50}**
Soft clay	0-1.77 m 0-70 in.	8.18 kN/m^3 0.030 pci	2.71-4.90 kPa 0.39-0.71 psi	0.02
	1.77-5.55 m 70-219 in.	8.69 kN/m^3 0.032 pci	9.21-11.65 kPa 1.34-1.69 psi	
	5.55-7.50 m 219-295 in.	9.62 kN/m^3 0.035 pci	26.00-28.13 kPa 3.77-4.08 psi	
	7.50-9.45 m 295-372 in.	9.80 kN/m^3 0.036 pci	33.98-35.54 kPa 4.93-5.15 psi	
CDSM improved soil	0-6D/9D/12D	8.69 kN/m^3	375 kPa	0.004
		0.032 pci	54 psi	
Dense sand	**Depth**	**Effective unit weight, γ'**	**Friction Angle**	**Initial modulus of subgrade reaction, *k***
	9.45-17.43 m 372-686 in.	10.33 kN/m^3 0.038 pci	38°	33,900 kN/m^3 125 pci

Table 4.3 Soil properties of centrifuge Test #2

Soil Type	Soil Parameters			
	Depth	**Effective unit weight, γ'**	**Undrained shear strength, c_u**	**Strain at 50% of the maximum principal stress difference, ε_{50}**
Soft clay	0-2.67 m 0-105 in.	8.18 kN/m^3 0.030 pci	2.81-5.34 kPa 0.41-0.77 psi	0.02
	2.67-5.16 m 105-203 in.	8.69 kN/m^3 0.032 pci	8.54-9.85 kPa 1.24-1.43 psi	
	5.16-7.41 m 203-292 in.	9.05 kN/m^3 0.033 pci	14.00-15.20 kPa 2.03-2.20 psi	
	7.41-9.93 m 292-391 in.	9.92 kN/m^3 0.034 pci	19.4-20.5 kPa 2.81-2.97 psi	
CDSM improved soil	0-6D/9D/12D	8.69 kN/m^3 0.032 pci	375 kPa 54 psi	0.004
Dense sand	**Depth**	**Effective unit weight, γ'**	**Friction Angle**	**Initial modulus of subgrade reaction, *k***
	9.93-18.00 m 391-709 in.	10.33 kN/m^3 0.038 pci	38°	33,900 kN/m^3 125 pci

4.2.2 Selection of a Test Pile

For the Test #1, the piles were selected to be aluminum piles (type: 6061-T4) with an outside diameter of 0.476 m (19 in.) and a wall thickness of 0.027 m (1 in.), which was motivated by the use of convential aluminum piles in centrifuge testing. The total length of the pile was 18.288 m (720 in.). The modulus of elasticity of the aluminum piles was 66.1 GPa (9587 ksi) and the yield strength was 167.5 MPa (24 ksi). After the first centrifuge test, no obvious permanent bending was observed on the aluminum piles. Therefore, smaller piles were selected for test #2 with the strength and stiffness similar to that of the standard steel piles recommended by the California Department of

Transportation (Caltrans). For the test #2, the piles used were steel tubes (type: A513 type 2 grade 1010) with the outside diameter of 0.286 m (11 in.) and wall thickness of 0.027 m (1 in.). All the piles were 20.388 m (803 in.) long. The modulus of elasticity of the steel piles was 192.5 GPa (27920 ksi) and the yield strength was 260.0 MPa (38 ksi).

In order to define the structural responses of the test piles in the LPILE analysis, section analysis was carried out using OpenSees. The material properties of the aluminum and steel piles were used as input parameters for the material model, steel02, in the program. The moment-curvature curves for the two test piles are shown in Figure 4.6, and are compared with that of the Caltrans standard steel pile with an outside diameter of 0.35560 m (14 in.), wall thickness of 0.01113 m (0.438 in.), and a yield strength of 310.3 MPa (45 ksi).

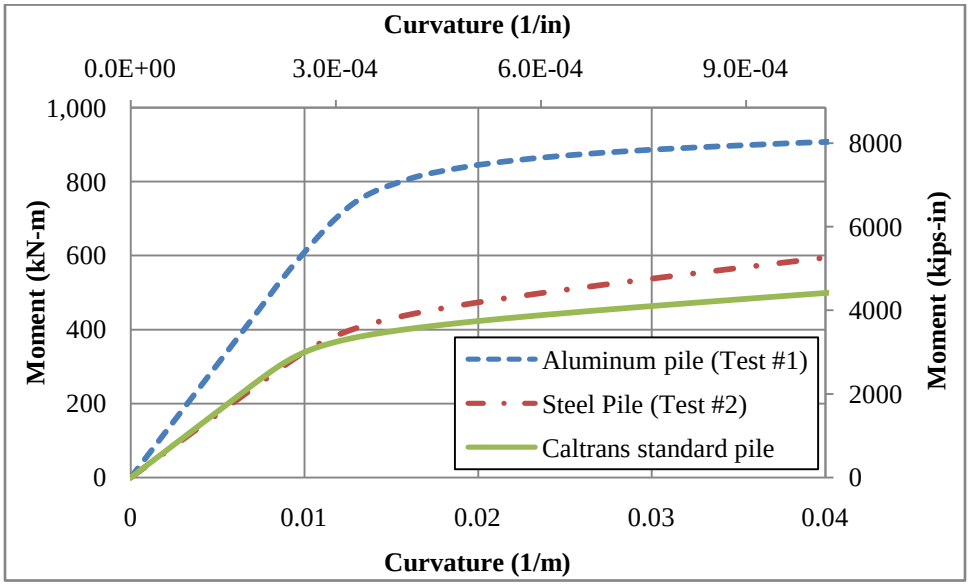

Figure 4.6 Moment-curvature curves for centrifuge test #1 and #2

4.2.3 Test Procedures

For the centrifuge Test #1, cyclic lateral loading tests were performed on one unimproved pile 1-0DGH and one CDSM-improved pile 1-9DST (see Figure 4.1). For the centrifuge test #2, cyclic lateral loading tests were conducted on piles 2-0DCD, 2-9DKL, 2-6DGH, 2-12DMN, 2-0DAB and 2-6DEF (see Figure 4.3) in sequence. During the tests, a displacement controlled hydraulic actuator was used to apply cyclic lateral loads to the pile head with ten target displacement increments. After the cyclic loading at each increment, the pile was pulled back to the initial starting point prior to loading to the next higher displacement increment. In Test #2, the target maximum lateral displacement for the pile 2-12DMN, which was improved by the largest CDSM block, was set at 0.229 m (9 in), although 0.724 m (28.5 in.) was the target maximum displacement for all other three piles. The main reason to apply a smaller maximum displacement for the pile 2-12DMN was to ensure that this pile behaves elastically and not to break the CDSM-improved soil block before the dynamic tests performed after the cyclic lateral loading test.

4.2.4 Test Results

Figures 4.7 and 4.8 present the pile head responses obtained from centrifuge Test #1 and #2, respectively. The load-displacement curves demonstrate that the CDSM soil improvement significantly increased the lateral stiffness of the piles and the lateral displacement can be effectively controlled. As shown in Figure 4.7, the slope of the improved pile (pile 1-9DST) in the elastic region was about six times higher than that of the unimproved pile (pile 1-0DGH), which were estimated to be 2500 kN/m (14.3

kips/in) and 350 kN/m (2.0 kips/in.), respectively. To reach the same maximum target displacement, an average of 420 kN (94.4 kips) force was applied to the improved pile, while only an average of 80 kN (18.0 kips) force was needed to the unimproved pile. In Figure 4.8, the slope of load-displacement curves in the elastic region increased as the dimensions of the CDSM improved soil block increases. This observation implies that the lateral stiffness of the piles can be regarded as an increase function of the soil improvement dimensions. However, the difference between the lateral stiffness of the piles 2-9DKL and 2-12DMN is not obvious, which indicates that the lateral stiffness of the piles will reach a stable condition or maximum value with a certain CDSM-improved zone.

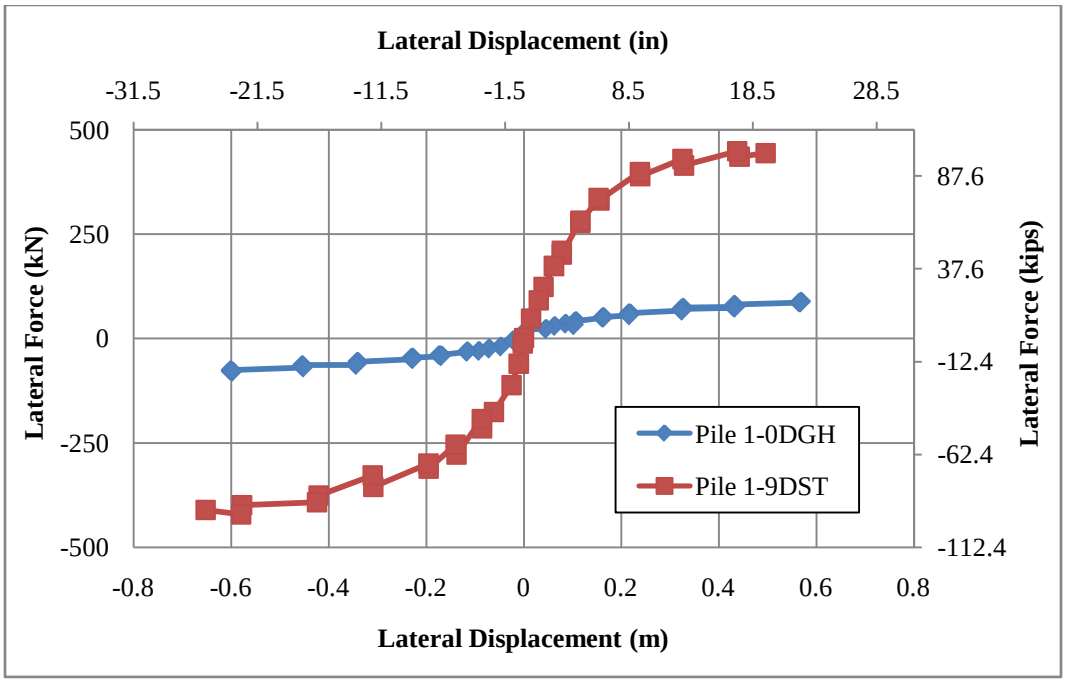

Figure 4.7 Load-displacement responses obtained from centrifuge Test #1

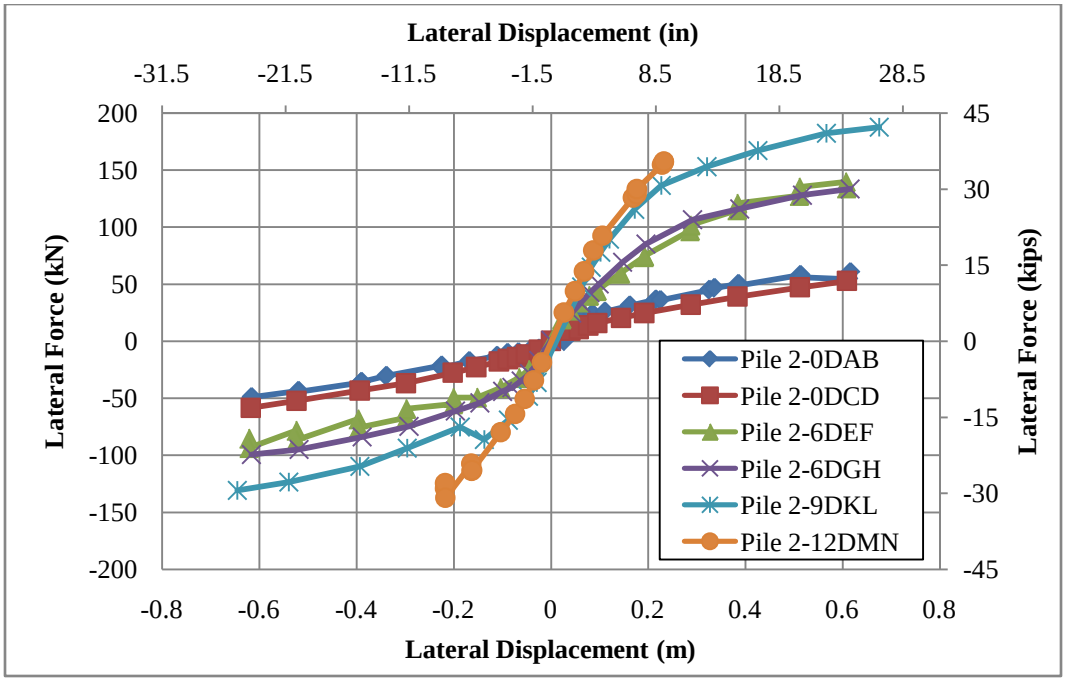

Figure 4.8 Load-displacement responses obtained from centrifuge Test #2

4.2.5 Analysis Results

Figures 4.9 through 4.14 present the load-displacement responses estimated using the Winkler analysis method and their comparison with the load-displacement measured responses from the centrifuge tests. The methodology proposed in Chapter 3 was used to establish the *p-y* curve modification factors for all the CDSM-improved piles, while LPILE was utilized to perform the lateral load analysis.

From the analysis results presented in Figures 4.9 through 4.14, following observations are made:

- the calculated elastic lateral stiffness for piles from centrifuge test #1 were slightly higher than that obtained from the experimental data;

- the calculated lateral load resistance for centrifuge test #1 increased from 100 kN (22.5 kips) to 420 kN/m (94.4 kips), which is in close agreement with the increase from 80 kN (18.0 kips) to 420 kN/m (94.4 kips) from the experimental data;
- the calculated elastic lateral stiffness for piles from centrifuge test #2 increased by 167% and 433% for CDSM soil improvement dimensions 9D×9D×6D and 13D×13D×9D, respectively, which agrees well to the 163% and 420% increase that observed from the experimental data;
- the calculated elastic lateral stiffness for piles with CDSM soil improvement dimensions 13D×13D×9D and 17D×17D×12D had no significant increase; and
- the calculated lateral load resistances for piles in centrifuge test #2 are in excellent agreement with the average value of the experimental data.

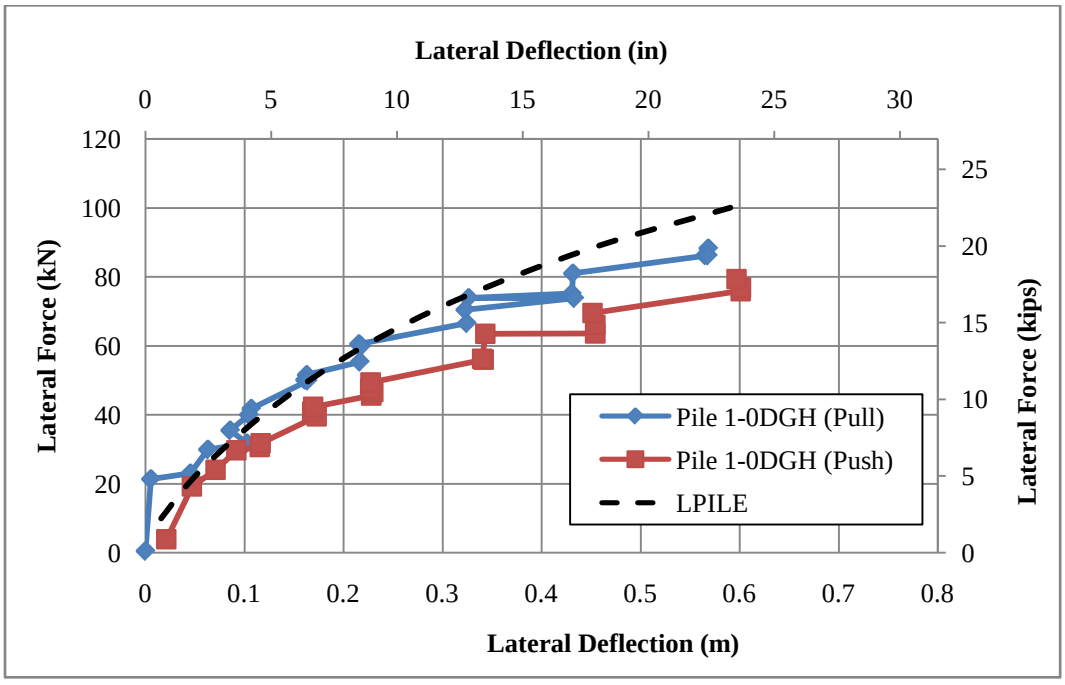

Figure 4.9 Comparison of measured load-displacement response envelopes with the computed load-displacement responses for pile 1-0DGH

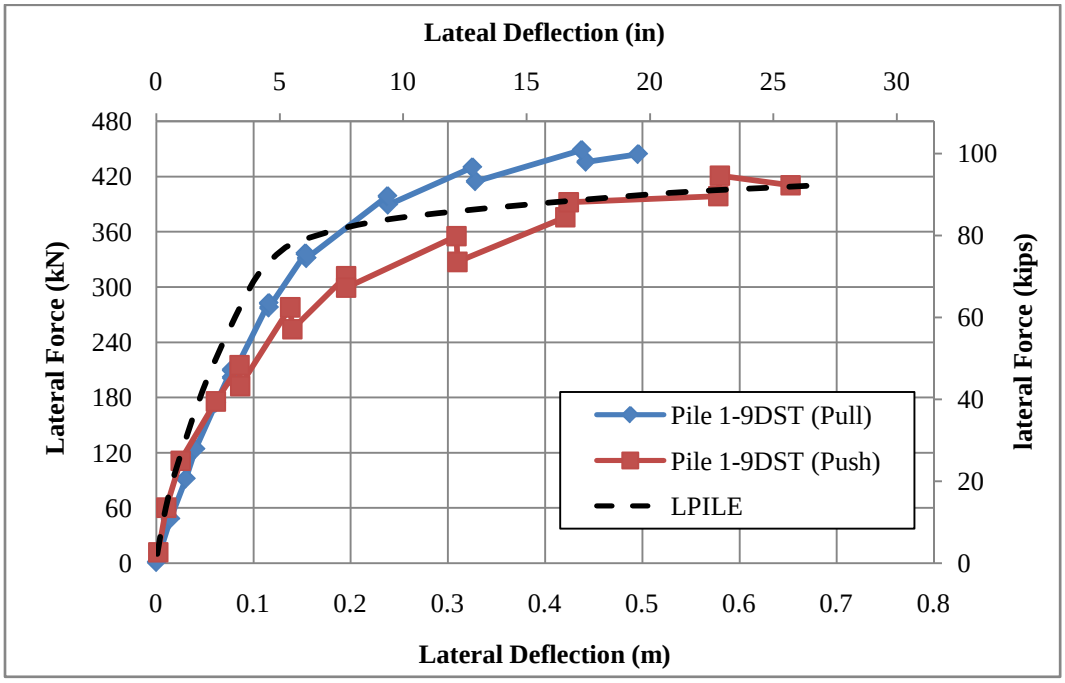

Figure 4.10 Comparison of measured load-displacement response envelopes with the computed load-displacement responses for pile 1-9DST

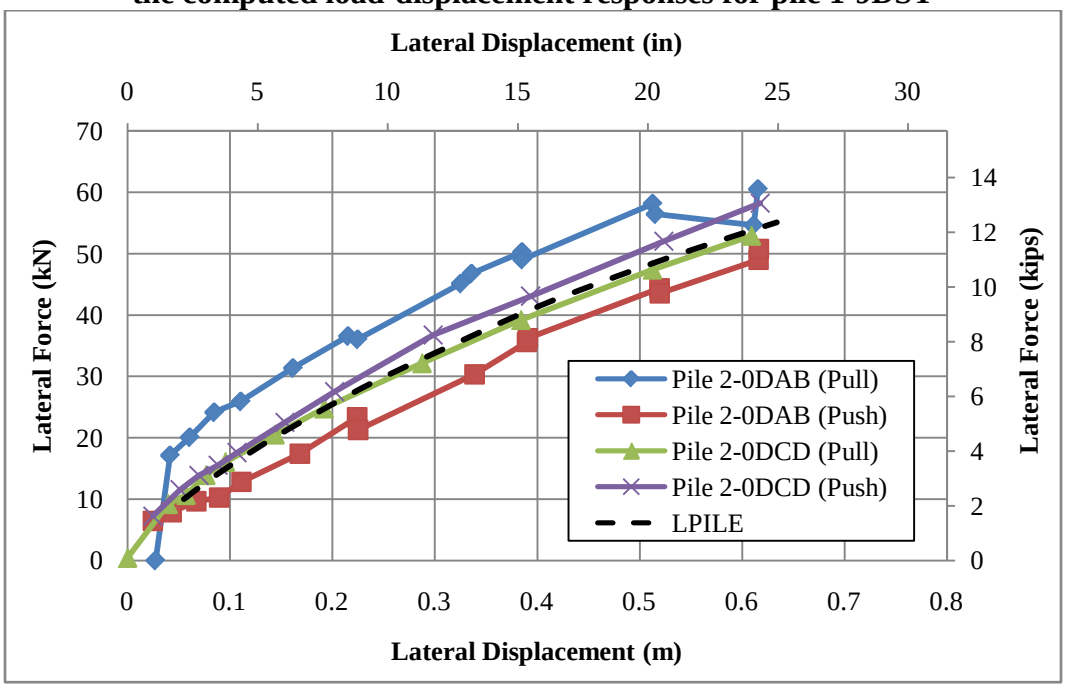

Figure 4.11 Comparison of measured load-displacement response envelopes with the computed load-displacement responses for piles 2-0DAB and 2-0DCD

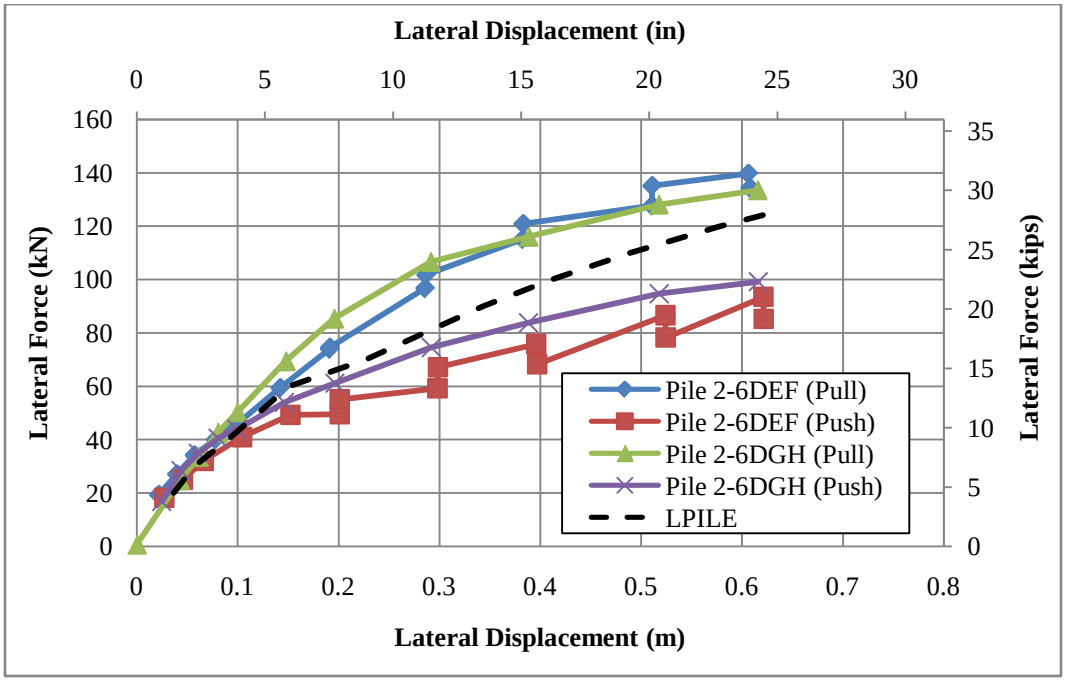

Figure 4.12 Comparison of measured load-displacement responses envelopes with the computed load-displacement responses for piles 2-6DEF and 2-6DGH

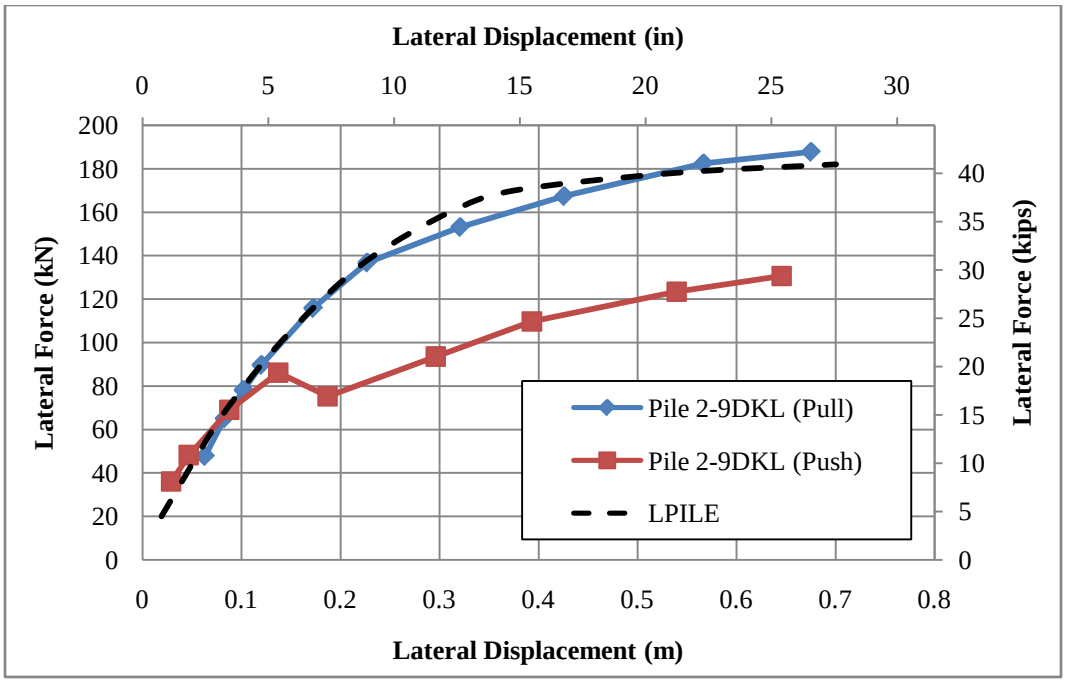

Figure 4.13 Comparison of measured load-displacement responses envelopes with the computed load-displacement responses for piles 2-9DKL

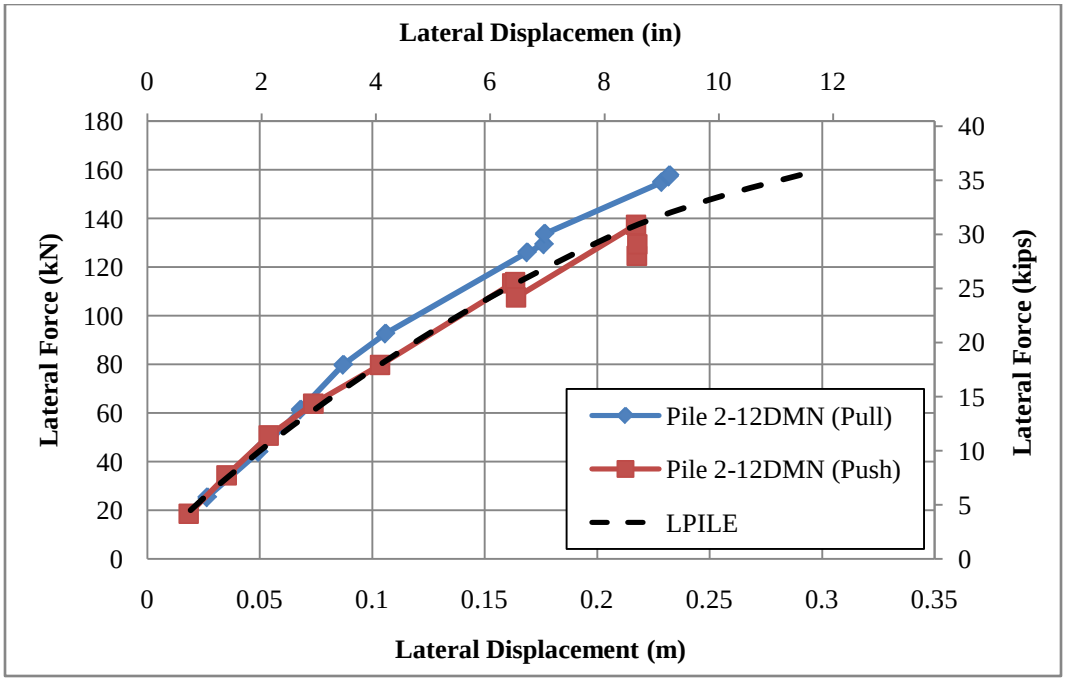

Figure 4.14 Comparison of measured load-displacement responses envelopes with the computed load-displacement responses for piles 2-12DMN

Therefore, the comparison of the analysis results with the centrifuge test results demonstrates that by using the proposed *p-y* curve modification factors, the global responses of a single pile embedded in a volume of CDSM-improved soil surrounded by soft clay can be adequately captured using the Winkler analysis method. The effectiveness of the CDSM soil improvement can be evaluated accurately with the newly developed methodology.

4.3 Large-Scale Field Testing

As a part of the current study, a series of lateral load tests were performed by Fleming et al. (2010) on full-scaled steel piles in a soft clay site located in Miami, Oklahoma, to study the lateral behavior of pile foundation with and without soil improvement. Two test piles were installed at the site with the soil surrounding one of

the piles improved using the CDSM technology. Both static and dynamic load tests were performed on the piles, the results from the static load test are used to investigate the ability of the proposed analysis method on capturing lateral responses of pile foundation in a volume of improved soil surrounded by unimproved soil.

4.3.1 Soil Properties

The test site was located at the east bank of Neosho River in Miami, Oklahoma. The soil profile consists of a layer of lean clay with gravel at the top, medium stiff to very soft silt and clay layers from a depth of 1.1 m (3.6 ft) to 4.3 m (14.1 ft), and sandy gravel layers from 4.3 m (14.1 ft) down. The water table was at a depth of 2.75 m (9.0 ft). A series of cone penetration test (CPT) test was conducted on the soil samples from the test site and the result is shown in Figure 4.15. The CDSM was installed on the test site with a specialty, purpose-built hollow stem and mixing tool arrangement. The cement slurry was mechanically blended with the on-site soils to make the soil-cement mixture with an unconfined shear strength of 2367 kPa (343 psi) after 28 days of curing time. The area of the CDSM soil improvement was 3.96 m × 3.96 m × 3.96 m (13 ft × 13 ft × 13 ft).

Based on the soil properties obtained from the CPT test of the test-site soil samples and the unconfined compression test of the CDSM improved soil samples, an equivalent soil profile was established for the use of development *p-y* curve modification factors and the lateral load analysis using LPILE. The parameters of the equivalent soil profile are summarized Tables 4.4.

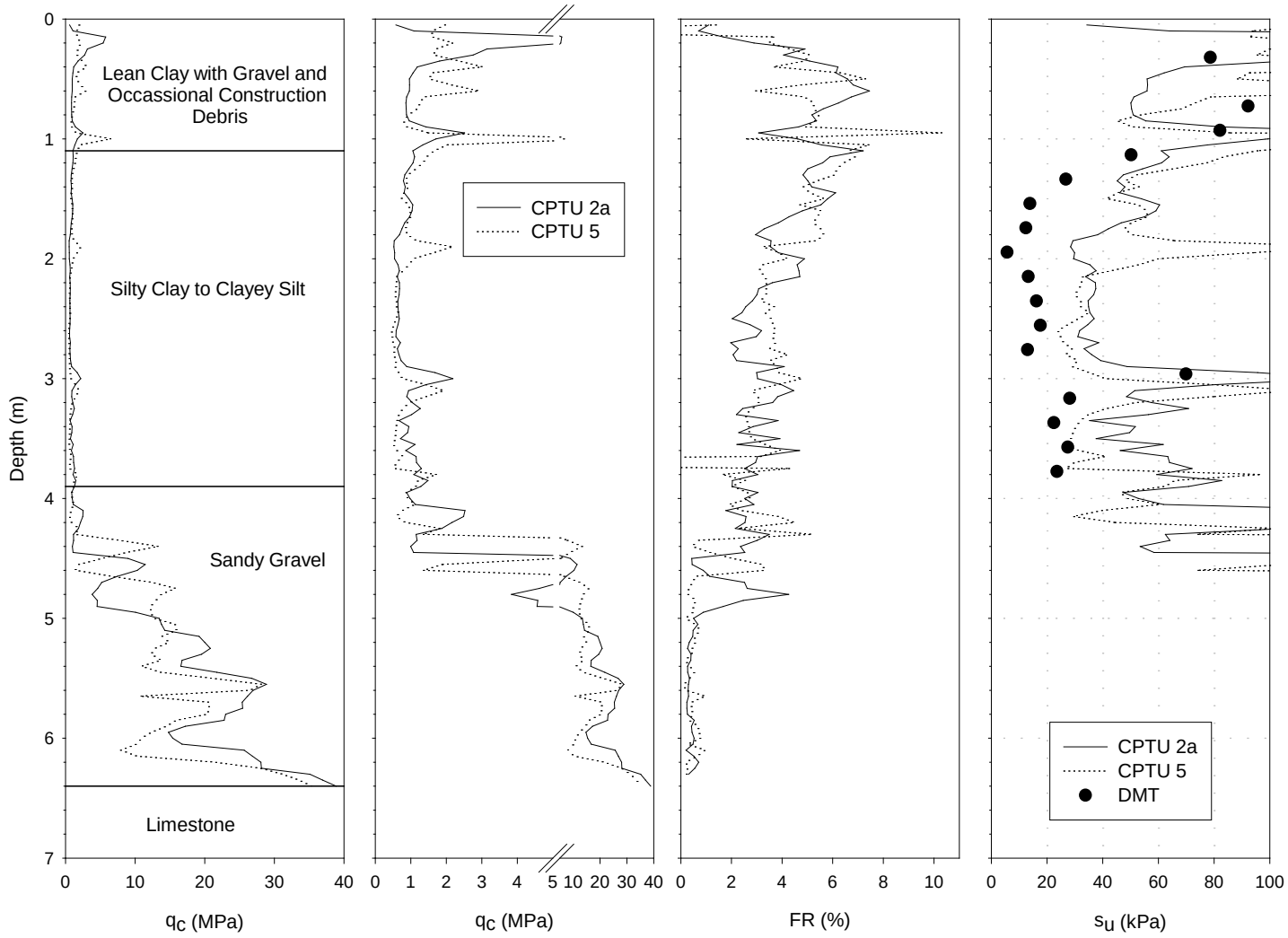

Figure 4.15 CPTU soundings completed at the east bank of Neosho River in Miami, Oklahoma (Fleming et al., 2010)

Table 4.4 Soil properties estimated for the field test

Soil Type	Soil Parameters			
	Depth	**Effective unit weight, γ'**	**Undrained shear strength, c_u**	**Strain at 50% of the maximum principal stress difference, ε_{50}**
Soft clay	1.10-2.05 m 43-81 in.	18.50 kN/m^3 0.068 pci	55 kPa 8.0 psi	0.01
	2.05-2.75 m 81-108 in.	18.50 kN/m^3 0.068 pci	33 kPa 4.8 psi	0.02
	2.75-2.92 m 108-115 in.	8.69 kN/m^3 0.032 pci	35 kPa 5.1 psi	0.02
	2.92-3.30 m 115-130 in.	8.69 kN/m^3 0.032 pci	66 kPa 9.6 psi	0.01
	3.30-3.60 m 130-142 in.	8.69 kN/m^3 0.032 pci	38 kPa 5.5 psi	0.02
	3.60-4.30 m 142-169 in.	8.69 kN/m^3 0.032 pci	68 kPa 9.9 psi	0.01
CDSM improved soil	0-3.96 m 0-116 in.	8.69 kN/m^3 0.032 pci	2367 kPa 343 psi	0.004
Dense sand	**Depth**	**Effective unit weight, γ'**	**Friction Angle**	**Initial modulus of subgrade reaction, *k***
	4.30-4.60 m 169-181 in.	10.33 kN/m^3 0.038 pci	42.8°	33,900 kN/m^3 125 pci
	4.60-4.85 m 181-191 in.		36.1°	
	4.85-5.40 m 191-213 in.		43.3°	
	5.40-5.85 m 213-230 in.		46.2°	
	5.85-6.20 m 230-244 in.		41.6°	
	6.20-7.71 m 244-304 in.		47.2°	

4.3.2 Selection of a Test Pile

The test piles were selected to be steel piles with an outside diameter of 0.324 m (12.75 in.) and a wall thickness of 0.0095 m (0.375 in.). They were driven open-ended to a depth of approximately 6.41 m (252.4 in.) below the ground surface. Since the top layer of the lean clay with gravel was excavated around the test piles, the total embedded length of the piles was 5.31 m (209.0 in.). A cubic yard of reinforced concrete cap was clamped at the pile top to model the superstructure dead weight. The steel of the pile conformed to ASTM A106 Grade B specifications and was tested to have a yield strength of 372.2 MPa (54.0 ksi), ultimate strength of 587.6 MPa (85.2 ksi) and Young's modulus of 212.7 GPa (30,845 ksi). To define the structural responses of the test piles in the Winkler analysis method, section analysis was carried out using OpenSees and the moment-curvature curve of the test pile is shown in Figure 4.16.

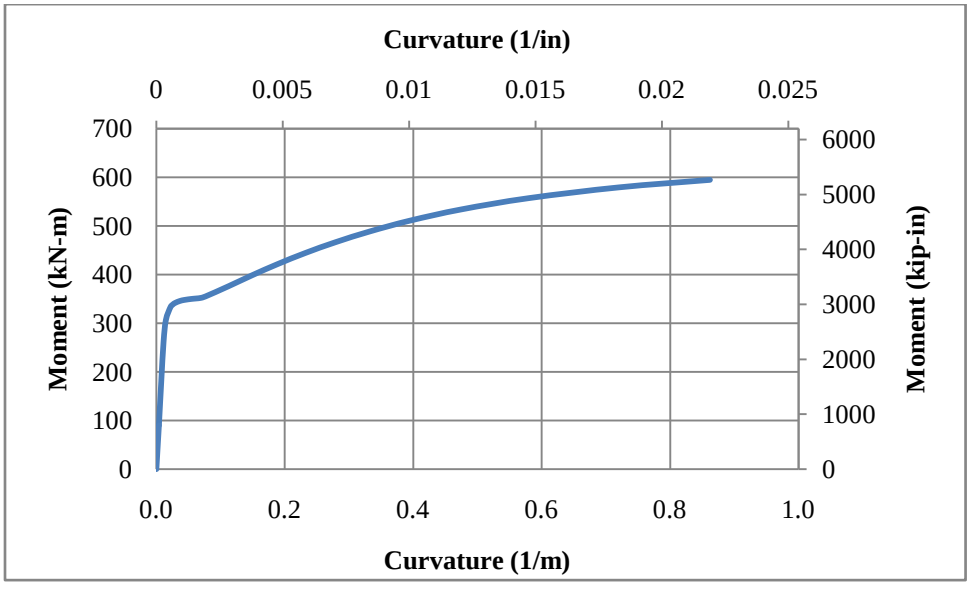

Figure 4.16 Moment-curvature curve for field testing pile

4.3.3 Test Procedures

The quasi-static tests were conducted using a hydraulic actuator to apply lateral load to the piles at the pile caps. A displacement control approach was used in the tests with target pile cap displacement increments of ±25, 51, 76, 102, 152, 203, 305, 406 and 483 mm (±1, 2, 3, 4, 6, 8, 12, 16 and 19 in.). During this process the actuator pushed or pulled the pile at a slow rate, allowing the applied loads to be treated as static loading. After each cyclic loading at the selected increment, the piles were pulled back to the original starting point prior to loading to the next higher displacement increment.

4.3.4 Test Results

Figures 4.17 and 4.18 present the load-displacement responses obtained from the quasi-static tests for unimproved pile and CDSM-improved pile, respectively. By improving the soil around the test pile to an extent of 3.96 m × 3.96 m × 3.96 m (13 ft × 13 ft × 13 ft), the elastic lateral stiffness increased by 420% from 778 kN/m (4.44 kips/in.) to 4042 kN/m (23.1 kips/in.), while the lateral displacement at yielding of the pile decreased by 67% from 0.152 m (5.98 in.) to 0.051 m (1.99 in.). The pile with CDSM soil improvement has a lateral load resistance of 220 kN (49.6 kips), which is 47% higher than the 150 kN (33.7 kips) of lateral load resistance provided by the pile without CDSM soil improvement. All the observations made above further confirm that the CDSM soil improvement techniques significantly increases the lateral stiffness of a pile foundation, while effectively controls the lateral displacement at the pile head.

In Figure 4.18, the force-displacement curves show that the pile with CDSM soil improvement was only tested to a maximum displacement increment of 203 mm (8 in.),

which was significantly lower than the target maximum displacement of 483 mm (19 in.). This early termination of the test was because the test pile failed at the end of first cycle of loading at lateral displacement of 203 mm (8 in.), primarily due to local buckling occurring at the side wall of the pile just above the ground surface, and fracturing the pile as a result of low cycle fatigue. This observation implies that in cases where CDSM soil improvement were used, the failure of a laterally loaded pile will most likely be controlled by local buckling mechanism. Therefore, the designer must check the buckling criteria while considering strength and serviceability limits in this case.

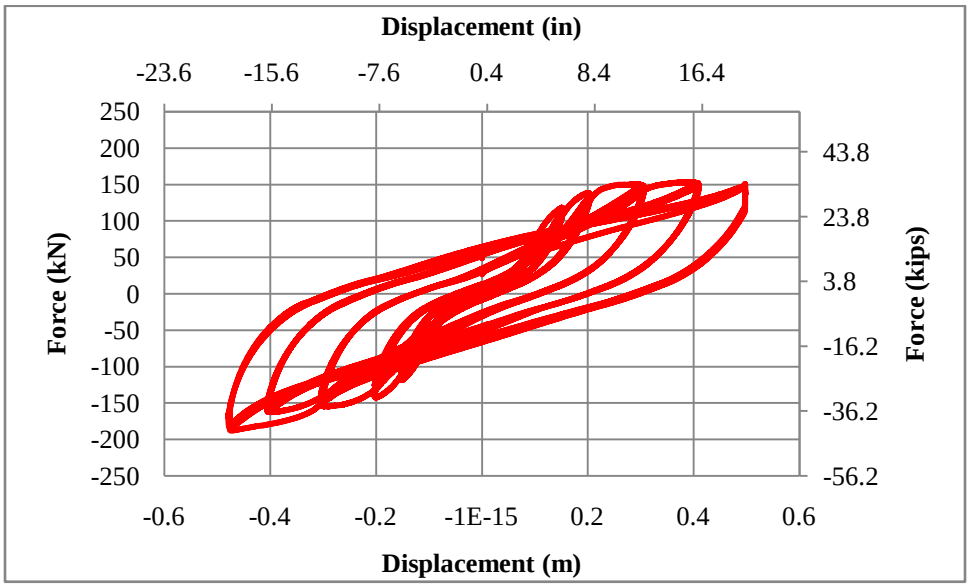

Figure 4.17 Load-displacement responses from field test for pile without CDSM soil improvement

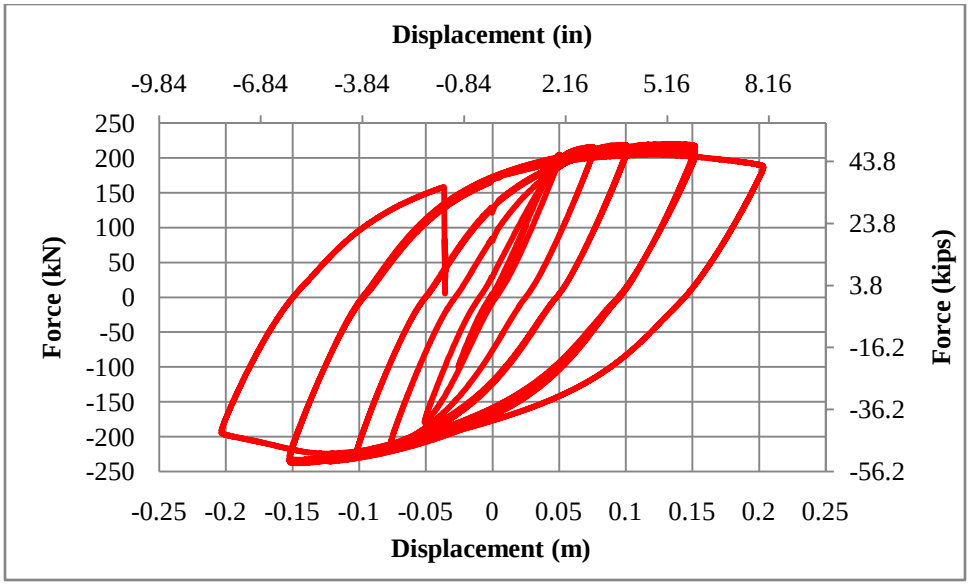

Figure 4.18 Load-displacement responses from field test for pile with CDSM soil improvement

4.3.5 Analysis Results

Figures 4.19 and 4.20 present the force-displacement response envelopes estimated using the Winkler analysis approach and their comparison with the force-displacement measured responses obtained during the field testing. Figure 4.21 and 4.22 shows the moment profile estimated using LPILE at the pile-head displacement of ±0.305 m (±12 in.) for pile without CDSM improvement and ±0.152 m (±6 in.) for pile with CDSM improvement and their comparison with the moment profile measured during the field testing. Again, the proposed methodology was used to calculate the *p-y* curve modification factors for pile embedded in CDSM improved soil profile and the lateral load analysis was performed utilizing LPILE.

From the analysis result presented in Figures 4.19 to 4.22, the following observations are made:

- the calculated elastic lateral stiffness increased by 480 % from 759 kN/m (4.3 kips/in.) to 4396 kN/m (25.1 kip/in.), which agrees well to the 420% increase obtained from the field test results;
- the calculated lateral displacement at first yielding of the pile decreased by 76 % from 0.158 m (6.2 in.) to 0.038 m (1.5 in.), which is close to the 67% decrease observed from the field test results;
- the calculated lateral resistance at maximum target displacement increased by 43% from 141 kN (31.7 kips) to 201 kN (45.2 kips), which is in an good agreement with 47% increase obtained from the field test;
- the calculated maximum moment location is about 1.5 m (4.9 ft) below the ground for pile with no ground improved, and at the ground surface for pile with ground improvement. This agrees very well with the experimental data; and
- the moment decreased to zero at a depth of 1.4 m (4.6 ft) below the ground surface in both calculated and measured moment profiles for the improved pile, which indicates that the effective depth of the ground improvement is a lot less the actual improvement depth used in the test.

The graphic comparison in Figures 4.19 and 4.20 shows that the Winkler analysis with proposed *p-y* modification factors is able to capture the full range of elastic and inelastic pile response envelopes with slopes that correspond well with the results obtained from field testing, while the observations made from the analysis results further confirm that the effectiveness of the CDSM soil improvement can be adequately evaluated using the newly developed methodology. However, the plastic hinge in the pile with CDSM soil improvement was predicted by the Winkler analysis to be developed at a lower lateral

load level compare to the test data, and the piles in both unimproved and improved soil are predicted to have a slightly lower lateral load resistance than that observed from the field test. This underestimation of the lateral load will result in an inadequately capturing shear forces within the pile sections. Therefore, appropriate safety factors should be introduced when designing the horizontal reinforcement in the pile.

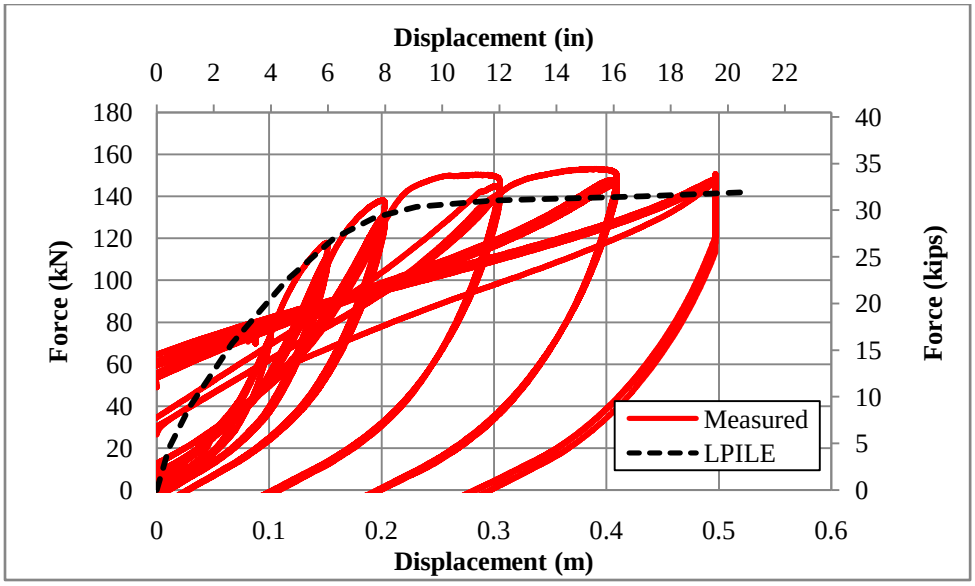

Figure 4.19 Comparison of measured cyclic force-displacement response of TPU from the field test and the computed response envelope from LPILE analysis for pile without CDSM soil improvement

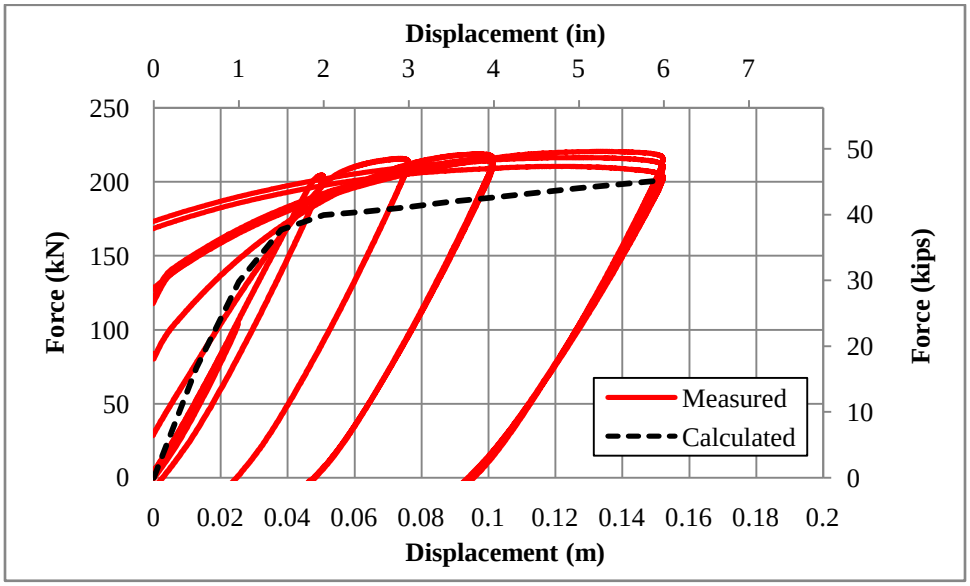

Figure 4.20 Comparison of measured cyclic force-displacement responses of TPI from field test and the computed response envelope from LPILE analysis for pile with CDSM soil improvement

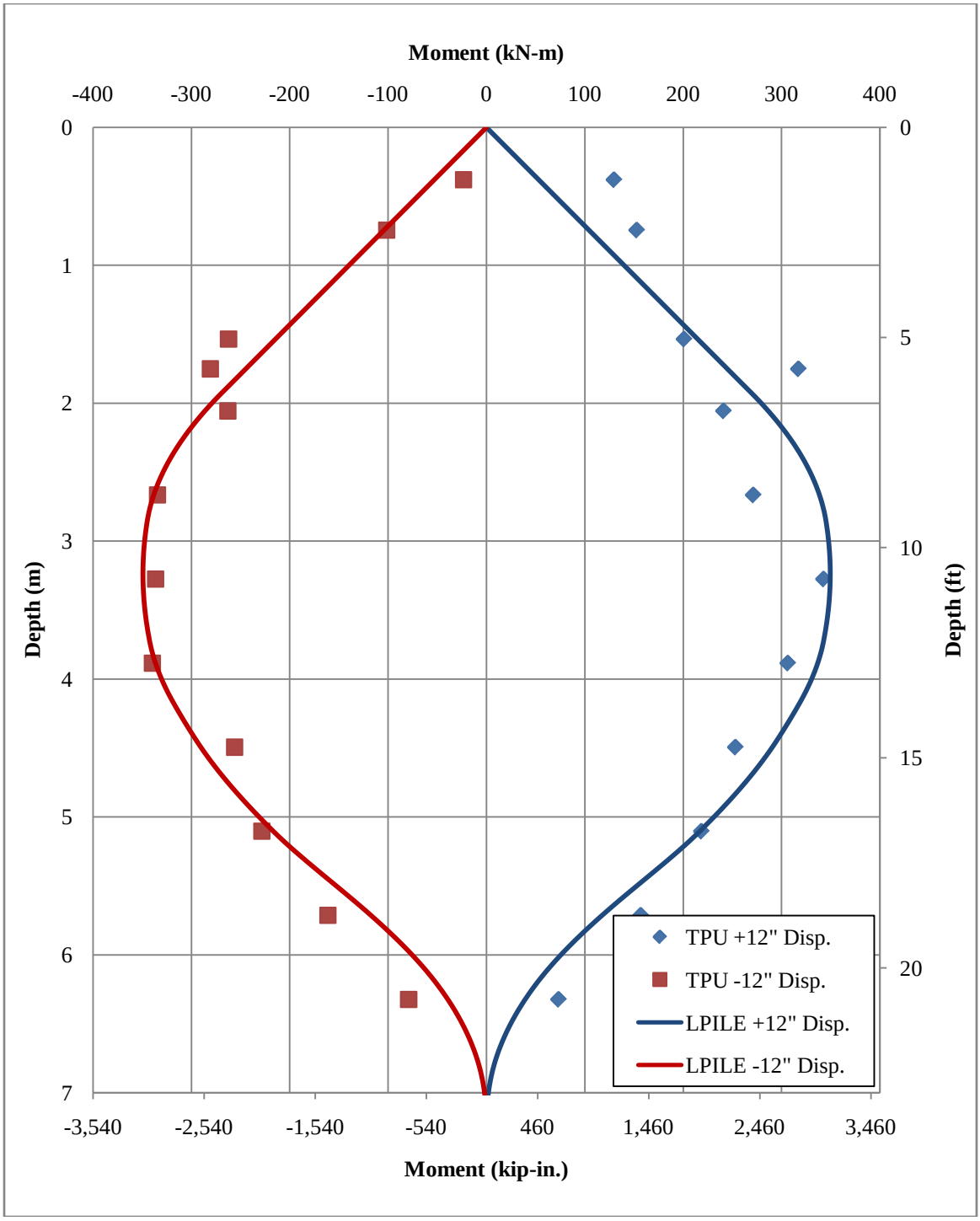

Figure 4.21 Comparison of measured moment along the pile length for TPU from field test and the computed pile moment profile from LPILE analysis for pile without CDSM soil improvement

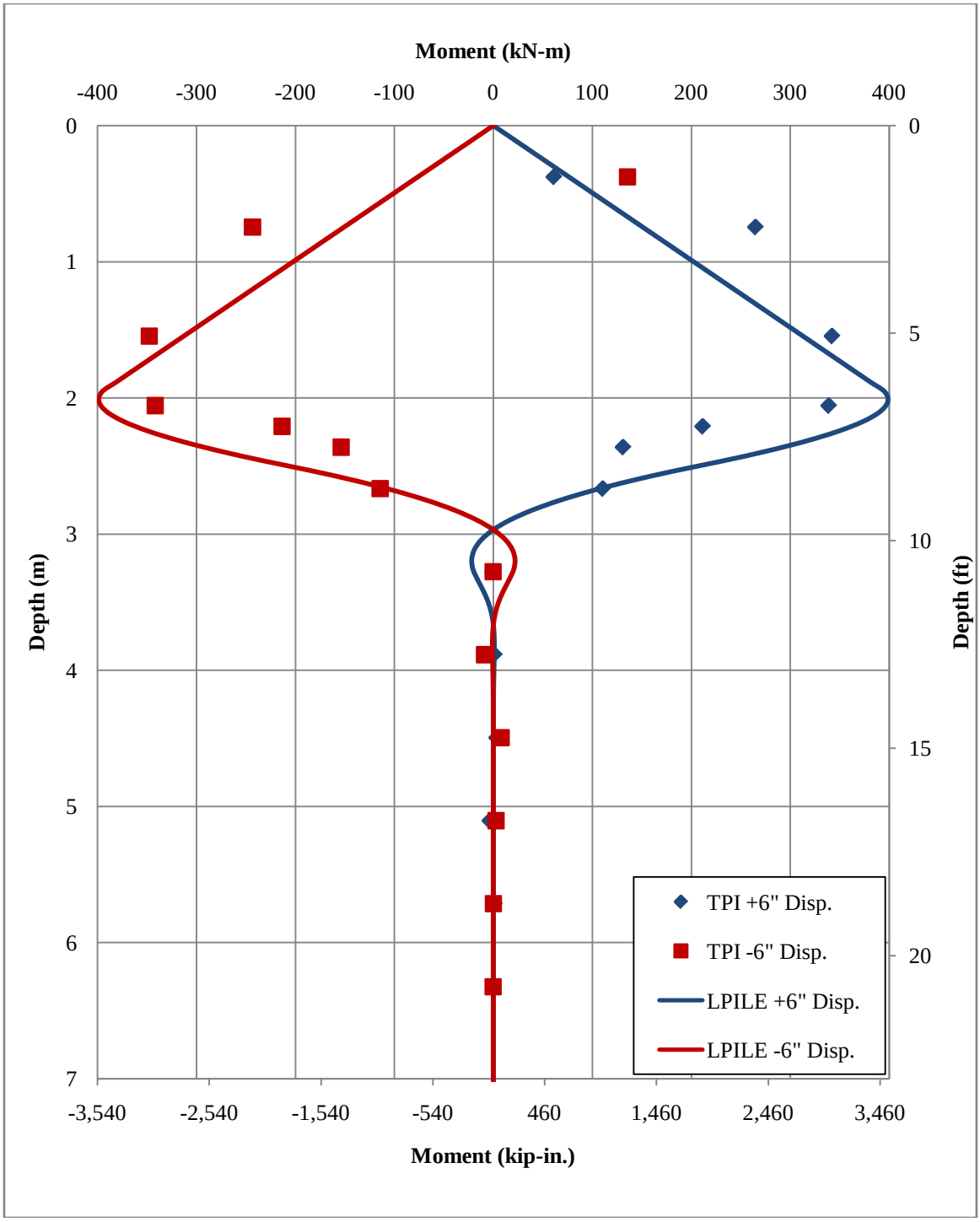

Figure 4.21 Comparison of measured moment along the pile length for TPI from field test and the computed pile moment profile from LPILE analysis for pile with CDSM soil improvement

CHAPTER 5 PERMISSIBLE LATERAL DISPLACEMENT FOR SINGLE PILE FOUNDATIONS IN CLAY SOIL WITH AND WITHOUT SOIL IMPROVEMENT

5.1 Introduction

Chapter 4 provided results from experimental tests performed on laterally loaded single pile foundations that were embedded in soft clay with and without CDSM soil improvement. The results showed that by using the CDSM soil improvement technique, the lateral displacement of a pile foundation was effectively controlled while the lateral resistance of the pile was significantly increased with increasing stiffness of the pile-soil system. The comparisons between the experimental data and results from the Winkler analysis performed using newly developed *p-y* curve modification factors demonstrated that the proposed methodology was able to capture the lateral responses of a pile foundation in a volume of CDSM-improved soil surrounded by soft clay. The effectiveness of the soil improvement can be accurately evaluated using the Winkler analysis method with modified *p-y* curve. With this in mind, a set of lateral load analyses was performed utilizing the proposed methodology to establish permissible displacements and further study the lateral behavior of single pile foundation in clay soil with and without CDSM soil improvement.

5.2 Overview of Permissible Lateral Displacement

The lateral load analyses presented herein were aimed to establish permissible limits of lateral displacements for precast, prestressed concrete piles and open-ended steel

pipe pile in different clay soil conditions by utilizing curvature capacities obtained from moment-curvature analysis of the pile sections. The “permissible limit” eventually defines the displacement that a specific pile, in a given soil, can undergo prior to experiencing failure. Failure is a term engineers use to describe partial or total collapse of a structure, and is generally associated with ultimate limit state. For laterally loaded piles, an ultimate limit state is reached if the resistive stresses in the soil attain the limit (yield) value over a substantial portion of the pile length so that plastic flow occurs within the soil mass resulting in large lateral deflection, translation or rotation of pile and eventual collapse of the structure. Such failures would mostly occur in the case of rigid piles. For flexible piles, a plastic wedge of soil may form at the front leading to excessive lateral deflection and bending. In addition to soil collapse, collapse of the pile itself is also possible. Plastic hinges may be formed in flexible piles due to excessive bending, which may eventually lead to collapse. In this study, the ultimate limit state is defined by the first flexural failure of a plastic hinge and the curvature associated with this limit state was used to define the permissible lateral displacement of the precast, prestressed concrete piles. However, ultimate limit states generally do not govern the failure of a laterally loaded steel pipe pile due to the ductile properties of steel. As observed in the field test presented in chapter 4, pile failure caused by local buckling at the side wall of the steel test pile happened much before the ultimate limit state is reached. Therefore, to define the permissible lateral displacement of a steel pile, curvature associated with local buckling should be used instead of the ultimate curvature.

5.3 Lateral Load Analysis

To establish the permissible lateral displacement limits for precast, prestressed piles in different clay soil conditions with and without CDSM soil improvement, LPILE was utilized to perform the lateral load analysis. Twe different boundary conditions at the pile head were investigated: 1) fixed head; 2) pinned head.

5.3.1 Pile Choice

A variety of prestressed precast concrete piles are standardized by the precast industry. The cross sections of these piles may be square and solid, square and hollow, octagonal and solid, octagonal and hollow, circular and solid or circular and hollow. Of the different cross sections, the precast, prestressed piles with solid square cross sections and solid octagonal cross sections are the most commonly used types in design practice in seismic regions (Arulmoli, 2006). This is due to the fact that the square piles types are easier to cast, while the octagonal piles minimize the impact of spalling on the moment-curvature response of these piles. Given the typical length requirements, it is convenient to cast the precast, prestressed piles in a horizontal position rather than in a vertical position. With the piles being cast horizontally, the square piles, in particular, provide an ease to the casting process. The most common sizes utilized in current seismic design practice are 12-inch, 14-inch, and 16-inch square piles, and 16-inch and 24-inch octagonal piles.

Over 200 moment-curvature analyses were performed by Fanous et al. (2010) on different octagonal and square pile sections in a study of newly developed confinement equations for design of prestressed concrete piles. The compressive strength of

unconfined concrete, the compressive stress in the concrete gross section due to prestress (after losses), and the axial load ratio were the primary variables in these analyses. Table 5.1 represents the ultimate curvatures that were established for the 16-inch octagonal prestressed pile sections. In this table, Pile 1 through Pile 7 represent the identified maximum and the minimum curvature capacities, including their f_{pc}, $f_c^{'}$ and axial load ratio values. Given that these piles represent the boundaries of the curvature capacities, only these seven 16-inch octagonal prestressed piles were selected for the lateral load analysis to establish the displacement limits.

Table 5.1. Ultimate curvature values of 16-inch octagonal prestressed piles using confinement reinforcement based on the newly developed equation, English unit (Fanous et al., 2010)

	Axial Load Ratio						
	0.2	**0.25**	**0.3**	**0.35**	**0.4**	**0.45**	**0.5**
16-inch Octagonal Pile with $f_c^{'}$ = 6000 psi							
fpc-700	0.00363 (Pile 1)	0.00338	0.00320	0.00305	0.00292	0.00280	0.00269 (Pile 7)
fpc-900	0.00356	0.00335	0.00317	0.00301	0.00288	0.00276	**x**
fpc-1100	0.00348	0.00328	0.00311	0.00298	0.00287	0.00277	**x**
fpc-1200	0.00340	0.00357	0.00310	0.00297	0.00287	0.00276 (Pile 4)	**x**
16-inch Octagonal Pile with $f_c^{'}$ = 8000 psi							
fpc-700	0.00364 (Pile 2)	0.00337	0.00318	0.00302	0.00288	0.00275	**x**
fpc-1000	0.00273	0.00335	0.00316	0.00299	0.00285	0.00273	**x**
fpc-1300	0.00343	0.00344	0.00309	0.00295	0.00282	0.00271	**x**
fpc-1600	0.00334	0.00317	0.00303	0.00291	0.00280	0.0027 (Pile 5)	**x**
16-inch Octagonal Pile with $f_c^{'}$ = 10000 psi							
fpc-700	0.00364 (Pile 3)	0.00336	0.00316	0.00299	0.00284	0.00272	**x**
fpc-1200	0.00348	0.00327	0.00310	0.00295	0.00282	0.00270	**x**
fpc-1600	0.00339	0.00320	0.00304	0.00291	0.00279	0.00268 (Pile 6)	**x**
fpc-2000	0.00333	0.00316	0.00301	0.00288	0.00277	**x**	**x**

x Not considered due to $\phi_{cr} > \phi_{sp}$

In order to compare the lateral behavior of concrete pile with that of a steel pile, the open-ended steel pipe pile from full-scaled field testing presented in chapter 4 was also selected for the lateral load analysis to establish permissible displacement for steel pile, and is designated as Pile S2 in this study. As shown in Figure 5.1, the moment-curvature responses compares very well with the selected 16-inch octagonal concrete pile 2. A buckling curvature of 0.0874 m^{-1} (0.00222 in^{-1}) was use to define the permissible displacement for this pile with fixed-head boundary condition. This was found by identifying the curvature associated with the strain at the outer wall of the pile section equal to the compressive strain induced at the buckling location during the experimental test, which was 0.023. For the pinned-head boundary condition, the maximum curvature of this pile was expected to happen below the ground surface. Due to the support provided by the surrounding soil at outer wall of this pile section, the buckling is expected to happen in the direction of towards the pile axis. Therefore, a buckling curvature of 0.0906 m^{-1} (0.00230 in^{-1}) was found for the pile with pinned head by identifying the curvature associated with the strain at the inner wall of the pile section equal to the compressive strain induced at the buckling location during the experimental test.

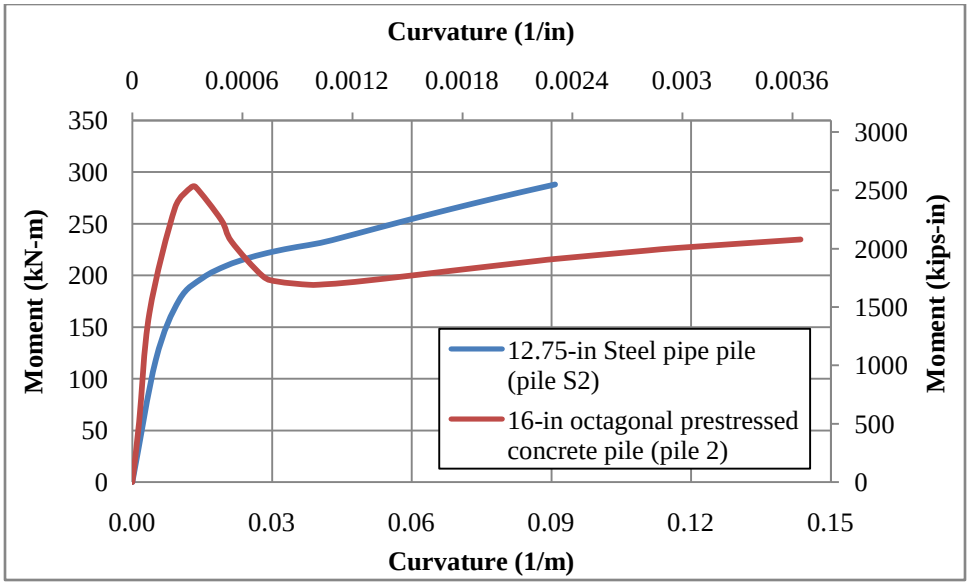

Figure 5.1 Moment-curvature responses for Pile 2 and Pile S2

5.3.2 Soil Type

Five different clay soil types and the corresponding parameter values were established for the lateral load analyses after consultation with Earth Mechanics, Inc. These soil models were selected in order to cover the full range of the soil conditions defined in Table 20.3-1 of ASCE 7-05. Table 5.2 gives the s_u, ε_{50}, k, and γ_{dry}, of the clay chosen for the LPLIE analysis, where

- s_u = average undrained shear strength;
- ε_{50} = strain at 50% of the strength;
- γ_{dry} = effective unit weight; and

ASCE 7 soil conditions and the corresponding parameter values are also included in Table 4.2 for the purpose of classification and comparison.

In addition to the soil conditions provided in Table 4.2, a CDSM soil improvement with improvement volume of 9D×9D×9D (D stands for the diameter of the pile) was also used in the analyses with following parameter:

- s_u = 375 kPa (54.4 psi);
- ε_{50} = 0.004; and
- γ_{dry} = 13.039 kN/m^3 (0.048 pci).

5.3.3 Sample Analysis

This section provides a sample lateral load analysis of fixed-headed Pile 1 embedded in very stiff clay. The properties of this pile are as follows:

- $f_c^{'}$ = 41.4 MPa (6000 psi);
- f_{pc} = 4.83 MPa (700 psi);
- $P_e / f_c^{'} A_g$ = 0.2;
- length = 9.144 m (30 ft);
- moment of inertia = 0.00164 m^4 (3952 in.^{4}); and
- modulus of elasticity = 30.4 GPa (4415 ksi).

The moment versus curvature response of this pile section was obtained using OpenSees, which is comprised of 250 data points. This 250 data set was then condensed to approximately 20 data points, which were included in the form of M vs. EI in LPILE. Figure 5.2 plots the complete moment versus curvature response with that based on the condensed number of data points. The comparison between the two curves ensures that the moment-curvature response of the pile was accurately represented in the LPILE analyses.

Table 5.2. Parameters selected for the soil models used in LPILE for the ASCE 7 soil classes (Fanous et al., 2010)

Site Class (ASCE 7-05)	Site Description (ASCE 7-05)			Soil Type (Interpreted)	Soil Parameters (Interpreted for prestressed pile study)		
	V_s (average shear wave velocity)	$\overline{N}$ (average field standard penetration resistance for top 100 ft)	s_u (undrained shear strength)		s_u	ε_{50}	γ_{dry}
A. Hard rock	> 5000 ft/s	NA	NA	NA	NA	NA	NA
B. Rock	2500 to 5000 ft/s	NA	NA	NA	NA	NA	NA
C. Very dense soil and soft rock	1200 to 2500 ft/s	> 50	> 2000 psf	Hard clay (Matlock)	192-383 KPa 4000-8000 psf	0	14.0 kN/m^3 108 pcf
				Very stiff clay (Matlock)	96-192 KPa 2000-4000 psf	0	
D. Stiff soil	600 to 1200 ft/s	15 to 50	1000 to 2000 psf	Stiff clay (Matlock)	48-96 KPa 1000-2000 psf	0.01	
E. Soft clay soil	< 600 ft/s	< 15	< 1000 psf	Medium clay (Matlock)	24-48 KPa 500-1000 psf	0.01	11.5-14.6 kN/m^3 73-93 pcf
				Soft clay (Matlock)	12-24 KPa 250-500 psf	0.02	
F. Soil requiring site analysis	NA						

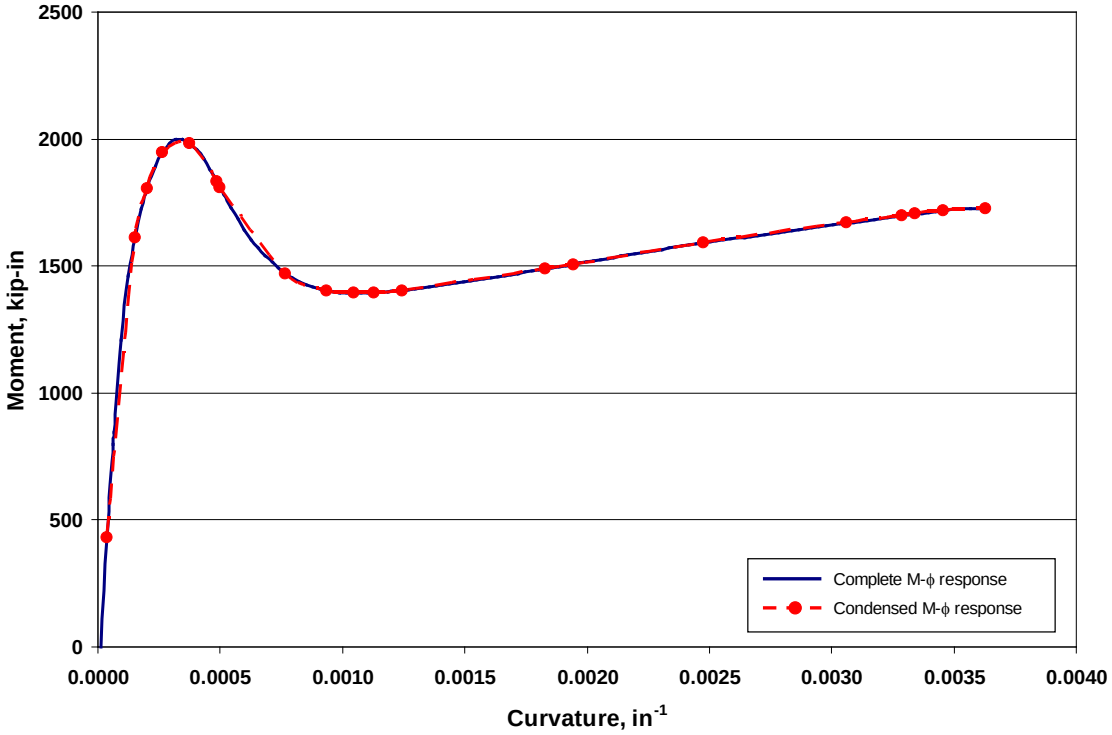

Figure 5.2. Complete moment versus curvature response of Pile 1 section from OpenSees with the condensed moment versus curvature relationship input used in LPILE (Fanous et al., 2010)

After entering the pile properties as well as the moment versus curvature relationship, the soil parameters were defined in LPILE. The following values were used to compose the very stiff clay:

- $\gamma = 0.0625$ lb/in^3;
- undrained cohesion, $c = 20.83$ lb/in^2; and
- strain factor, $\varepsilon_{50} = 0.004$.

For soil profiles contain the CDSM soil improvement, the *p-y* curve modification factors established using the proposed methodology should be entered in addition to the soil parameters.

The final step in the analysis was to define the boundary conditions. To simulate a fixed head at the pile top, the pile head was maintained at zero slope, while the lateral displacement of the pile at this location was progressively increased. Figure 5.3 depicts the boundary condition input for this particular case, where condition 1 represents the lateral displacement at the pile head, while condition 2 represents the slope at the pile head.

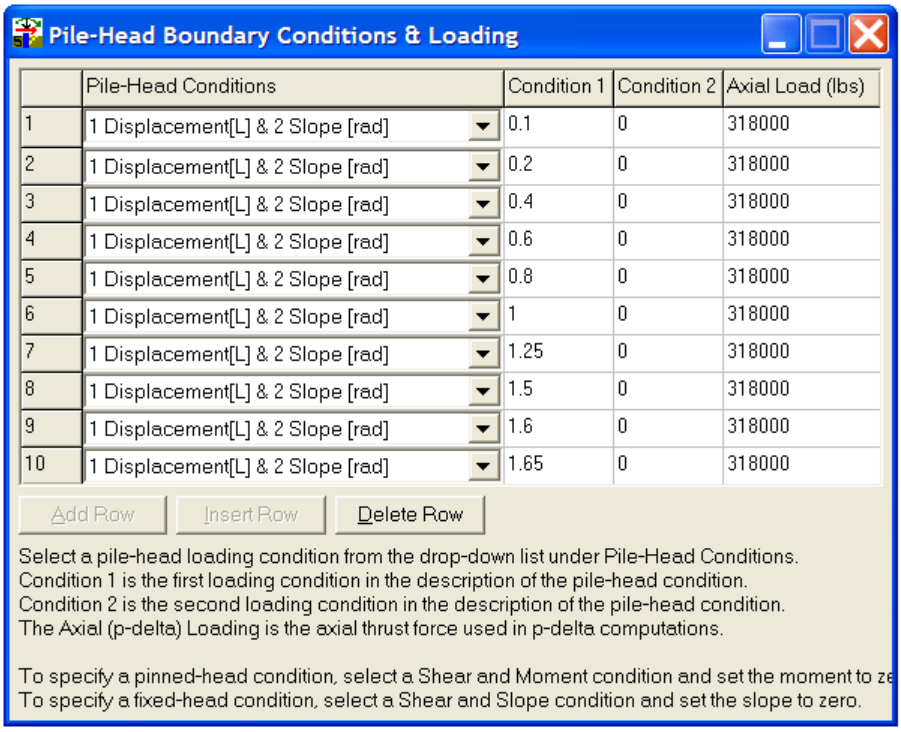

Figure 5.3. An example of boundary conditions input in LPILE (Fanous et al., 2010)

Once the boundary conditions are entered in LPILE, the execution of the analysis followed. With the completion of running the analysis, LPILE provides an output along the length of the pile for each target lateral displacement. The LPILE output along the pile length includes:

- deflection;

- moment;
- shear;
- slope;
- total stress;
- flexural rigidity; and
- soil resistance.

To assure that LPILE was utilizing the moment versus curvature relationship provided as an input to define the pile section characteristics, the maximum curvature that the pile sustained was determined at each lateral displacement step, and then they were compared with the input data. Figure 5.4 shows this comparison in a graphical form, which confirms that the pile response was accurately modeled in LPILE.

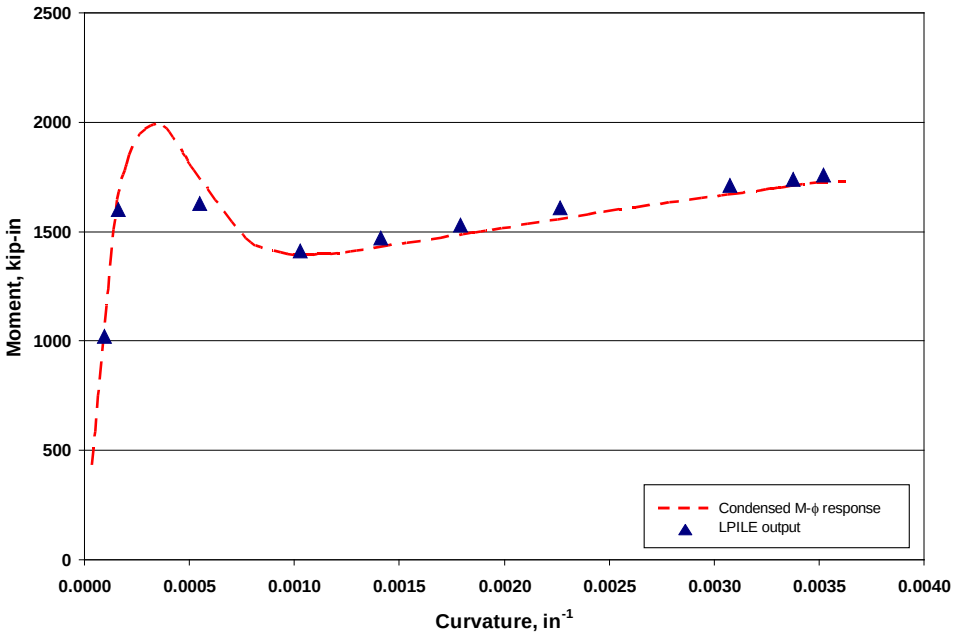

Figure 5.4. Comparison of LPILE output against the moment versus curvature response used as the input in LPILE for Pile 1 (Fanous et al., 2010)

The maximum lateral displacement of the 16-inch octagonal pile embedded in very stiff clay was 0.04191 m (1.65 in), which was attained when the curvature corresponding to the maximum moment reached the ultimate curvature of the pile. Figure 5.5 compares the displacement, shear, and moment profiles obtained for this analysis case, at lateral displacements of 0.00254 m (0.1 in) and 0.042 m (1.65 in).

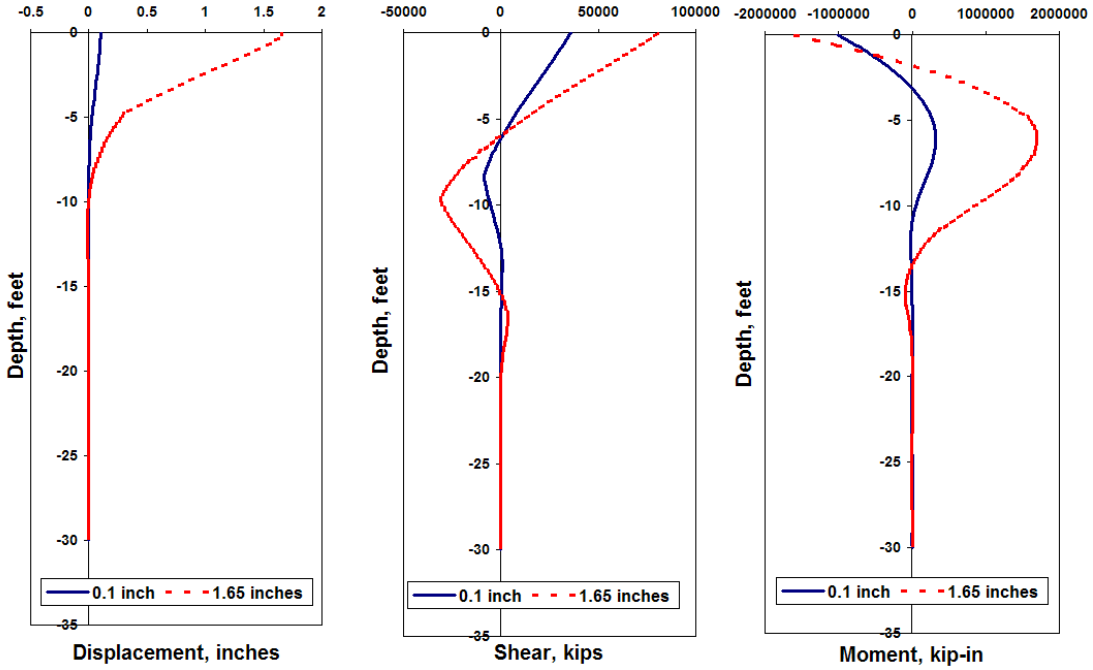

(a) (b) (c)

Figure 5.5 (a) Displacement, (b) Shear, and (c) Moment profiles of a 16-inch octagonal prestressed fixed-head pile in a very stiff clay at a small and ultimate displacements (Fanous et al., 2010)

4.6.4 Analyses Results

A summary of the results obtained from the LPILE analysis of the seven prestressed precast concrete piles and the steel pipe pile are presented in this section. Tables 5.3(a) and 5.3(b) provide the permissible displacement limits that were established

for each of the concrete piles analyzed with a fixed pile head and a pinned pile head in clay with and without CDSM soil improvement. A summary of the compressive strength of the unconfined concrete, $f_c^{'}$, the compressive stress in the concrete at the centroid of the cross section due to prestress (after losses), f_{pc}, and the axial load ratio used in the LPILE analysis are included in the same table. The upper-bound values of the permissible displacement limits in the tables were obtained from the pinned-head analyses, while the lower-bound values were established by the fixed-head analyses. Table 5.4 shows the permissible displacement limits that were established for steel pile, and is compared with the permissible displacement limits established for concrete pile No.2.

From the results presented in Tables 5.3(a), 5.3(b) and 5.4, the following observations can be made:

- a pile with a pinned head will experience a larger lateral displacement at the pile head than that with a fixed head, when embedded in the same soil profile;
- the lateral displacement limits of piles embedded in clay with both fixed head and pinned head conditions decrease as the undrained shear strength and the effective unit weight increase;
- at large lateral displacements, the displacement component induced by the axial load (i.e., the P-Δ effect) was larger than that caused by the lateral load acting on the pile, which was analyzed in several different soil conditions with a pinned pile head (these values are identified by " * " in Table 4.3 and 4.4). Consequently, the ultimate condition could not be reached for these cases, and thus the reported results do not appear to always follow some of the aforementioned trends.

However, it is important to realize that the displacements calculated for these piles far exceed the displacements that may be permitted for these piles to experience under seismic lateral load without causing instability to the entire structure, which in turn implies the need of soil improvement to control the excessive displacements in these cases;

- the steel pile with a pinned head will experience a larger lateral displacement at the pile head than the concrete piles with a pinned head will experience, when embedded in the same soil profile;
- the steel pile with a fixed head will experience same level of lateral displacement at the pile head than the concrete piles with a fixed head will experience, when embedded in the same soil profile;
- by providing an volume of CDSM soil improvement around the prestressed precast concrete piles embedded in medium clay and soft clay, the permissible displacement limit reduced by an average of 66%; and
- by providing an volume of CDSM soil improvement around the steel pipe pile embedded in medium clay and soft clay, the permissible displacement limit reduced by an average of 79%.

Table 5.3(a). Permissible displacement limits established for 16-inch octagonal prestressed piles with a fixed pile head and a pinned pile head in clay soils with and without CDSM improvement (SI unit)

Soil Type (Interpreted for prestressed pile study)	Permissible Displacement Limits (m)						
	Pile 1 $f'_c = 41.4$ MPa $f_{pc} = 4.8$ MPa $P/f'_cA_g = 0.2$	**Pile 2** $f'_c = 55.2$ MPa $f_{pc} = 4.8$ MPa $P/f'_cA_g = 0.2$	**Pile 3** $f'_c = 68.9$ MPa $f_{pc} = 4.8$ MPa $P/f'_cA_g = 0.2$	**Pile 4** $f'_c = 41.4$ MPa $f_{pc} = 8.3$ MPa $P/f'_cA_g = 0.45$	**Pile 5** $f'_c = 55.2$ MPa $f_{pc} = 11.0$ MPa $P/f'_cA_g = 0.45$	**Pile 6** $f'_c = 68.9$ MPa $f_{pc} = 11.0$ MPa $P/f'_cA_g = 0.45$	**Pile 7** $f'_c = 41.4$ MPa $f_{pc} = 4.8$ MPa $P/f'_cA_g = 0.5$
Hard clay	0.033-0.036	0.034-0.047	0.037-0.501	0.027-0.076	0.028-0.086	0.028-0.081	0.024-0.032
Very stiff clay	0.042-0.064	0.048-0.056	0.051-0.060	0.036-0.103	0.042-0.113	0.039-0.105	0.029-0.041
Stiff clay	0.062-0.081	0.066-0.084	0.071-0.077	0.051-0.128	0.071-0.154*	0.060-0.142*	0.041-0.051
Medium clay	0.099-0.112	0.107-0.113	0.114-0.119	0.095-0.164	0.105-0.155*	0.107-0.117*	0.065-0.069
Soft clay	0.166-0.165*	0.174-0.154*	0.191-0.168*	0.140-0.123*	0.164-0.100*	0.136-0.091*	0.105-0.108
Medium clay with CDSM improvement	0.033-0.081	0.046-0.088	0.041-0.089	0.032-0.086	0.039-0.091	0.042-0.098	0.024-0.056
Soft clay with CDSM improvement	0.046-0.093	0.051-0.100	0.053-0.100	0.039-0.097	0.051-0.108	0.051-0.108	0.032-0.064

* Ultimate condition did not reach due to significantly high P-Δ effects

Table 5.3(b). Permissible displacement limits established for 16-inch octagonal prestressed piles with a fixed pile head and a pinned pile head in clay soils with and without CDSM improvement (English unit)

Soil Type (Interpreted for prestressed pile study)	Permissible Displacement Limits (in.)						
	Pile 1 $f'_c = 6000$ psi $f_{pc} = 700$ psi $P/f'_cA_g = 0.2$	**Pile 2** $f'_c = 8000$ psi $f_{pc} = 700$ psi $P/f'_cA_g = 0.2$	**Pile 3** $f'_c = 10000$ psi $f_{pc} = 700$ psi $P/f'_cA_g = 0.2$	**Pile 4** $f'_c = 6000$ psi $f_{pc} = 1200$ psi $P/f'_cA_g = 0.45$	**Pile 5** $f'_c = 8000$ psi $f_{pc} = 1200$ psi $P/f'_cA_g = 0.45$	**Pile 6** $f'_c = 10000$ psi $f_{pc} = 1600$ psi $P/f'_cA_g = 0.45$	**Pile 7** $f'_c = 6000$ psi $f_{pc} = 700$ psi $P/f'_cA_g = 0.5$
Hard clay	1.30-1.40	1.35-1.85	1.45-2.00	1.05-3.00	1.10-3.40	1.10-3.20	0.95-1.25
Very stiff clay	1.65-2.50	1.90-2.20	2.00-2.35	1.40-4.05	1.65-4.45	1.55-4.15	1.15-1.60
Stiff clay	2.45-3.20	2.60-3.30	2.80-3.05	2.00-5.05	2.80-6.05*	2.35-5.60*	1.60-2.00
Medium clay	3.90-4.40	4.20-4.45	4.50-4.70	3.75-6.45	4.15-6.10*	4.20-4.60*	2.55-2.70
Soft clay	6.55-6.50*	6.85-6.05*	7.50-6.60*	5.50-4.85*	6.45-3.95*	5.35-3.60*	4.15-4.25*
Medium clay with CDSM improvement	1.30-3.20	1.80-3.45	1.60-3.50	1.25-3.40	1.55-3.60	1.65-3.85	0.95-2.20
Soft clay with CDSM improvement	1.80-3.65	2.00-3.95	2.10-3.95	1.55-3.80	2.00-4.25	2.00-4.25	1.25-2.50

* Ultimate condition did not reach due to significantly high P-Δ effects

Table 5.4. Permissible displacement limits established for a 16-inch octagonal prestressed pile with a partially-fixed pile head in different soil types

Soil Type	Permissible Displacment Limits (m)			
	Pile with fixed head		Pile with pinned head	
	Pile 2 (Prestressed precast concrete pile)	Pile S2 (Steel pipe pile)	Pile 2 (Prestressed precast concrete pile)	Pile S2 (Steel pipe pile)
Hard Clay	0.034 m (1.35 in)	0.029 m (1.15 in)	0.047 m (1.85 in)	0.098 m (3.85 in)
Very stiff clay	0.048 m (1.90 in)	0.042 m (1.65 in)	0.056 m (2.20 in)	0.140 m (5.50 in)
Stiff clay	0.066 m (2.60 in)	0.062 m (2.45 in)	0.084 m (3.30 in)	0.191 m (7.50 in)
Medium clay	0.107 m (4.20 in)	0.097 m (3.80 in)	0.113 m (4.45 in)	0.248 m (0.75 in)
Soft clay	0.174 m (6.85 in)	0.169 m (6.65 in)	0.15 m* (6.05 in*)	0.288 m (11.35 in)
Medium clay with CDSM improvement	0.046 m (1.80 in)	0.024 m (0.95 in)	0.088 m (3.45 in)	0.050 m (1.95 in)
Soft clay with CDSM improvement	0.051 m (2.00 in)	0.030 m (1.20 in)	0.100 (3.95 in)	0.065 m (2.55 in)

* Permissible displacement falls outside the range established for the fixed-head and pinned head analyses

CHAPTER 6 SUMMARY, CONCLUSIONS AND RECOMMENDATIONS

6.1 Introduction

The research of developing a method to account for the effect of soil improvement specifically the cement-deep-soil-mixing on the lateral behavior of a single pile in soft clay using the Winkler analysis approach was the focus of this thesis. This research was motivated by the lack of study on the topic of laterally loaded piles in soft clay and improved soils. Despite the widespread presence of this soil type in high seismic regions and the frequent need to locate bridges and buildings in soft clay, only a few investigations have been carried out to guide engineers in evaluating the effectiveness of ground improvement techniques on increasing the lateral resistance of pile foundation embedded in soft clay, and no numerical models have been validated to evaluate this approach. Thus, the objective of this research was to develop modified *p-y* curves for Winkler analysis to characterize the lateral load behavior of a single pile embedded in a volume of CDSM-improved clay surrounded by unimproved soft clays. The sections to follow provide a summary of the completed work, conclusions of the project, as well as recommendations that have developed throughout the investigation of the project.

6.2 Summary

The project began with an overall introduction of laterally loaded piles with emphasis on the load transfer mechanism. The pile performances in soft clay were

investigated through the observations during past earthquakes and quantitative analysis results. Available analysis methods for soil-pile interaction problem and types of ground improvement techniques were briefly discussed and the scope of research was defined.

A detailed literature review was completed, aiming to gain knowledge on the development and fields of applications together with limitations of each ground improvement techniques. The ability of each available analysis method for lateral loaded piles have been assessed for determining lateral responses of pile foundation in a volume of improved soil surrounded by unimproved soil. Previous analytical work and case studies on laterally loaded pile in soft clay with ground improvement have been investigated to study the effectiveness of the ground improvement on increasing lateral resistance of pile foundations.

A method of developing *p-y* curve modification factors to account for the effect of the CDSM-improved soil on enhancing the lateral load behavior of a single pile embedded in soft clay was developed by integrating the effectiveness of the improved soil into the procedures of constructing *p-y* curves for stiff clay recommended by Welch and Reese (1972). It was achieved by estimating the effective length for a infinitely long soil layer with CDSM so that the fraction of the load resisted by the soil improved over a limited horizontal extent could be accounted for by taking the ratio between the soil resistance attenuation at actual length of the soil improvement and the effective length. The accuracy of the method was verified against the centrifuge test data from Liu et al. (2010) and the full scale field test from Fleming et al. (2010).

A set of lateral load analyses was performed to establish permissible displacements for precast, prestressed concrete piles as well as open-ended steel pipe pile

prior to reaching the curvature capacity of piles. Different clay soil conditions with and without CDSM ground improvement were used in the analysis in order to analytically study the effectiveness of the CDSM ground improvement technique on controlling the lateral displacement of pile foundations.

6.3 Conclusions

The following conclusions were drawn based on the completed study presented in this report:

- From the detailed literature reviews completed for this study, following knowledgments were learned:
  - soil mixing is a versatile ground improvement method which can be used to stabilize a wide range of soils, including soft clays, silts and fine grained sands. The main areas of soil mixing applications are foundation support, retention systems, ground treatment, liquefaction mitigation, hydraulic cut-off walls and environmental remediation;
  - among the available analysis methods for SSI problem, elastic continuum and finite element approaches have the ability to analyze lateral loaded piles embedded in a volume of improved soil surrounded by soft clay due to their three-dimensional nature. However, the computational cost of these fully coupled analysis methods is expensive and do not provide simple, practical steps for use in routine design practice; and
  - the study of previous investigations on laterally loaded pile in soft clay with ground improvement showed that the ground improvement dose have the

potential for being more cost-efficient to solve the problem of poor pile performance in soft clay, however, no numerical model have been validated for evaluating this approach.

- A method was developed to establish *p-y* curve modification factors for soil profile which consist of a volume of CDSM improved soil surrounded by soft clay. With the newly developed modification factors, Winkler analysis method can be easily performed to analyze laterally loaded pile in improved soft clay and provide simple, practical steps for use in design.
- Verifications using the experimental data by Liu et al. (2010) and Fleming et al. (2010) demonstrated that the Winkler analysis with proposed *p-y* modification factors is able to capture the full range of elastic and inelastic pile responses with slopes that correspond well with the results obtained from field testing, the effectiveness of the CDSM soil improvement can be adequately evaluated. The following conclusion was drawn from the verifications:
  - the lateral resistance increased by 320% for CDSM soil improvement dimensions 13D×13D×9D, which is in close agreement with the 340% increase obtained from the centrifuge test #1;
  - the elastic lateral stiffness for piles from centrifuge test #2 increased by 167% and 433% for CDSM soil improvement dimensions 9D×9D×6D and 13D×13D×9D, respectively, which agrees well to the 163% and 420% increase that observed from experimental data;

- the calculated elastic lateral stiffness for piles with CDSM soil improvement dimensions 13D×13D×9D and 17D×17D×12D has no significant increase, same trend have been observed in centrifuge test #2;
- the elastic lateral stiffness increased by 480% comparing to the 420% increase obtained from the field test results;
- the lateral displacement at yielding of the pile decreased by 7.6 % comparing to the 6.7% decrease observed from the field test results;
- the lateral resistance increased by 43% comparing with 47% increase obtained from the field test; and
- the plastic hinge in the pile with CDSM soil improvement was developed at a lower lateral load level compare to the test data, and the lateral load resistance of the piles was slightly lower than that observed from the field test.

- From the analytical study of the permissible displacement limit of prestressed precise concrete pile and steel pipe pile, following conclusion was drawn:
  - the lateral displacement limits of piles embedded in clay with both fixed head and pinned head conditions decrease as the undrained shear strength and the effective unit weight increase;
  - the steel pile with a pinned head will experience a larger lateral displacement at the pile head than the concrete piles with a pinned head will experience, when embedded in the same soil profile;
  - the steel pile with a fixed head will experience same level of lateral displacement at the pile head than the concrete piles with a fixed head will experience, when embedded in the same soil profile;

- by providing an volume of CDSM soil improvement around the prestressed precast concrete piles embedded in medium clay and soft clay, the permissible displacement limit reduced by an average of 66%; and
- by providing an volume of CDSM soil improvement around the steel pipe pile embedded in medium clay and soft clay, the permissible displacement limit reduced by an average of 79%.

6.4 Recommendations

Though the duration of this project, the lack of studies on the topic of laterally loaded piles in soft clay with ground improvement was noticed, and no numerical model of analyzing piles with ground improvement have been validated. This motivated the author to develop *p-y* curve modification factors for use in the Winkler analysis to capture the lateral responses of a single pile embedded in a volume of CDSM-improved clay surrounded by soft clays. The newly developed methodology was verified against the centrifuge test data from Liu et al. (2010) and field test data from Fleming et al. (2010). Through the performed analysis during this study, the following recommendations are established:

- to gain more confidence in the proposed method, verifications on capturing the local responses (e.g. maximum moment location) of laterally loaded piles are required;
- the experimental test data used for verification of the proposed method were obtained from steel pipe pile. Therefore, it is recommended that the ability of the

proposed method on capturing lateral behavior of concrete piles should be investigated further;

- more analytical study can be performed for piles embedded in different ground improvement scenarios (e.g. vary the horizontal extent of the improvement while keeping the depth of the improvement the same); and
- pile group effect should be investigated to further expand the capability of the proposed method.

REFERENCES

ACI Committee 318. *Building Code Requirements for Structural Concrete (ACI 318-05) and Commentary (318R-05)*, American Concrete Institute, Farmington Hills, Michigan, 2005.

Al-Tabbaa, A. and Evans, Ch. "Geoenvironmental research and applications of Deep Soil Mixing in the UK, *Proceedings of Deep Mixing Workshop 2002 in Tokyo,* Port and Airport Research Institute & Coastal Development Institute of Technology, 2002.

American Society of Civil Engineers. *ASCE-7 Minimum Design Loads for Buildings and Other Structures*. American Society of Civil Engineers, 2005.

Baguelin, F., Frank, R. & Saïd, Y. H. Theoretical study of lateral reaction mechanism of piles. *Geotechnique* 27, No. 3, 405-434, 1977.

Basack, S., and Purkayastha, R.D. "Behavior of Single Pile Under Lateral Cyclic Load in Marine Clay." *Asian Journal of Civil Engineering (Building and Housing)*, 8(4), 443-458, 2007.

Basu, Dipanjan. *Analysis of Laterally Loaded Piles in Layered Soil,* PhD. Dissertation, Purdue University, West Lafayette, Indiana, 2006.

Bergado, D.T., Anderson, L.R., Miura, N., Balasubramaniam, A.S. *Soft Ground Improvement in Lowland and Other Environments*, ASCE, 1996.

Bhomik, S. and Long, J. "An Analytical Investigation of the Behavior of Laterally Loaded Piles," *Proc. Geotech. Eng. Congress*, Vol. 2, ASCE Spec. Pub. 27, 1307-1318, 1991.

Boulanger, R.W., Curras, C.J., Kutter, B.L., and Wilson, D.W. "Seismic Soil-Pile-Structure Interaction Experiments and Analyses." *Journal of Geotechnical and GeoenvironmentalEngineering*, ASCE, 125(9), 750-759, 1999.

Boulanger, R.W., and Tokimatsu, K. (Eds.). "Seismic Performance and Simulation of Pile Foundations in Liquefied and Laterally Spreading Ground." In *Geotechnical Special Publication No. 145*, ASCE, New York, 2006.

Broms, B. B., "Design of laterally loaded piles". *Journal of Soil Mechanics and Foundation Division,* ASCE 91, No. SM3, 79-99, 1965.

Brown, D., Shie, C., and Kumar, M. "P-Y Curves for Laterally Loaded Piles Derived from Three Dimensional Finite Element Model," *Proc. 3rd Intl. Symposium on Numerical Models in Geomechanics*, Niagra Falls, 683-690, 1989.

Brown, D. and Shie, C. "Modification of P-Y Curves to Account for Group Effects on Laterally Loaded Piles," *Proc. Geotech. Eng. Congress*, Vol. 1, ASCE Spec. Pub. 27, 479-490, 1991.

Cai, Y., Gould, P., and Desai, C. "Numerical Implementation of a 3-D Nonlinear Seismic S-P-S-I Methodology," in Seismic Analysis and Design for Soil-Pile-Structure Interactions, Geotech. Spec. Pub. 70, ASCE, 96-110, 1995.

CEN TC 288, *Execution of Special Geotechnical Works – Deep Mixing*, Provisional Version, presented during Deep Mixing Workshop, Tokyo, 2002.

Davisson, M. T. & Gill, H. L. Laterally loaded piles in a layered soil system. *J. Soil Mech. Fdn. Div., Am. Soc. Civ. Engrs.* 89, No. SM3, 63-94, 1963.

Desai, C. and Appel, G. "3-D Analysis of Laterally Loaded Structures," *Proc. 2nd Intl. Conf. on Numerical Methods in Geomechanics*, ASCE, Blacksburg, 405-418, 1976.

Einav, I. Energy and variational principles for piles in dissipative soil. *Geotechnique* 55, No. 7, 515-525, 2005.

Ensoft, Inc. LPILE Plus 5.0. Ensoft, Inc., 2005.

Essler, R. and Yoshida, H. "Jet Grounting", *Ground Improvement*, Spon Press, New York, NY, 2004

Evans, L.T. Jr. and Duncan, J.M. Simplified Analysis of Laterally Loaded Piles. *Report UCB/GT/82-04*, University of Califormia, Berkley, 1982.

Fanous, A. F. *Development of Rational Design Methodology for Sprial Reinforcement in Prestressed Concrete Piles in Regions of High Seismicity*, Thesis, Iowa State University, Ames, Iowa, 2007.

Fleming, W. G. K., Weltman, A. J., Randolph, M. F. & Elson, W. K. (1992). Blackie & Son Ltd.

Georgiadis, M. & Butterfield, R., "Laterally loaded pile behavior". *Journal of Soil Mechanics and Foundation Division*, ASCE, 108, No. GT1, 155-165, 1982.

Georgiadis, M. Development of p-y curves for layered soils. *Proc. Conf. Geotech. Pract. Offshore Engng., Am. Soc. Civ. Engrs.* 536-545, 1983.

Guo, W. D. & Lee, F. H. Load transfer approach for laterally loaded piles. *Int. J. Numer. Anal. Meth. Geomech.* 25, No. 11, 1101-1129, 2001.

Hamada, M. "Damage to Piles by Liquefaction-Induced Ground Displacements," *Proc. 3rd U.S. Conference Lifeline Earthquake Eng.*, ASCE, Los Angeles, 1172-1181, 1991.

Hetényi, M. Beams on elastic foundation. Univ. Michigan Press, Ann Arbor, 1946.

Matlock, H. & Reese, L. C. Generalized solutions for laterally loaded piles. *J. Soil Mech. Fdn. Div., Am. Soc. Civ. Engrs.* 86, No. SM5, 63-91, 1960.

Matlock, H. Correlations for Design of Laterally Loaded Piles in Soft Clay, Offshore *Technology Conference Proceedings*, Offshore Technology Conference, Houston, Texas, 1970, Vol. I, Paper No. 1204, pp. 577-594, 1970.

Mayoral, J.M, Pestana, J.M., Seed, R.B. "Determination of Multidirectional p-y Curves for Soft Clays." *Geotechnical Testing Journal*, ASTM, 28(3), 1-11, 2005.

Mazzoni, S., F. McKenna, M.H. Scott, and G.L. Fenves. "Open System for Earthquake Engineering Simulation," *Pacific Earthquake Engineering Research Center*, University of California, Berkeley California, Ver. 1.6., 2004.

McClelland, B. & Focht Jr., J. A. Soil modulus for laterally loaded piles. *Trans. Am. Soc. Civ. Engrs.* 123, 1049-1063, 1958.

Mindlin, D. "Force at a Point in the Interior of a Semi-Infinite Solid," *Physics*, 7, 195-202, 1936.

Ismael, N. "Behavior of Laterally Loaded Bored Piles in Cemented Sand", *Journal of the Geotechnical Engineering Division*, ASCE: 1678-1699, 1970.

Kamon, M. and Bergado D. T. "Ground Improvement Techniques", *9th Asian Region Conf. on Soil Mechanics and Foundation Engieering.*, Bangkok, Vol. 2, pp. 526-546, 1991.

Kirupakaran, K., Cerato, A.B., Liu, C., Miller, G.A., Muraleetharan, K.K., Pinilla, J.D., Price, S., and Thompson, Z.M., "Simulation of a Centrifuge Model Test of Pile Foundations in CDSM Improved Soft Clays", *Proceedings of GeoFlorida 2010: Advances in Analysis, Modeling & Design.*, 2010.

Koojiman, A. "Comparison of an Elastoplastic Quasi Three-Dimensional Model for Laterally Loaded Piles with Field Tests," *Proc. 3rd Intl. Symposium on Numerical Models in Geomechanics*, Niagra Falls, 675-682, 1989.
Kutter, B. L. "Dynamic centrifuge modeling of geotechnical structures." *Transportation Research Record*. 1336, Transportation Research Board, Washington, D.C., 24-30, 1992.

Lee, S. L., Kog, Y. C. & Karunaratne, G. P. Laterally loaded piles in layered soil. *Soils Fdns.* 27, No. 4, 1-10, 1987.

Levy, N.H., Einav, I. and Randolph, M.F. "Effect of Recent Load History on Laterally Loaded Piles in Normally Consolidated Clay." *International Journal of Geomechanics*, ASCE, 7(4), 277-286, 2007.

Lok, T. "Numerical Modeling of Seismic Soil-Pile-Structure Interaction in Soft Clay." *Ph.D. Dissertation*, University of California, Berkeley, California, 1999.

Liu, C., Soltani, H., and Muraleetharan, K. "Centrifuge Investigation of Static loading tests on single piles in soft clays", University of Oklahoma, unpublished, 2010.

Ohtomo, K. "Soil force on conduit pile system due to liquefaction-induced lateral flow." *Proceedings, 6th Japan-U.S. Workshop on Earthquake Resistant Design of Lifeline Facilities and Countermeasures for Soil Liquefaction,* Technical report NCEER-96-0006, NCEER, Buffalo, NY, 541-550, 1996.

Peck, R.B., Hanson, W.E., and Thornburn, T.H. *Foundation Engineering (2nd Edition)*, John Wiley & Sons, New York, 1974.

Poulos, H., "An Approach for the Analysis of Offshore Pile Groups," *Proc. 1st Intl. Conf. on Numerical Methods in Offshore Piling*, London, 119-126, 1980.

Poulos, H. G. "Behavior of laterally loaded piles: I – single piles", *Journal of Soil Mechanics and Foundation Division,* ASCE, 97, No. SM5, 711-731, 1971a.

Poulos, H. G. "Behavior of laterally loaded piles: II – pile groups", *Journal of Soil Mechanics and Foundation Division,* ASCE, 97, No. SM5, 733-751, 1971b.

Poulos, H. G. "Behavior of laterally loaded piles: III – socketed piles". *Journal of Soil Mechanics and Foundation Division,* ASCE, 98, No. SM4, 341-360, 1972.

Poulos, H. G. & Davis, E. H. *Pile foundation analysis and design*. John Wiley & Sons, Inc., 1980.

Reese, L. C. and Welch, R. C. "Lateral loading of deep foundations in stiff clay." *Journal of geotechnical engineering division* 101(GT7): 633-649, 1975.

Reese, L., Cox, W. and Koop, F. "Analysis of Laterally Loaded Piles in Sand," *Proceedings to the 5th Annual Offshore Technology Conference.*, No. OTC 2080, pp. 473–485, 1975.

Reese, L. C. "Laterally Loaded Piles: Program Documentation," *J. Geotech. Eng.*, ASCE, 103(4), 287-305, 1977.

Reese, L. C. *Handbook on Design of Piles and Drilled Shafts under Lateral Load.* FHWA-IP-84-11, 360 pp. US department of Transportation, Federal Highway Administration, 1984.

Reese, L. and Wang, S. "Documentation of Computer Program SHAFT1 Version 1.1: Drilled Shafts Under Axial Loading," Ensoft, Inc., 1989.
Reese, L., "Analysis of Piles in Weak Rock," *Journal of the Geotechnical and Geoenvironmental Engineering Division*, ASCE, Vol. 123, no. 11, Nov. 1997, pp. 1010-1017, 1997.

Reese, J. C. & Van Impe, W. F. *Single piles and pile groups under lateral loadings*. A. A. Balkema, Rotterdam, 2001.

Rollins, K., T. Gerber, J. Lane, and S. Ashford, "Lateral Resistance of a Full-Scale Pile Group in Liquefied Sand," *submitted to Journal of the Geotechnical and Geoenvironmental Engineering Division*, American Society of Civil Engineers, 2003.

Rollins, K. M., Adsero, M.E. and Brown, D.A. "Jet grouting to increase lateral resistance of pile group in soft clays", In Geotechnical Special Publication No. 185: Contemporary topics in deep foundations. IFCEE'09, Iskander, M., Laefer, D.E. and Hussein, M.H. (Eds.) 265-272, 2010.

Terzaghi, K. Evaluation of coefficients of subgrade reaction. *Geotechnique* 5, No.4, 297-326, 1955.

Tomisawa, K. and Miura, S., "A design approach for composite ground pile and its verification", Advances *in Deep Foundations*, Taylor & Francis Group, London, 2007.

Topolnicki, M. "In Situ Soil Mixing", *Ground Improvement*, Spon Press, New York, NY, 2004

Trochianis, A., Bielak, J., and Christiano, P. "A Three-Dimensional Nonlinear Study of Piles Leading to the Development of a Simplified Model," *Rpt. R-88-176*, Dept. of Civil Eng., Carnegie Inst. of Technology, December, 1988.

Prakash, Shamsher and Sharma, Hari D. *Pile Foundations in Engineering Practice*, John Wiley and Sons, Inc, 1990
Pyke, R. & Beikae, M. A new solution for the resistance of single piles to lateral loading. *Laterally Loaded Deep Fdns., ASTM STP 835,* 3-20, 1984.

Salgado, R. *The engineering of foundations. The McGraw-Hill Companies*, Inc. 2008.

Seed, R., Dickenson, S., Riemer, M., Bray, J., Sitar, N., Mitchell, J., Idriss, I., Kayen, R., Kropp, A., Harder, L. Jr., and Power, M. "*Preliminary Report on the Principal*

Geotechnical Aspects of the October 17, 1989 Loma Prieta Earthquake," Rpt. No. UCB/EERC-90/05, Earthquake Eng. Research Ctr., Univ. of California, 1990.

Semprich, S. and Stakler, G. "Grouting", *Geotechnical Engineering, Geotechnical Handbook,* Ernst & Sohn, Berlin.

Sondermann W. and Wehr, W. "Deep Vibro Techniques", *Ground Improvement,* Spon Press, New York, NY, 2004

Sun, K. Laterally loaded piles in elastic media. *J. Geotech. Engng., Am. Soc. Civ. Engrs.* 120, No. 8, 1324-1344, 1994a.

Swane, I. and Poulos, H. "Shakedown Analysis of Laterally Loaded Pile Tested in Stiff Clay," *Proc. 4th Australia-New Zealand Conf. on Geomechanics*, Perth, Vol. 1, 165-169, 1984.

Thompson, G. R., *Application of Finite Element Method to the Development of p-y Curves for Saturated Clays.* Thesis, University of Texas, Austin, 1977.

Ulitskii, V. M. and Alekseev S. I. *Preservation of Buildings during the Installation of Foundation Pits and the Laying of Utilities in Saint Petersburg*, Soil Mechanics and Foundation Engineering, Volume 39, Number 4, 2002.

Wilson, D.W., Boulanger, R.W., and Kutter, B.L. "Soil-pile-superstructure interaction at soft or liquefiable soils sites-Centrifuge Data Report for CSP4." *Report No. UCD/CGMDR-97/04*, Center for Geotechnical Modeling, Dept. of Civil Engineering, University of California, Davis, California, February, 1997a.

Wilson, D.W., Boulanger, R.W., and Kutter, B.L. "Soil-pile-superstructure interaction at soft or liquefiable soils sites-Centrifuge Data Report for CSP5." *Report No. UCD/CGMDR-97/06*, Center for Geotechnical Modeling, Dept. of Civil Engineering, University of California, Davis, California, February, 1997b.

Winkler, E. Die Lehre von der Elasticitaet und Festigkeit, Prag, Dominicus, 1867.

Wong, P., Kulhawy, F., and Ingraffea, A. "Numerical Modeling of Interface Behavior for Drilled Shaft Foundations Under Generalized Loading," in Foundation Eng.: Current Principles and Practices, ASCE, Vol. 1, 565-579, 1989.

Wood, H. "*Distribution of Apparent Intensity in San Francisco*," in The California Earthquake of April 18, 1906, Rpt. of the State Earthquake Investigation Comm., Carnegie Inst. of Washington, Washington, D.C., 220-245, 1908.

Yegian, M. and Wright, S. "Lateral Soil resistance - Displacement Relationships for Pile Foundations in Soft Clays," *Proc. 5th Offshore Technology Conf.*, OTC 1893, Houston, Vol. 2, 663-676, 1973.

Zelinski, R., Roblee, C.J., and Shantz, T. “Bridge foundation remediation considerations, earthquake-induced movements and seismic remediation of existing foundations and abutments.” In *Geotechnical Special Publication No. 55*, S. Kramer and R. Siddharthan (Eds.), ASCE, New York, 1995.

ACKNOWLEDGEMENTS

The research described herein was carried out as part of the George E. Brown, Jr. Network for Earthquake Engineering Simulation (NEES) research project (Grant No. CMMI-0830328) “NEESR-SG: Understanding and Improving the Seismic Behavior of Pile Foundations in Soft Clays”. Dr. Richard J. Fragaszy at the National Science Foundation serves as the program manager for this grant.

The author would like to recognize Dr. Sri Sritharan for the opportunity to work on this project. His commitment to the success of this project was greatly appreciated.

The author would like to thank her parents, husband, and friends for their support through the duration of this project. The author is blessed to be surrounded by such an amazing group of people and knows that this experience is one that will always be remembered.